

UNIVERSITY OF OKLAHOMA

GRADUATE COLLEGE

STABILITY OF AQUEOUS FOAMS AT HIGH PRESSURE AND THE IMPACT OF
CONTAMINANTS

A THESIS

SUBMITTED TO THE GRADUATE FACULTY

in partial fulfillment of the requirements for the

Degree of

MASTER OF SCIENCE

By

OYINDAMOLA OBISESAN

Norman, Oklahoma

2021

STABILITY OF AQUEOUS FOAMS AT HIGH PRESSURE AND THE IMPACT OF
CONTAMINANTS

A DISSERTATION APPROVED FOR THE
MEWBOURNE SCHOOL OF PETROLEUM AND GEOLOGICAL ENGINEERING

BY THE COMMITTEE CONSISTING OF

Dr. Ramadan Ahmed, Chair

Dr. Catalin Teodoriu

Dr. Hamidreza Karami

Dr. Mahmood Amani

© Copyright by OYINDAMOLA OBISESAN 2021

All Rights Reserved.

ACKNOWLEDGEMENTS

I thank God first and foremost for the successful completion of this research. My profound appreciation also goes to Dr. Ramadan Ahmed for his support provided. He has been a strong pillar for me during the project. It would have been impossible to have achieved this feat without the encouragement, knowledge, and constructive feedback from Dr. Ahmed. The resources I have gained during my time in graduate college with Dr. Ahmed are of utmost importance and would take me far in my life pursuit and research. I am also grateful to Dr. Mahmood Amani for his insights and knowledge on this project.

I appreciate my parents, whom I call my earthly gods for their love, support, and care all these years. Through sunshine and rain, you always supported me. I love you a lot. I would also send my love and thanks to my sisters; Yetunde, Bidemi, Bolu, and sister Tundun for their support and contributions and my adorable brother Richard Obisesan. I also thank my wards Obaloluwa, Anike, Owen, and Michelle Fasanya.

My heartfelt gratitude goes to my professors for helping me become the well-rounded engineer that I am today. I appreciate Dr. Catalin for his knowledge and expertise in one of my first classes as a Masters' student at the University of Oklahoma. I am also very grateful for the knowledge and insight I gained from Dr. Hamidreza's advanced production class. I am so grateful to have been surrounded by such resourceful and knowledgeable professors.

I am grateful to Dr. Rida Elgaddafi for his initial insights on the project and putting me through with the resources I needed and walking me through the experimental setup and taking time to

teach me the data analysis required for the project. I express my thanks to Jeff McCaskill for his help in the laboratory and for always being willing to explain the tools and help as much as possible.

I would like to finally my friends Judah Odiachi and Michael Olubode for their support and friendship during my degree program and this thesis. You made this journey as fun and interactive as practically possible. I am so thankful for Layefa Timiyan for being my best friend during this time and listening to my project insights and giving me constructive feedback. I am also grateful to have Okeoghene Agbawe as a dear friend and support system. I am so happy to have you all in my life as friends.

This research was made possible by NPRP grant 10-0115-170165 from the Qatar National Research Fund (QNRF). I would like to thank the Qatar National Research Fund for providing the research fund for this project. Also, I would like to express my gratitude and appreciation to the Texas A&M University at Qatar and the University of Oklahoma for supporting the project.

TABLE OF CONTENTS

ACKNOWLEDGEMENTS	iv
TABLE OF CONTENTS	vi
LIST OF FIGURES	x
LIST OF TABLES	xiv
ABSTRACT.....	xv
CHAPTER ONE	1
1.1. Factors Affecting Foam Stability	2
1.2. Applications of Foam.....	3
1.2.1. Drilling	3
1.2.2. Enhanced Oil Recovery	3
1.2.3. Hydraulic Fracturing	4
1.2.4. Cementing	4
1.3. Properties of Foam.....	4
1.3.1. Stability	5
1.3.2. Quality.....	6
1.3.3. Rheology	7
1.4. Effects of External Factors.....	8
1.4.1. Pressure	8
1.4.2. Surfactant	8
1.4.3. Temperature	9
1.4.4. Foam Generation Technique	10
1.4.5. Bubble Size and Distribution	10

1.4.6. Effect of Height.....	10
1.4.7. Column Diameter.....	11
1.5. Objectives and Scope of Work.....	11
CHAPTER TWO	12
2.1. Foam Structure.....	12
2.2. Drainage Mechanisms.....	13
2.3. Drainage Models.....	14
2.4. Effect of Pressure	14
2.5. Literature on Foam Contaminants.....	15
2.5.1. Salt	15
2.5.2. Oil	23
2.5.3. Clay	27
CHAPTER THREE.....	32
3.1. Channel Dominated Drainage Model.....	32
3.1.1. Model Assumptions	32
3.2. Node Dominated Drainage Model	33
3.2.1. Model Assumptions	33
3.2.2. Computational Grid Simulation	34
CHAPTER FOUR	36
4.1. Experimental Setup.....	36
4.2. Test Procedure.....	37
4.2.1. Base Fluid Preparation.....	37
4.2.2. Rheology and Stability.....	38

4.3. Experimental Scope and Test Materials	40
4.3.1. Salt	40
4.4.2. Clay	41
4.4.3. Oil	42
4.4. Data Analysis	43
CHAPTER FIVE	46
5.1. Aqueous Foam without Contaminants.....	46
5.1.1. Foam Rheology.....	46
5.1.2. Drainage Measurement	50
5.2. Effect of Pressure on Drainage	54
5.3. Aqueous Foam with Salt.....	56
5.3.1. Effect of Mono and Divalent Salt on Surface Tension.....	56
5.3.2. Effect on Viscosity.....	57
5.3.3. Effect of Salt Concentration on Foam Drainage	58
5.4. Aqueous Foam with Oil	71
5.4.1. Foam Generation Technique in the Presence of Crude Oil	71
5.4.2. Effect Oil Type	71
5.4.3. Effect of Crude Oil Types.....	72
5.4.3. Effect of Mineral Oil.....	76
5.5. Aqueous Foam with Clay	79
5.5.1. Effect of Bentonite	79
5.5.2. Effect of Kaolinite	82
5.6. Comparison of Model Predictions with Measurements	84
5.6.1. Aqueous Foam without Salt	85
5.6.2. Aqueous Foam with 9% Salt	87

CHAPTER SIX	89
6.1. Conclusions	89
6.1.1. Aqueous Foam without Contaminant	89
6.1.2. Aqueous Foam with Salt.....	89
6.1.3. Aqueous Foam with Oil.....	90
6.1.4. Aqueous Foam with Clay.....	90
6.2. Recommendations	90
NOMENCLATURE	92
SUBSCRIPTS	93
REFERENCES	94
Appendix A: Drainage Measurements.....	105
A.1 Results for Clay Contaminated Foams.....	105
Appendix B: Foam Rheology Measurements.....	109
B.1 Results for Salt Contaminated Foams	109
B.2 Results for Oil Contaminated Foams	111
Appendix C: Mathematical Modelling Results	113
Appendix D.....	117

LIST OF FIGURES

Figure 2.1. Hexagonal Foam Structure	14
Figure 2.2. The effect of salinity on foam stability at CD conc 0.005 wt.% in brine solution of NaCl and <i>CaCl2</i> solution weight ratio 3:1 after 90 minutes (Liu et al. 2005).....	20
Figure 2.3. The effect of salinity on foam stability at CD conc 0.005 wt.% in NaCl solution after 90 minutes (Liu et al. 2005)	21
Figure 2.4. Effect of Salinity on Foam Stability at CD Conc 0.005 Wt.% in <i>CaCl2</i> Solution after 90 Minutes (Liu et al. 2005)	21
Figure 2.5. Effect of crude oil API gravity on foam stability (Rojas et al. 2001)	27
Figure 2.6. Half-life of foams stabilized by the mixtures of 0.4 wt.% of AOS surfactant and clay particles concentration (Chen et al. 2019)	30
Figure 2.7. Drainage time of foams stabilized with Laponites/CTAB system as a function of CTAB concentration at different particle concentrations (Zhang et al. 2008).	31
Figure 3.1. Simulated foam column with 36 grids (Govindu 2019).....	35
Figure 4.1. Experimental Setup	37
Figure 4.2. (a) Flowrate vs. time (b) Differential pressure variations with time	40
Figure 4.3. Pressure distribution in the vertical test section	43
Figure 4.4. (a) Normalized density plot for the column sections (b) Pressure distribution at different times	44
Figure 5.2: Power-law exponent.....	48
Figure 5.3. Apparent viscosity vs quality at 25oC and 6.89 MPa @ 5000 1/s	48
Figure 5.4. Normalized density curves a) 45% b) 50% c) 55% d) 60% e) 65% f) 70%.....	49

Figure 5.5. Drainage fraction versus time for aqueous foams a) 45% b) 50% c) 55% d) 60% e) 65% and f) 70%	52
Figure 5.6. The effect of pressure on average drainage curves of different quality foams: a) 40%; c) 50%; and e) 60%	55
Figure 5.7. Surface tension measurement for NaCl and CaCl₂	57
Figure 5.8. Viscosity changes with salt (NaCl and CaCl₂) concentration.....	58
Figure 5.9. Density changes with NaCl and CaCl₂ concentration.....	58
Figure 5.11. Effect of NaCl salt on the drainage volume of aqueous foam at 50% quality a.) 0% wt. b.) 5% wt. c.) 7% wt. d.) 9% wt. e.) 14% wt. f.) 18% wt.	64
Figure 5.12. Effect of NaCl salt on the drainage volume of aqueous foam at 60% quality a.) 0% wt. b.) 5% wt. c.) 7% wt. d.) 9% wt. e.) 14% wt. f.) 18% wt.	65
Figure 5.13: Effect of NaCl concentration on the AMDF of different quality foams	66
Figure 5.15. Effect of CaCl₂ salt on the drainage volume of aqueous foam at 50% Quality a.) 0% wt. b.) 5% wt. c.) 9% wt. d.) 14% wt. e.) 18% wt.	68
Figure 5.16. Effect of CaCl₂ salt on the drainage volume of aqueous foam at 60% Quality a.) 0% wt. b.) 5% wt. c.) 9% wt. d.) 14% wt. e.) 18% wt.	69
Figure 5.17. Effect of CaCl ₂ concentration on the AMDF of (a) 40% and 50% quality foams (b) 60% quality foam.....	70
Figure 5.18. Effect of crude oil type on AMDF of different quality foams: (a) 40%, (b) 50%, and (c) 60%	73
Figure 5.19. Fractional drainage vs. time for different quality foams: (a) 40%, (b) 50%, and (c) 60%	75

Figure 5.20. Fractional drainage vs. time for 40% quality foam at different mineral oil concentration: (a) No Oil, (b) 5%, (c) 10%, and (d) 20%	77
Figure 5.21. Fractional drainage vs. time for 50% quality foam at different mineral oil concentration: (a) No Oil, (b) 5%, (c) 10%, and (d) 20%	77
Figure 5.22. Drainage rate at 60% Quality (a) No Oil (b) 5% (c) 10% (d) 20%	78
Figure 5.23. Drainage rate at 40% quality foam with different bentonite concentrations: (a) 0.0%, (b) 2.5%, and (c) 5.0%	80
Figure 5.24: Rheology of bentonite containing foam at different qualities: a) 40%, b) 50%, and c) 60%	81
Figure 5.25. Drainage rate at 40% quality foam with different Kaolinite concentrations: (a) 0.0%, (b) 2.5%, and (c) 5%	83
Figure 5.26. Rheology of kaolinite containing foam at different qualities: a) 40%, b) 50%, and c) 60%	84
Figure 5.27. Drainage fraction versus clay concentration	84
Figure 5.28. Quality profiles at 60% quality foam at 0% salt: (a) 15 minutes, (b) 30 minutes, (c) 60 minutes, (d) 100 minutes, and (e) 120 minutes.....	86
Figure 5.29. Quality profiles at 60% quality foam at 9% salt: (a) 15 minutes, (b) 30 minutes, (c) 60 minutes, (d) 100 minutes, and (e) 120 minutes.....	88
Figure A.1.1. Drainage fraction versus time at 50% Quality (a) No Bentonite (b) 2.5% Bentonite (c) 5% Bentonite	105
Figure A.1.2. Drainage rate at 50% Quality (a) No Kaolinite (b) 2.5% Kaolinite (c) 5% Kaolinite	106

Figure A.1.3. Drainage rate at 60% Quality (a) No Bentonite (b) 2.5% Bentonite (c) 5% Bentonite	107
Figure A.1.4. Drainage rate at 60% Quality (a) No Kaolinite (b) 2.5% Kaolinite (c) 5% Kaolinite	108
Figure B.1.1. Shear stress vs. nominal Newtonian shear rate for: a) 5%; b) 9%; c) 14%; and d) 18% NaCl foams	109
Figure B.1.2. Shear stress vs. nominal Newtonian shear rate for: a) 5%; b) 9%; c) 14%; and d) 18% CaCl ₂ foams	110
Figure B.2.1. Effect of the Mineral Oil on Foam Rheology a.) 40% Quality b.) 50% Quality c.) 60% Quality	111
Figure B.2.2. Effect of the Crude Oil on Foam Rheology a.) 40% Quality b.) 50% Quality c.) 60% Quality	112
Figure C.1. Drainage Rate at 40% Quality of Model vs Experiment at 0% Salt (a) 15 Minutes (b) 30 Minutes (c) 60 Minutes (d) 100 Minutes (e) 120 Minutes.....	113
Figure C.2. Drainage Rate at 50% Quality of Model vs Experiment at 0% Salt (a) 15 Minutes (b) 30 Minutes (c) 60 Minutes (d) 100 Minutes (e) 120 Minutes.....	114
Figure C.3. Drainage Rate at 40% Quality of Model vs Experiment at 9% Salt (a) 15 Minutes (b) 30 Minutes (c) 60 Minutes (d) 100 Minutes (e) 120 Minutes.....	115
Figure C.4. Drainage Rate at 50% Quality of Model vs Experiment at 9% Salt (a) 15 Minutes (b) 30 Minutes (c) 60 Minutes (d) 100 Minutes (e) 120 Minutes.....	116

LIST OF TABLES

Table 4.1. Experiment Matrix – Salt.....	40
Table 4.2. Experiment Matrix – Clay	41
Table 4.3. FTIR Analysis for Bentonite and Kaolinite.....	42
Table 4.4. Experimental matrix for oil contamination study	42
Table 4.5. Properties of crude oils used in the experiment.....	42
Table 5.1: Rheology measurements of base fluids with bentonite	81
Table 5.2: Rheology measurements of base fluids with Kaolinite	83

ABSTRACT

Foam is a mixture of gas bubbles dispersed in a continuous liquid phase that exhibits some form of structure. Foam is used in various oil and gas industry operations such as drilling, cementing, and fracking. The properties of foam that make it applicable for use in the oil and gas industry are its low density and high viscosity. These unique properties make foam applicable in drilling underbalanced while maintaining good hole cleaning and pressure management. However, the thermodynamically unstable structure of foam makes it prone to collapse after a stipulated time based on factors such as the foam quality, base fluid, temperature, and pressure. The half-life of the foam which is the time required for the foam to drain half of its liquid should be sufficient to allow the circulation of foam in the wellbore without significant degradation of relevant properties.

While drilling through various formations, foam can encounter certain contaminants such as salt, oil, clay, and other substances. These substances can change some of the properties of the foam. This study investigates the effect that salt, oil, and clay have on the drainage behavior of the foam. Foam drainage/stability experiments were conducted on the stability of aqueous foams at high pressure (6.89 MPa) and the ambient temperature of 25°C. The test was performed by trapping the foam in a vertical test section that has 10 differential pressure sensors to measure the pressure profile. Experiments were conducted at the various quality of foam (40%, 50%, 60%) to determine drainage rate and drainage volume at various sections (segments) of the test section for two hours.

The results show that the drainage rate decreases with foam quality indicating that foam stability increases with foam quality. Various contaminants have varying effects on the stability of the aqueous foam. The NaCl and CaCl₂ salts have the effect of improving the stability of the foam at

lower salt concentrations. However, at higher concentrations, they destabilize the foam, and this effect is known as the “W” effect of increase and decrease based on salt concentration. The CaCl_2 had a higher impact on foam stability due to its greater valency. This behavior was observed across all the qualities investigated.

The effect of mineral oil on the stability of foam is sensitive to its quality. At lower qualities (40% and 50%), foam stability improves with the mineral oil content. But at higher quality, a decrease in the drainage was observed with mineral oil concentration. Both light and heavy crude oils have a destabilization effect on the foam across all qualities. Increasing the concentration of crude oils decreased the foam stability. The heavy oil had a lower destabilization effect than the light crude oil.

The introduction of bentonite and kaolinite clays improved the stability of the foam across all the qualities investigated. Increasing the concentration of clays increased the stability of the foam. Bentonite has a more significant effect on increasing stability than kaolinite.

CHAPTER ONE

INTRODUCTION

Foam is a thermodynamically unstable fluid with a large surface area. It has wide use in many industries such as the oil and gas, chemical, petrochemical, and food industries. The properties of foam such as its high viscosity and low density justify its widespread use. Foam is a fluid created by the entrapment of gas in a liquid. The liquid forms a thin film coat around the gas pockets.

There are two certain requirements to be met for foam to occur.

- I. The presence of mechanical stress in form of agitation or shearing. The agitation disturbs the molecules of the two fluids in the mixture and creates foam.
- II. The presence of surfactant. The surfactant reduces the surface tension of the liquid phase and stabilizes the surface created by the mixing.

Foam exhibits a fluid structure with distributed gas bubbles in a continuous liquid phase. Often the foams used in the oilfield consist of a liquid phase between 5-40% and the gas phase of 95%-60%. The presence of structure makes foams thermodynamically unstable particularly at low energy state when they undergo processes such as gravitational drainage, coalescence, and Ostwald ripening (Sinha et al. 2019; Bhakta and Ruckenstein 1997; Gallego-Juárez et al. 2015).

Gravity drainage is caused by the density differential between the gas and liquid phases, which is the primary reason for foam breakdown or decay. The heavier liquid flows to the bottom due to the forces of gravity. When the bubbles collide, the pressure differences between small foam bubbles with higher pressure and large foam bubbles with lower pressure cause the bubbles to coalesce. The coalescence or merging of the bubbles destabilizes the foam as the large bubbles are

more prone to collapse or unstable (Govindu et al. 2019). Ostwald Ripening happens when smaller gas bubbles merge with larger bubbles that are unstable due to their thin-film (Eren 2004).

1.1. Factors Affecting Foam Stability

Quality, presence of surfactant, contaminants, pH, surface tension, presence of polymers, temperature, foam formation method, and type of base fluid are all factors that affect foam stability (Gallego-Juárez et al. 2015; Sherif et al. 2016).

The foam's quality is an essential property in its long-term stability. These foams can be classified based on foam quality as wet foam or dry foam. Wet and dry foams have some liquid in them; however, wet foams have more liquid than dry foams (Govindu et al. 2019; Okpobiri et al. 1986). The transition from wet to dry foam occurs when the quality exceeds 75%. Dry foam has a lesser drainage volume and higher stability compared to wet foam. This is because of the higher viscosity of the gas and liquid network. The foam structure changes with the quality of the foam because the structure of the foam is formed by the volume of liquid and gas in the fluid (Ahmed et al. 2003; Sherif et al. 2016). The change from wet to dry foam allows bubble deformation which affects the foam structure under dynamic conditions. With increasing foam quality, the foam structure also changes from a spherical to polyhedral shape (Rehm and Paknejad 2012).

Particle absorption at the gas-liquid interface, stratification of non-absorbing particles, and variations in capillary pressure produced by the presence of tiny, adsorbed particles are three major processes that allow the formation of foam. Surfactants are then added to the foam to increase its stability by reducing interfacial tension and forming stable layers. Surfactant molecules cling to the gas-liquid interface, resulting in a thicker, more stable layer. The molecules of the surfactant

adsorbed to the plateau boundary, bubble surface, and lamella between the foam bubbles (Zhang et al 2008). At the plateau border, they coagulate to produce a thick film across the surface of the bubble at the start of drainage, improving foam stability by minimizing coalescence when the foam bubbles meet. In the coherent phase, the molecules jammed at the film lamella produce a web structure, and bubbles become trapped in the collection of molecules, resulting in improved foam stability. The surfactant lowers the interfacial tension of the film at the gas-liquid contact surface.

1.2. Applications of Foam

Foams are utilized in several industrial applications because of their distinctive characteristics. In the petroleum industry, they are applied in drilling, completion, fracking, cementing, and enhanced oil recovery operations.

1.2.1. Drilling

For use in the drilling process, the foam must be stable and maintain its properties to avoid wellbore instability and formation damage. When used in underbalanced drilling, foam can improve well stability, increase penetration rate, reduce swelling in sensitive shale formations, eliminate the risk of lost circulation and differential sticking, and minimize formation damage, which causes invasion zones and distorts the true representation of formation properties. The high viscosity of the foam ensures optimum hole cleaning and cutting carrying capacity.

1.2.2. Enhanced Oil Recovery

Enhancing Oil Recovery (EOR) is used to provide external energy such as thermal, miscible gas injection, or chemicals into the reservoir to increase the amount of hydrocarbon extracted after the

reservoir's natural energy has depleted (Sunmonu et al. 2013; Farzaneh and Sohrabi 2013). Poor sweep efficiency and lower oil recovery owing to viscous instability, which may be attributed to the low density and low viscosity of the fluid injected, have been some of the challenges faced by EOR in recent years. This is where foam's low density and high viscosity properties become beneficial, as they increase vertical and areal sweep.

1.2.3. Hydraulic Fracturing

Foam can increase proppant placement efficiency over the total fracture length due to its high proppant carrying capacity (Harris 1996). A critical part of hydraulic fracturing is the recovery of the liquid flow back to the surface. When foam is used for fracturing, the gas phase improves liquid clean-up.

1.2.4. Cementing

Foam cementing is a cementing technique in the oil industry required especially when low-density cement is required to avoid fracture during cementing (Taiwo et al. 2011). The benefits of foam cementing include better mud removal, reduction of gas migration and fluid loss, and good elasticity. Foam cement is more resistant to cyclic stress than conventional cement. It exhibits unique properties such as low density, low permeability, and high strength that are required in weak formations with low fracture gradients.

1.3. Properties of Foam

There are certain properties that foam possess that enable it to be useful for the applications that are discussed previously. These properties depend on factors such as foam quality, foam generation

method, presence of surfactant, temperature, base fluid type, pH, impurities, presence of polymers, surface tension (Gallego-Juárez et al. 2015; Sherif et al. 2016). The three most important properties of the foam that affect its application are quality, stability, and rheology.

1.3.1. Stability

Stability is a particularly important feature of foam because it determines the rate of degradation of its property (Gallego-Juárez et al. 2015). If foam is left without mixing or shearing, destabilization and decay occur immediately after it is generated. The three mechanisms for foam destabilization are gravity separation, Ostwald ripening, and bubble coalescence. Gravity separation is a major factor for foam destabilization by triggering liquid drainage. This involves the flow of liquid down the column due to its higher density and flow of gas upwards. This segregation continues until the surface tension cannot be handled by thinning gas bubble walls. The surface tension relationship is between the gas bubble wall and liquid film. The pressure exertion on the bubbles is equalized by the pressure in the bubbles. The coalescence of the bubble involves the larger bubble; which has a lower pressure in contact with the small bubble; which has a higher pressure. When the two bubbles are in contact, the gas diffuses between the bubbles, and the smaller bubble is absorbed by the larger one (Ostwald Ripening) (Tuna 2004).

During the drainage process, the capillary pressure gradient, which acts along the foam column height, opposes the liquid drainage process. The drainage rate also varies along the column height, as a result, the capillary pressure and liquid drainage processes can be balanced at a certain foam column height. The inclusion of a surfactant is required to lower the surface tension and improve foam stability. Moreover, other factors such as bulk and surface viscosity, mechanical resistance, ability to resist film thinning influence the stability of foam (Argillier et al. 1998).

1.3.2. Quality

The quality of foam is an important parameter that determines its characteristics and performance. It denotes the volumetric ratio of gas in the foam. Mathematically, the foam quality (Γ) at a given pressure (P) and temperature (T) is expressed as:

$$\Gamma(P, T) = \frac{V_g}{V_f} = \frac{V_g}{V_g + V_L} \quad (1.1)$$

where V_f and V_g are the volumes of foam and gas phase at a given pressure and temperature, respectively. V_L is the volume of liquid. Foams are categorized as wet or dry foam depending on the foam quality (Okpobiri et al. 1986). Wet foams have a high liquid content, and they are prone to drainage. Dry foams are high-quality foams that exhibit structure and limited drainage due to the viscous resistance created by the foam network structure.

The stability of foam is strongly influenced by the foam quality. Foam properties would differ based on the quality of the foam. As foam quality increases above 75% it is more challenging to describe the foam behavior due to complex foam structure. The quality of the foam influences the structure of the foam (Sherif et al. 2016; Ahmed et al. 2003). This is because the foam quality determines the bubble shape. Bubble-shaped transformation occurs when the quality is above 75% and this causes a change in the foam structure. As liquid drains out, the foam shape transforms from spherical to polyhedral, improving foam stability (Davis 2013). Wet foams have a low quality (< 75%) and spherical shape while dry foams exhibit a polyhedral structure with thin separating films (Rehm and Paknejad 2012).

The influence of quality on stability was investigated by Govindu et al. (2019). The drainage rate decreased with quality. Liquid drainage is delayed in high-quality foams due to the rigid and then bubble structure. Besides this, the viscosity of foam is directly related to its quality; therefore, as the quality of the foam improves, so does the viscosity (Ahmed et al. 2003). Wellbore cleaning is an important part of the drilling process. Foam hole cleaning is determined by annular velocity and its rheology, which is primarily controlled by base fluid viscosity and foam quality (Li and Kuru 2004). The carrying capacity of the foam is one of the primary benefits of foam drilling. Due to the structure of the foam, which contains bubbles trapped in the foam structure, foam systems exhibit strong hole cleaning properties. Even when there is no circulation, the structure of foam keeps the cuttings from falling out (Martins et al. 2000). The more rigid the foam structure is, the better the lifting capacity of the foam and therefore good hole cleaning property.

1.3.3. Rheology

The structure of foam makes it fluid with complex rheology. The rheology of foam is defined by the temperature, pressure, foam quality, texture, base fluid properties, and the type of surfactant in foam (Bonilla et al. 2000). At low qualities (less than 40%), aqueous foam is usually assumed to be a Newtonian fluid but at high qualities (greater than 40%), it develops structure and exhibits shear-thinning and yielding behaviors that are the characteristics of non-Newtonian fluids (Akhtar et al. 2018).

The rheology of the foam is determined by the quality of the foam and the base liquid viscosity (Sherif et al. 2016). The rheology of the base fluid used for the generation of foam also influences the stability of the foam. Ibizugbe (2012) carried out an investigation and observed the reduction in the stability with decreasing base fluid viscosity. The half-life of the foam was found to vary

significantly when the rheological parameters of the base fluid were changed. The rheology of the base fluid can be improved by adding polymer (Chen et al. 2005). The base fluid viscosity was varied by changing polymer concentration in the base fluid. The viscosity difference between the various concentration shows a change in flow consistency index and flow behavior index which shows that increasing polymer concentration increases foam viscosity (Sherif et al. 2016).

1.4. Effects of External Factors

The drainage behavior of foam is influenced by various factors including pressure, temperature, surfactant type, foam generation method, bubble size and texture, and column height and diameter.

1.4.1. Pressure

The effect of pressure with foam drainage has been studied in literature (Rand and Kraynik 1983). The research by Rand and Kraynik (1983) investigated the drainage time by increasing generating pressure. An increase in the drainage time was observed with increasing pressure. The bubble size was reduced due to the pressure increase resulting in improved foam stability.

1.4.2. Surfactant

Surfactants are the required addition to the base liquid mixture. The properties of the surfactant included in foam generation can influence the stability of the foam. The hydrophobic tendency, electrical properties, water-solubility, and the molecular weight of surfactant can affect foam stability (Soleymani et al. 2013; Zhang et al. 2008). The foam stabilization of surfactant involves three mechanisms; adsorption of the particles at the gas-liquid interface, the stratification of non-absorbing particles, and the changes in capillary pressure caused by the presence of small, adsorbed

particles. A surfactant reduces the interfacial tension by lining the contact surface between the gas/liquid phases. This is due to the structure of surfactant molecule which has both hydrophilic and lipophilic parts that have a strong affinity for water and nonpolar hydrocarbon, respectively.

According to Ibizugbe (2012), foams have a weak bubble film which makes them unstable. Surfactants can be added to the foam to strengthen the film and make the foam more stable and last longer. The surfactant can impede excessive thinning of the bubble films to reduce the foam destabilization by bubble coalescence. Surfactant mixtures can increase the surface viscosity of the base fluid which impedes liquid drainage through the bubble film.

1.4.3. Temperature

The effect of temperature on foam stability was studied by (Maini and Ma 1986). The increase in temperature reduces the stability of foam. An increase in liquid drainage was observed with temperature. This is partly due to the reduction in liquid viscosity with an increase in temperature. An increase in temperature also causes the vaporization of liquid films between bubbles and weakens the bubble film (Soleymani et al. 2013). The study also concluded that if a stabilizing agent is not used on the foam, increasing the temperature can be detrimental to the stability of the foam. However, on some foaming agents, better stability is observed with an increase in temperature due to the inability of some solvents to dissolve at a lower temperature. The effect of temperature also depends on the type of foaming agent used. At higher temperatures, the type of surfactant used should be able to withstand elevated temperatures.

1.4.4. Foam Generation Technique

Foam can be generated by using various methods (Garrett 1993; Bhakta and Ruckenstein 1995a; 1995b; Hirt et al. 1987; Skauge et al. 2020) including aeration and agitation of liquid with dissolved gas such as the formation of the bubble at orifices and formation of the bubbles in the rotary mixer, by liquid phase vaporization, and by gas release through microbial and chemical reactions. The method of foam generation would determine the initial bubble size distribution of the foam, and its stability (Garrett 1993; Rand and Kraynik 1983). The initial bubble size could either be spherical and polyhedral and distribution could either be monodispersed or polydispersed.

1.4.5. Bubble Size and Distribution

Foam structure and the bubble shape and size depend on foam quality and the method by which the foam is formed. Foam bubbles most commonly have a spherical monodisperse structure (Engelsen et al. 2002). However, as the quality increases, the bubble structure becomes polydispersed to conserve the spherical shape. Higher quality foams therefore have mostly polyhedral-shaped polydispersed bubbles. This polydispersed structure of the bubbles influences foam instability due to the varying pressure distribution caused by nonuniform bubble size which causes bubble coalescence at higher pressures. Blackwell and Sobolik (1987) stated that the ideal structure of foam bubbles is a pentagonal dodecahedron. According to David and Marsden's (1969) research, bubble diameters range from 100 to 800 micrometers.

1.4.6. Effect of Height

The physical and chemical properties of foams are not the only properties that affect foam drainage. Other factors such as the height of the test section or shape and initial vertical liquid

distribution influence the drainage (Saint-Jalmes 2006). Ramani et al. (1993) studied the effect of foam height on the foam drainage rate. The amount of liquid drained from a foam column varied with time. The work concluded that the foam column with the highest height would have the least drainage rate.

1.4.7. Column Diameter

Ramani et al. (1993) studied the effect of test section diameter on the drainage rate. The experiments were performed using glass columns of diameter 0.03 and 0.05 m. The results from this experiment showed the minor effect of column diameter on the foam drainage.

1.5. Objectives and Scope of Work

The objectives of this study are to investigate the impacts of pressure, and contaminants on the foam drainage rate, and to evaluate the performance of the foam drainage model in predicting the stability of foam under elevated pressure. These objectives were achieved by performing drainage experiments at various pressure and introducing oil contaminants into the surfactant solution at different concentrations and using a test setup and method that can allow measuring drainage at different locations in a foam column. The numerous applications of foam cause foam to be in processes where it encounters various contaminants such as oil, salt, and clay. These are the three contaminants that are investigated in this work. The aim is to determine how the presence of these contaminants affects the drainage behavior of aqueous foams. The experiments were conducted at three different foam qualities (40%, 50%, and 60%). This is to investigate the behavior of the foam with changing quality both in clean and contaminated foams.

CHAPTER TWO

LITERATURE REVIEW

This chapter discusses existing literature in the areas of foam structure, drainage mechanisms, and drainage modeling. Studies conducted on the effects of contaminants such as salt, oil, and clay on the stability and drainage behavior of foams are also presented.

2.1. Foam Structure

The most stable shape of an individual gas bubble surrounded by liquid is a sphere, which has the smallest possible area for a volume of gas. In foams, gas dispersed in liquid would have a bubble with a sphere or polyhedral shape (Vries 2010). Foams are generally classified as wet foams (spherical foams) and dry foams (polyhedral foams) (Leonard and Lemlich 1965). Most stable foams do not contain spherical bubbles but regularly built cells of polyhedral bubbles with nearly uniform size distribution. Foams can be studied in terms of structural elements such as films, bubbles, junctions, and plateau borders. Thin film separates gas bubbles pressed together to form foam; the rupture of this film is one of the mechanisms for drainage and foam decay. The Plateau border is the liquid-filled interstitial channel formed when films converge along a line or curve. Only three films can meet at a Plateau border, and these three films meet at equal angles. Junctions are interconnected networks formed when several Plateau borders meet, and only four Plateau borders can meet at a junction (Weaire and Phelan 1996).

As the quality of foam increases, it reaches a point where it is called a dry foam i.e., if its quality is greater than 95%. The structure of the dry foam is polyhedral with curved bubble walls. High-quality dry foams have a polyhedral bubble structure. But at low qualities, this structure disappears

and the bubbles become spherical. Close to this limit, bubbles have a shape slightly different and deformed due to the high-density packing (Stefan et al. 2005).

2.2. Drainage Mechanisms

Drainage occurs when a trapped foam attempts to attain static equilibrium. Liquid films surrounding the gas bubbles drain into the plateau border due to the capillary forces that trigger curvature of plateau border walls and suck liquid from the liquid film surrounding the gas bubble and the liquid drains out of the foam due to gravitational force. A trapped foam in a vertical column is the best to analyze for drainage evaluation.

The decay and collapse of a bubble film occur as a result of uninhibited growth of thermal and mechanical disturbances on the film surface (Ruckenstein and Bhakta 1996). If the force which opposes the film thinning increases in response to the local thinning due to the disturbance, the decay process becomes self-controlled, and no film rupturing occurs. The major reason for film rupturing is however the reduction in differential pressure in the film as the thickness of the film decreases. The forces such as gravity, surface tension, and viscous drag have a major role in the drainage of the foams. Electrostatic double layer (EDL), hydration, and van der Waals forces determine the stability of thin foam films.

Haas and Johnson (1967) stated that most of the drainage occurs through the plateau borders (Figure 2.1). Two variations of foam drainage regions are often considered, the channel-dominated drainage regime where the major resistance occurs in the plateau border, and the node-dominated drainage regime, where the viscous resistance occurring in the nodes becomes the controlling mechanism.

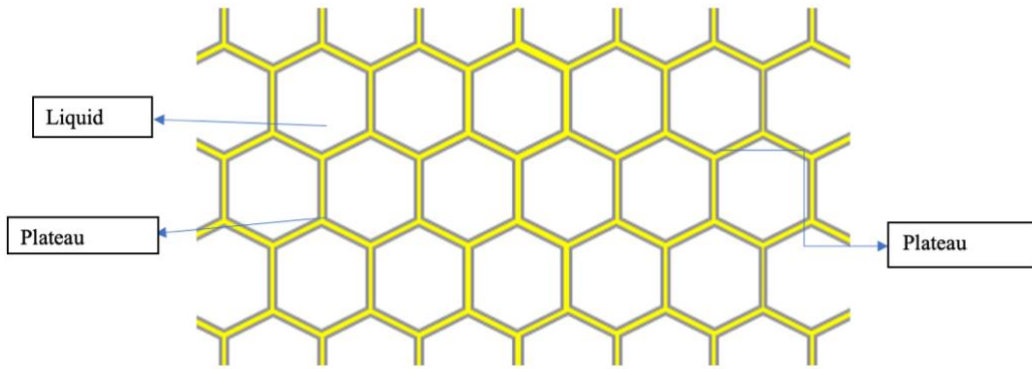


Figure 2.1. Hexagonal Foam Structure

2.3. Drainage Models

Several models for the analysis of the drainage of the foam have been developed over the years. The three modeling approaches consider the structure of the plateau border as uniform cylinders with immovable walls (Bhakta and Ruckenstein 1995b). The models also have deliberations over when the foam drainage ends, and the system achieves equilibrium. Other modeling studies (Ramani et al. 1993; Bhakta and Ruckenstein 1997) concluded that liquid would continue to drain until all the liquid in the system is drained before the system achieves its equilibrium and the drainage process ends. This argument is considered in this work. The draining of the fluid occurs during the time in which the experiment is conducted (Bhakta and Ruckenstein 1995b).

2.4. Effect of Pressure

The effect of pressure with foam drainage has been studied in literature (Rand and Kraynik 1983). An increase in pressure on the foam causes a change in the bubble size of the foam which influences the drainage time of the foam. The bubble size change due to the pressure change is due to the expansion of the gas in the foam as the pressure increases. Experiments were done with the different base fluid types; oil and water, with various surfactant types at low and high

pressure and it concluded that drainage time was not dependent on the chemistry between the gas-oil but on pressure. The bubble size decreases with an increase in pressure and the drainage time increases with decrease in bubble size.

2.5. Literature on Foam Contaminants

The drilling process introduces contaminants such as oil, salt, and rock cuttings into the drilling fluid. An accurate investigation of the drilling foam is required to understand the effect of the contamination on the properties of the fluid. The contaminants that are considered in this work are salt, oil, and clay. The type and concentration of the contaminants in the foam have varying effects on the behavior of the foam.

2.5.1. Salt

During the drilling process, salt can be encountered in numerous forms. Some of the forms include Sodium Chloride (NaCl), Potassium Chloride (KCl), Calcium Chloride (CaCl₂), Magnesium Chloride (MgCl₂). The salt present in the drilling fluid can be introduced in many forms which include additives that are introduced to improve some of the drilling foam properties or contaminants from the rock formation. Salt additives in drilling fluids can increase the density of the base fluid and reduce the freezing point. Salt-based foam can inhibit shales and reduce clay hydration and/or dispersion. The increase in salt concentration in the foam lowers the rate of salt absorption from salt beds while drilling through them. This helps to reduce wellbore enlargement and/or instability.

2.5.1.1. Effect of Surfactant and Salt Concentration on Foam Stability

Surfactant molecules converge to create aggregates of different forms and microstructures depending on the foam composition, temperature, and surfactant type. The critical micelle concentration (CMC) is defined as the lowest surfactant concentration for the development of the critical micelle with a spherical shape (Dong et al. 2008). The interfacial behavior of ionic surfactants at a fluid-fluid interface is a critical phenomenon in understanding colloidal occurrences which includes thin film stability, surface tension, micellization (Warszyński et al. 2002). The surfactant CMC is reduced because of growth in the binding of counterions to surfactant. The strength of the counterion bind increases with an increase in polarization and valency of counterions and decreases with an increase in hydrated radius. The surface tension of aqueous sodium dodecyl sulfate (SDDS) is lowered more efficiently for smaller, less hydrated counterions. The effect of ions of inorganic salt on the surfactant adsorption was studied by Bott and Wolff (1997); Oh and Shah (1993); Warszyński et al. (2002) on the surface tension of the liquid/gas interface.

Bubble coalescence is influenced by the ionic surfactant adsorption at the air-water interface (Giribabu et al. 2008). The adsorption of ionic surfactant is affected by the presence of inorganic salt. The results from these reviewed studies have reported that the valency of salt required to inhibit coalescence varies in the sequence: $\text{NaCl} > \text{MgCl}_2 > \text{AlCl}_3$. Ghosh (2004) measured air bubble coalescence by the bubble rest time which is the coalescence at the flat air-water interface. This work shows an increase in rest time with the concentration of the surfactant.

When a surfactant is present, certain salt ions cause an increase in the rest time of the air films. Adding NaCl immensely increased the film stability when a surfactant is present (Ghosh 2004). The surface tension of liquid was measured as the NaCl concentration was increased and the surface tension did not show any significant change as the Cetyltrimethylammonium Bromide; Hexadecyltrimethylammonium Bromide (CTAB) surfactant is completely saturated on the air-water interface and no additional adsorption was achievable.

Many attributes have been specified from research to increase foam stability in the presence of salt which are hydrophobic interaction (Craig et al. 1993), hydration effect (Isrealachvili 1997), double layer repulsion (Marčelja 2006). When NaCl presents, the stability increases due to a decrease in surface diffusivity because of the conglomeration of the tails of CTAB and a decrease in the repulsion between the positive head groups of CTAB. Foam bubble stability depends on the coalescence rate of the bubble. The absorption of two bubbles causes the generation of the thin liquid film. Further drainage at the interface occurs due to the continuous drainage of the film. The disjoining pressure effect is prominent when the electrostatic double layer and van der Waals forces become significant (Li and Slattery 1988)

Li and Slattery (1988) conducted experiments to determine the coalescence rate of bubbles varying the NaCl concentration. The surface tension of the aqueous solution was shown to decrease by about 60% in the first 0.1 sec. The addition of NaCl causes a decrease in the surface tension and the electrostatic forces. When NaCl is absent, the bubbles stay on the solution surface for many hours without breaking. The increase in the concentration of NaCl at a smaller concentration causes the rest time to decrease quickly, this is due to the reduction in repulsive electrostatic force.

With the increase in NaCl concentration, the electrostatic repulsive forces effect became negligible. This negligible effect causes a more prominent reduction in surface tension which increases the coalescence time. (Kumar and Ghosh 2006) work shows the effect of NaCl on the coalescence of air bubbles when ionic and cationic surfactants are present. The effect of NaCl on the surface tension was also studied. The NaCl addition significantly affects the surfactant adsorption at the air-water interface. A significant decrease in surface tension is observed in the presence of the surfactant. The surfactant used in the analysis were Sodium dodecyl sulfate (SDS), CTAB, Sodium Dodecylbenzene Sulfonate (SDBS). The surfactants were tested at various concentrations. The same results were observed for the surfactant solutions as NaCl concentration increases bubbles rest time.

In the presence of salt, a decrease in electrostatic double-layer repulsion between the interfaces lowers coalescence time (Li and Slattery 1988; Lu and Corvalan 2012). Coalescence resistance occurs as a result of the strong resistance caused by the solvation forces. Salt valency has variable effects on the surfactant solution stability. Films generated in the presence of Magnesium Chloride; a bivalent salt showed more stability and longer rest time than films generated from a monovalent salt like NaCl. The explanation for this observation is that the Mg^{2+} ions connect with the negatively charged headgroups of SDS at the surface of the film which causes an increase in elasticity and surface viscosity. This influence causes stagnancy of surface film and resistance to liquid drainage from the films (Angarska et al. 1997). The valency of salts also affects the adsorption of the surfactant to varying degrees due to their influence on the electrostatic charge screening (Behera et al. 2014; Giribabu et al. 2008).

Inorganic salts are naturally present or added in certain foam applications. Salt can alter the charge at the gas-liquid interface by affecting the adsorption of surfactant molecules at the interface (Behera et al. 2014; Giribabu et al. 2008). The salt type has a varying effect on the surfactant. The rate of coalescence differs based on the valency of the salt. Salt addition causes the growth of micellar conglomerates of some micellar long-chain cationic surfactants. Growth is immense and in one dimension and the micelles are huge and very elastic with a molar weight of 10^6 and they are called wormlike micelles. The wormlike micelles have viscoelastic behavior like a polymer solution and are characterized by elevated activity at the surface.

The presence of the salts significantly affects the formability and stability of the foam. The ions of different valence affect the adsorption of surfactants to different degrees due to their varied effect on the screening of electrostatic charge. The different valency of the ions has varying effects on the gas-liquid adsorption because of their effect on the electrostatic charge screening. The potential at the gas-liquid interface can be significantly reduced due to the binding of counterions. Foam stability is majorly dependent on the stability of the thin foam film. The addition of salt and increase in surfactant concentration can influence the diffusion of surfactant and foamability (Giribabu et al. 2008; Warszyński et al. 2002; Kumar and Ghosh 2006; Angarska et al. 1997; Kralchevsky et al. 1999).

2.5.1.2. The Effect of Salt on CMC and Foamability

Surfactant addition to aqueous foam reduces interfacial tension and enhances the stability of foam film and generates a stable foam structure (Liu et al. 2005). The surfactant concentrations affect the stability of the foam; as the surfactant concentration increases, the foam becomes more stable.

In the work by Liu et al. (2005), surfactant concentration was increased from 0.005 to 1 wt.% in 0.005 wt.% increments. Foam stability was insensitive to the increase in surfactant concentration when the concentration was above 0.01 wt.%.

The foam stability is sensitive to the surfactant concentration when salt is present. The stability is not sensitive to salinity at any concentration and any salt type (NaCl and CaCl₂) at a concentration higher than 0.025 wt.% (Liu et al. 2005). The stability however is affected by the salinity at low surfactant concentrations (less than 0.005 wt.%). The stability increases with salt concentration when the salt concentration is between 2 wt.% and 5%. Above 5 wt.%, the foam becomes stable and insensitive to further increase in salt concentration in the NaCl and CaCl₂ mixture (3:1). In the individual brine solutions of NaCl and CaCl₂, the stability curve exhibited a “W” shape as the salt concentration was increased using Chaser CD1045TM (CD) (Figures 2.2 to 2.4).

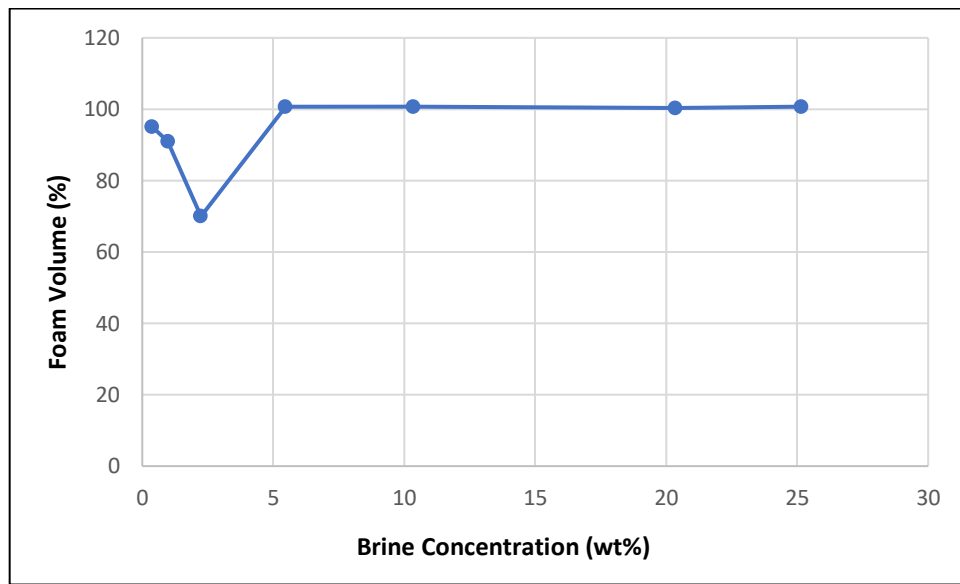


Figure 2.2. The effect of salinity on foam stability at CD conc 0.005 wt.% in brine solution of NaCl and CaCl₂ solution weight ratio 3:1 after 90 minutes (Liu et al. 2005)

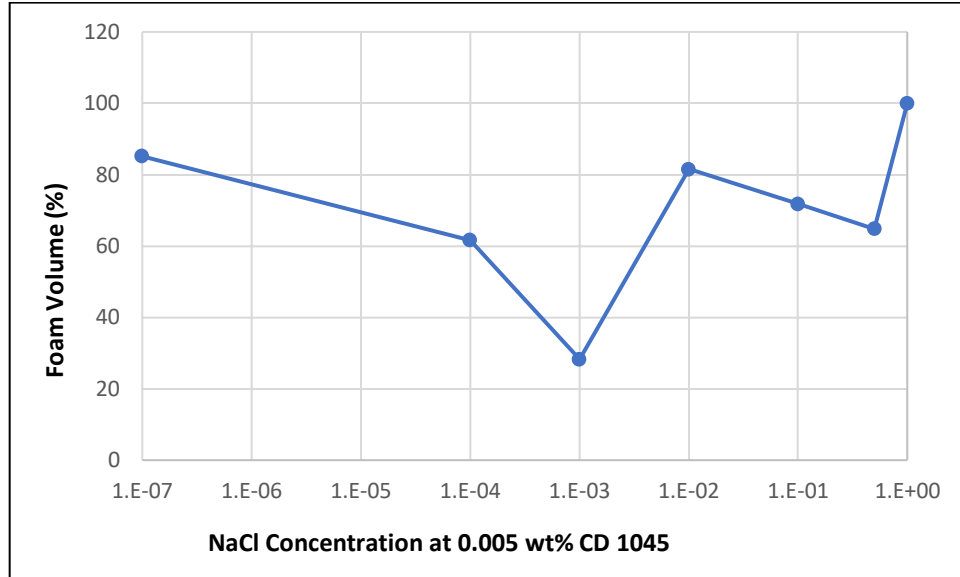


Figure 2.3. The effect of salinity on foam stability at CD conc 0.005 wt.% in NaCl solution after 90 minutes (Liu et al. 2005)

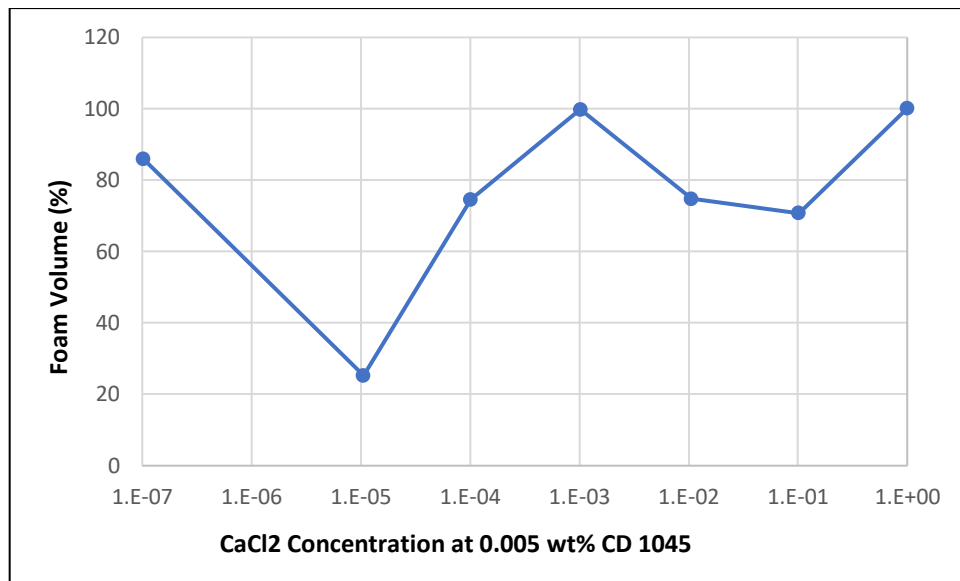


Figure 2.4. Effect of Salinity on Foam Stability at CD Conc 0.005 Wt.% in CaCl2 Solution after 90 Minutes (Liu et al. 2005)

The addition of salt affects the aqueous surfactant solution. The salt can modify the intramicellar and intermicellar interactions in the surfactant (Carale et al. 1994). Salt addition is also evident in

the phase behavior and the CMC. CMC is the concentration of a surfactant in a bulk phase. Beyond this concentration, the formation of micelles starts. The CMC is the smallest value of the surface tension and additional surfactant concentration increase does not cause a decrease in the value of the surface tension. Experimental studies show that salt addition to nonionic and ionic surfactants reduces the CMC of the surfactant (Varade and Ghosh 2017). The interface at the surface of the surfactant solution adsorbs the surfactant and this causes a decrease in surface tension of the liquid until the equilibrium value in the presence of surfactants is reached. The dynamic surface tension (DST) however depends on the type of the surfactant and the nature of fluid and presence of other additives (Qazi et al. 2020). Salts are added in many use cases and can enhance surfactant behavior. Salt addition can majorly affect surfactant behavior by changing the critical micellar concentration (CMC). According to studies by (Fang et al. 1997; Beyer et al. 2006) in the presence of salt, the CMC decreases, and equilibrium surface tension also decreases as the salt concentration increases.

2.5.1.3. The Effect of Salt on Fluid Rheology

The rheology of base fluid used for the generation of foam impacts its stability. The half-life of foam varies as the rheology of the base fluid is changed. Ibizugbe (2012) carried out an investigation and found that foam prepared with low viscosity base fluid was less stable as the liquid tended to form a larger surface area to accommodate the gaseous phase. Other studies (Chen et al. 2005; Ahmed et al. 2003; Sherif et al. 2016) showed that the foam apparent viscosity increases with foam quality and base fluid viscosity. The salt addition to the base fluid influences the viscosity and density of the base fluid which in turn affects the stability of foam. Ruckenstein

and Bhakta (1996) showed that salt and surfactant concentration strongly affects the surface viscosity.

2.5.1.4. Effect of Salt on Surface Tension

The adsorption at the gas-liquid interface of a zwitterionic surfactant depends on the electrostatic interactions among the charged molecules and the hydrophobic interactions (Zajac et al. 1996). Varade and Ghosh (2017) performed surface tension measurements for solutions with salt and without salt. According to their findings, the addition of NaCl decreases the surface tension of the surfactant solution. This shows that the air-water interface absorbs even more surfactant molecules. Salt has been shown to increase the adsorption of surfactants at the air-water interface. This effect is due to the reduction of the electrostatic double layer (EDL) repulsion between the charged head groups of the molecules of the surfactant (Iyota and Krastev 2009). The required salt quantity for surface tension reduction depends on the valency of the salt. The quantity of salt required rises in this trend $\text{NaCl} > \text{CaCl}_2 > \text{AlCl}_3$ (Varade and Ghosh 2017). The higher valency salt has a higher effect on the force of double-layer repulsive electrostatic which causes higher adsorption of surfactant at the air-water interface. The effect is shown in the research by Varade and Ghosh (2017) as an incessant reduction in surface tension of the solution and a lower CMC as the salt concentration increases.

2.5.2. Oil

There have been varying reports on the effect of oil on the stability of oil in the presence of oil. Denkov et al. (2002); Kuhlman (1990) reported that oil has a detrimental effect on the stability of the foam, but Li et al. (2011) reported that the oil can stabilize the foam.

The effectiveness of foam to overcome the gas-liquid barrier and break the foam structure was studied by Novosad and Mannhardt (1989). One of the objectives of this study has been to determine the effect of oil on the stability of aqueous foam. This analysis considers different experiments conducted on foam with varying oil concentration and type and trapping mechanisms to understand if the type and concentration of oil affect the film drainage. The effect of oil on the foam can be due to four effects (Novosad and Mannhardt 1989):

- a) Emulsification of the oil and aqueous phases
- b) Solubilization of surfactant in the oil
- c) The spreading of the oil at the gas-liquid interface
- d) Effect of polar, surface-active components in the oil.

The destabilization of foam due to emulsification of oil and aqueous phases and solubilization of surfactant in the oil is due to the consumption of the surfactant as a result of processes that compete for the surfactant concentrated at the gas-liquid interface. Crude oil might contain surface-active agents that displace some of the surfactants at the gas-liquid interface which can either result in stabilization or destabilization of the foam.

According to Novosad and Mannhardt (1989), the possibility of solubilization of surfactant in the oil and partitioning of the surfactant into the oil phase is based primarily on the structure of the surfactant. The sensitivity of the stability of foam to crude oil contamination is not strongly affected by the oil type but is more strongly influenced by the type of surfactant. In the presence of oil in surfactant solution, oil-water tend towards forming a stable emulsion. The tendency of the oil/water solution to form a stable emulsion is related to the interfacial tension of the system. The

lower the interfacial tension, the higher the tendency of forming stable foams. The formation of stable emulsions consumes surfactant and destabilizes the foam.

Soleymani et al. (2013) researched the stability of drilling foam using three crude oil types of different API gravities (27.3°, 35.5°, and 43.5°). The results from the research show that the stability of the drilling foam increases with the addition of crude oil. It was shown the major factor that influences how much the crude oil stabilizes the drilling foam is the API gravity of the crude oil. The crude oil sample with a lower API gravity has a higher impact on the stabilization of the foam and vice versa. According to the work, this trend was because of the viscosity change of the crude oil samples.

2.5.2.1. Mechanism of Foam Destabilization

There are several mechanisms for the destabilization of foam by oil (Andrianov et al. 2012; Arnaudov et al. 2001; Denkov and Marinova 2000). Princen and Goddard (1972) concentrated and investigated the case where the gas-liquid interface has the lens of oil present. According to this work, the oil lens extracts a minor component from the surface layer which reduces the stabilizing effect of surfactant. The experiment was carried out in the absence of paraffin oil and the presence of paraffin oil lens of varying thickness floating on the fluid surface. Nikolov et al. (1986) investigated the process that occurs during foam thinning in the presence of oil. The interaction mechanism between the droplets of oil, the thinning foam film, and plateau borders and the effect of the surface and interfacial tension changes on the stability of the foam. Three distinct foam films occur in the three-phase foam thinning process. These are:

- I. Foam Film (water film between the air bubbles)

- II. Emulsion film (water trapped between oil films).
- III. Pseudoemulsion films (water trapped between air and oil droplets).

The surface energy of foam with emulsified oil can be stabilized by forces that increase the surface energy of the foam such as electrostatic and van der Waals. Surfactants added to the foam also increase the surface action of the foam and enhance its stability. This surface activity would impede the entry of the oil droplets and therefore oppose the destruction of the foam. The addition of oil to already stable foam can enhance foam stability due to lowering of the surface tension of the solution (Basheva et al. 2001; Arnaudov et al. 2001) and by reduced water draining from the plateau border as a result of oil film obstructing the water flow (Koczo et al. 1992). Koczo et al. (1992) investigated foam stability in the presence of oil in two different forms:

- a) Soluble in the micelles (microemulsions)
- b) As individual drops (macro emulsions).

Both forms affect foam stability in different ways. The former results in the formation of micellar structure within the films which causes the micellar solution foam film to exhibit stepwise thinning (stratification). Also, the stability of pseudo-emulsions was investigated in the presence of emulsified oil and the effect of factors such as oil type, surfactant type, oil volume, oil volume fraction on foam stability. The tests were performed by measuring foam degradation in form of drainage rate, bubble disproportionation, and film rupture, and assessing the changes occurring in foam properties.

Rojas et al. (2001) studied the effect of the type of oil on the half-life of the foam using different crude oils with varying API gravity. The results from these experiments are shown in Figure 2.5, the foam stability assessment is based on the API gravity of the crude oil. The highly viscous crude

oil stabilizes the foam better than a less viscous one. The higher the API gravity of the crude oil, the lower the half-life of the foam and therefore the foam stability. The concentration of the crude oil also affects foam stability. However, this effect is not relevant until after 10% oil concentration. At or below this point, all the crude oil samples do not have any effect on the foam stability.

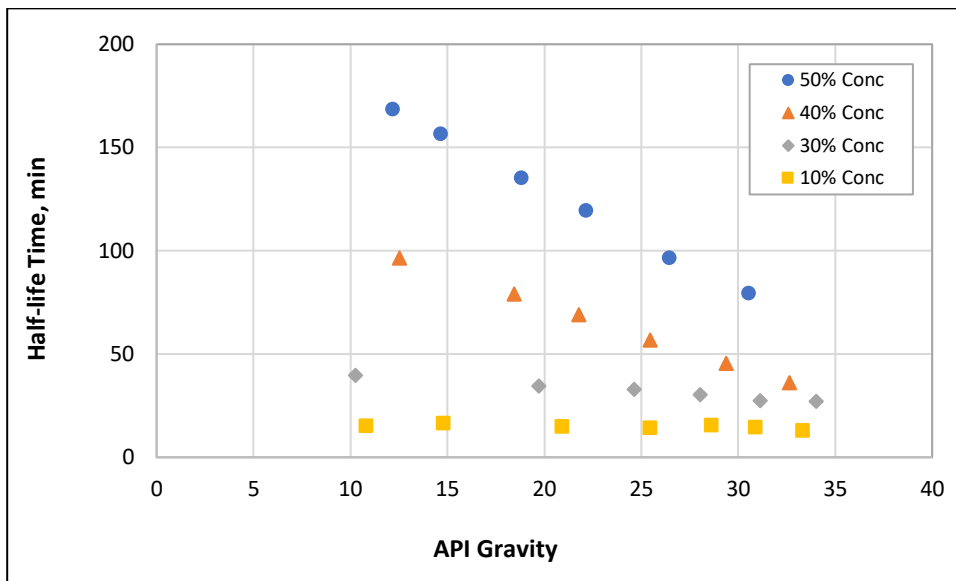


Figure 2.5. Effect of crude oil API gravity on foam stability (Rojas et al. 2001)

2.5.3. Clay

Some studies (Pickering 1907; Ramsden 1903) have been performed on the stabilization of foam by the addition of solid particles. The influence of solid particles on foam stability is dependent on the type of surfactant used, the size of the solid particles, and their concentrations (Pugh 1996). The stabilization effect of solids is dependent on how hydrophobic or hydrophilic the solids are. It has been established that very hydrophobic particles are very difficult to foam (Zhang et al. 2008). These particles tend to act as an anti-foaming agent at the gas-liquid interface due to the bridging-dewetting mechanism (Binks 2002).

The stabilization of foam due to solids occurs in two ways: the adsorption of colloidal particles at the gas-liquid interface (Gonzenbach et al. 2006; Binks 2002; Alargova et al. 2004) and the stratification of non-adsorbing particles intervening in a thin film that separates the dispersed phases. The former is key for the formation of stable foam and the latter improves the foam stability against drainage. The stability of foam is dependent upon strong attachment of the particles at the bubble surface and the network of particles at the interface. The hydrophobicity of colloidal particles is dependent on adsorption of colloidal particles at the gas-liquid interface (Gonzenbach et al. 2006; Binks 2002; Alargova et al. 2004).

According to Yang et al. (2006), the solid particles rupture the film by forming a bridge on the film. Various factors affect the stability of an emulsion stabilized by particles which include the wettability of the particle, concentration of the particle, ionic strength, and pH. The dispersion of solids in the aqueous or oleic phases tends to occur in strongly hydrophilic or hydrophobic particles. These particles form large droplets that are prone to coalescence.

Yu et al. (2020) studied the stability of oil-in-water emulsions in the presence of Nanomontmorillonite particles with changing salinity and pH. The clay particles are found to be adsorbed at the oil-water interface. The clay particle adsorption at the interface reduces the interfacial tension by 16.8% at 0.25 wt.% clay. This agrees that the adsorption at the interface is thermodynamically favored to decrease the energy at the oil/water interface (Levine et al. 1989). The adsorption of the clay particles increases the size of the oil-water interface which means smaller droplet size and more droplets. The stability of the foam is dependent on the bubble size distribution and shape (Engelsen et al. 2002). The smaller the bubble size, the higher the drainage

time of the foam. This also agrees with the analysis by Zhang et al. (2008), the most stable foam had the smallest particle size. The Na-montmorillonite was concluded to be an effective oil-water emulsion stabilizer.

According to Sani and Mohanty (2009), the addition of clay to the surfactant solution increases the surface tension slightly at 1% clay concentration. The low concentration of the clay was not sufficient to affect the density of the fluids. The clay structures create a linked structure that can slow down the rate of liquid drainage from the foam. The clay had no noticeable influence on the stability of foam and its half-life. Some nanoparticles strongly adsorb on the bubble surface when added to a foam system. The nanoparticles form a three-dimensional network between the surfaces of the droplets and the continuous phase. The three-dimensional network reduces the rate of bubble coalescence and subsequently stabilizes the foam.

According to Chen et al. (2019), clay particles are very hydrophilic and bad foaming agents. Chen et al. (2019) attempted to generate aqueous foams using only clay dispersions. The suspension however did not result in the generation of any foam. A suspension prepared with a mixture of 0.4 wt.% of surfactant and an increasing concentration of clay particles from 0 to 1.6 wt.% showed that the half-life of the foam increases significantly with the concentration of clay particles (Figure 2.6).

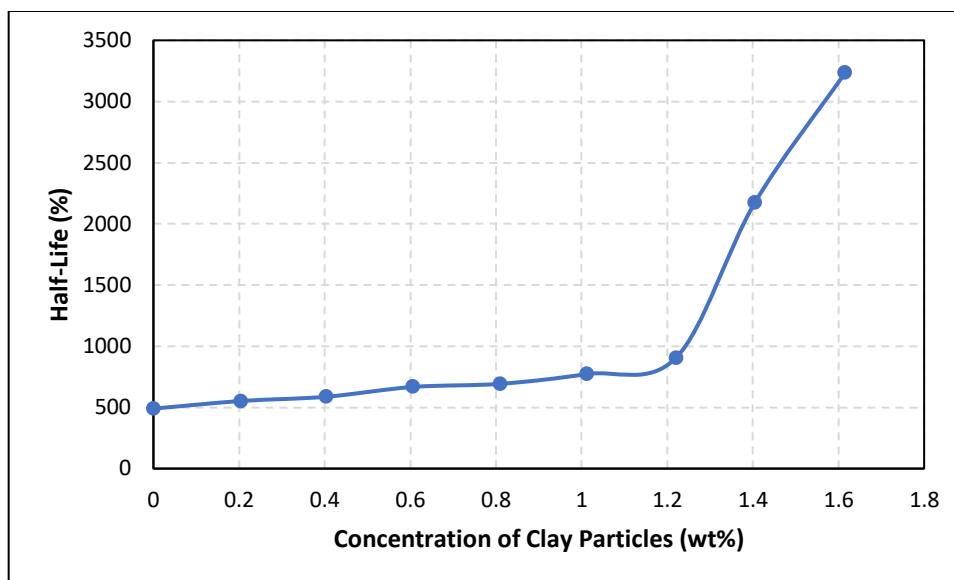


Figure 2.6. Half-life of foams stabilized by the mixtures of 0.4 wt.% of AOS surfactant and clay particles concentration (Chen et al. 2019)

Zhang et al. (2008) investigated the effect of Laponite clay on the stability of foam in the presence of CTAB surfactant. In the presence of only clay particles, the solution did not foam at all. The surfactant solution was characterized by increasing the stability of the foam as the surfactant concentration was increased until the CMC was reached. And a further increase in surfactant concentration did not cause an increase in the foam stability. The solution with the Laponite/CTAB was studied changing the Laponite concentration from 0 wt.% to 2.0 wt.% and changing of the surfactant concentration. The foam stability increased as the clay and surfactant concentration increased until a point was reached for the clay concentration where further increase in surfactant concentration reduces the foam stability (Figure 2.7). The analysis from other studies (Zhang et al. 2008; Chen et al. 2019) agrees with these findings. In the presence of clay particles and surfactant, the CTAB surfactant is adsorbed on the Laponite particles. As the concentration of the surfactant increases, the rate of flocculation and hydrophobicity of the particles increases until it reaches a maximum level at which the stability also reaches the maximum level. Further increase

in the surfactant concentration decreased the hydrophobicity of the particles due to the formation of a second surfactant layer that gradually reverses the hemimicelles formation (Zhang et al. 2008). The flocculated particles started to scatter, and the stability of foam began to diminish. The adsorption property of CTAB on Laponite particles determined the stability of the foam.

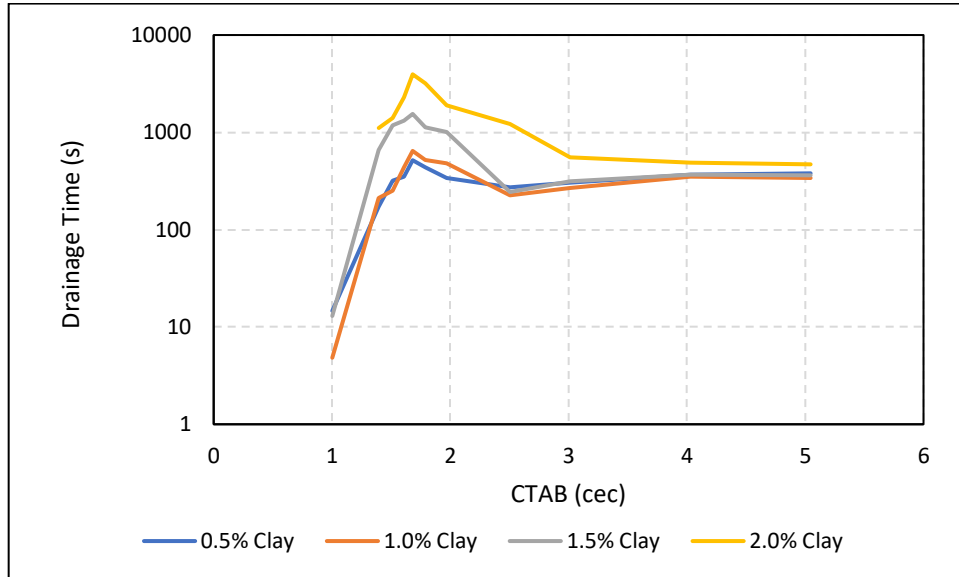


Figure 2.7. Drainage time of foams stabilized with Laponites/CTAB system as a function of CTAB concentration at different particle concentrations (Zhang et al. 2008).

CHAPTER THREE

MODELLING

This section presents the mathematical model formulation, assumptions, and limitations. The foam drainage process can be modeled using two generalized modeling approaches: channel-dominated method and node-dominated approach.

3.1. Channel Dominated Drainage Model

The channel-dominated model to describe the foam drainage process considered gravity and viscous resistance and the main phenomena involved in the drainage process of foam. The model assumes that the flow in the channels is Poiseuille type flow with triangular cross-sections (Leonard and Lemlich 1965).

3.1.1. Model Assumptions

- All the liquid in the foam is assumed to be from the channel and no contributions from the nodes or films.
- The viscosity is assumed to be constant and equal to the viscosity of the base liquid.
- The effect of surface tension is ignored.
- The changes caused by the deformation of channels are ignored.

For the channel-dominated model, the foam drainage equation which describes liquid content distribution can be expressed as:

$$\mu \frac{de}{dt} + K_1 \rho g L^2 \frac{\partial \varepsilon^2}{\partial z} - \frac{\sigma \delta \varepsilon^{0.5} K_1 L}{\varepsilon} \frac{\partial^2 \varepsilon^{1.5}}{\partial z^2} = 0 \quad (3.1)$$

$$k(\varepsilon) = K_1 L^2 \varepsilon \quad (3.2)$$

3.2. Node Dominated Drainage Model

The node-dominated model postulates where channels intersect a large liquid mass form at the node. In comparison to the contribution of node-dominated flow on the drainage volume, the contribution of channel-dominated flow is very small. The solution to the node-dominated flow is however more complex and requires the Navier-Stokes equations. This equation establishes the relationship between liquid flow velocity and liquid volume fraction. The complexity of the equations requires some simplification such as negligible contribution from the channel-dominated flow to simplify the model. However, recent studies (Saint-Jalmes and Langevin 2002; Koehler et al. 2000) have been performed to improve these models by considering the effects of channel flow, the effect of viscosity, and foam permeability.

$$\mu \frac{d\varepsilon}{dt} + K_2 \rho g L^2 \frac{\partial \varepsilon^{1.5}}{\partial z} - \frac{\sigma \delta_\varepsilon^{0.5} K_2 L}{\varepsilon} \frac{\partial^2 \varepsilon}{\partial z^2} = 0 \quad (3.3)$$

$$k(\varepsilon) = K_2 L^2 \varepsilon^{0.5} \quad (3.4)$$

In this study, the channel-dominated model developed by Koehler et al. (2000) has been used to generate predictions that can be compared with experimental measurements obtained from free drainage experiments conducted in a vertical test section.

3.2.1. Model Assumptions

The following are the assumptions that are made to find the numerical solutions of the models (Govindu 2019).

1. All foam bubbles are assumed to be monodispersed.

2. The bubbles are assumed to retain a spherical shape in the quality interval considered (40% to 60%). This assumption makes it reasonable to set the length of the channel as less than the channel length for dry foam which is $\frac{d_b}{2.8}$.
3. The surface tension is assumed to be constant due to the uniform surfactant concentration throughout the vertical test section.
4. The direction of liquid flow was assumed to be along the vertical axis.
5. The effects of container geometry and wall are ignored due to the assumption that the foam is unbounded.
6. In the foam stability model, the assumption made for the value of δ_ϵ is 0.1711. Koehler et al. (2000) populated this value using software evaluation used for determining surface tension-shaped surfaces (Surface Evolver).

3.2.2. Computational Grid Simulation

Govindu (2019) simulated foam quality profile along the vertical test section with time using the channel-dominated model for the initial qualities of 40%, 50% and 60%. The model simulates the physical measurements obtained from a vertical test section. The height in the simulation is the total height of the test section (1.08 m). The prediction of the model is the quality profile of the foam from the top of the column to the bottom of the column. The modeling is performed considering different sections that simulate the 9 segments that the test section is divided into. The column height is divided into 36 competition grids (i_1 to i_{36}). Two imaginary grids are added at the top of the simulated column and at the bottom for the purpose of modeling the column numerically (Figure 3.1). The two imaginary columns were employed to define the boundary conditions: at time $t = 0$; $\epsilon = 1 - \varphi$ and at $t = N * \Delta t$; $z = H$.

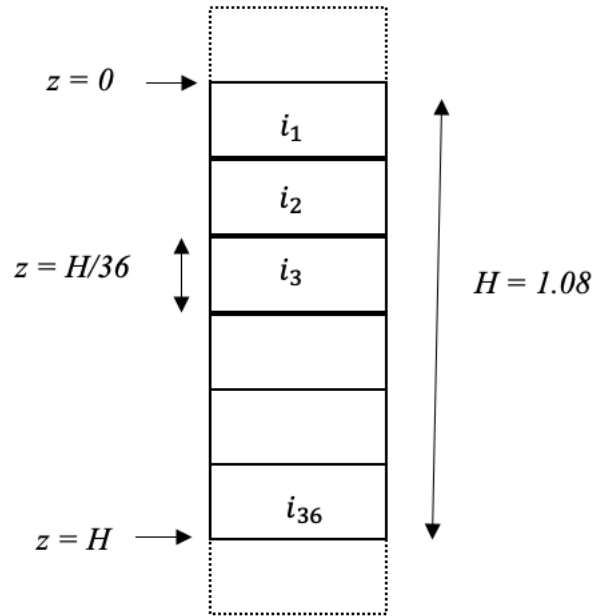


Figure 3.1. Simulated foam column with 36 grids (Govindu 2019)

The properties of the fluid in the simulation are the viscosity of the base fluid at standard temperature and pressure, surface tension of the fluid and density. Permeability constraints K_1 used was 0.05 (after multiple iterations). The results of these simulations are compared with the measured foam quality obtained from experiments (Chapter Five).

CHAPTER FOUR

EXPERIMENTAL STUDY

The experiment involves measuring the rheological properties and drainage behavior of the foam. The effect of various contaminants was studied. The contaminants considered include salt, clay, and oil. Foam quality and the concentration of the contaminants were varied. The surface tension of the base fluid was also measured with increasing surfactant concentration and the CMC was selected. The repeatability of the experiments was investigated and all tests in this work were repeated to ensure the consistency of the experimental outcomes.

4.1. Experimental Setup

The equipment used to perform the experimental investigation is shown in Figure 4.1. The test setup includes liquid tank, nitrogen cylinder, Foam Generation Section (FGS): differential pressure transmitter (P2), static mixers and needle valve, injection pump (Pump 1) and circulation pump (Pump 2), Coriolis flow meter to measure mass flow rate and fluid density, pipe viscometer (6.22 mm) to obtain fluid rheology measurements, vertical test section (stability cell) having ten pressure differential pressure transducers, pressure and temperature sensors, pressure regulators, and relief valves.

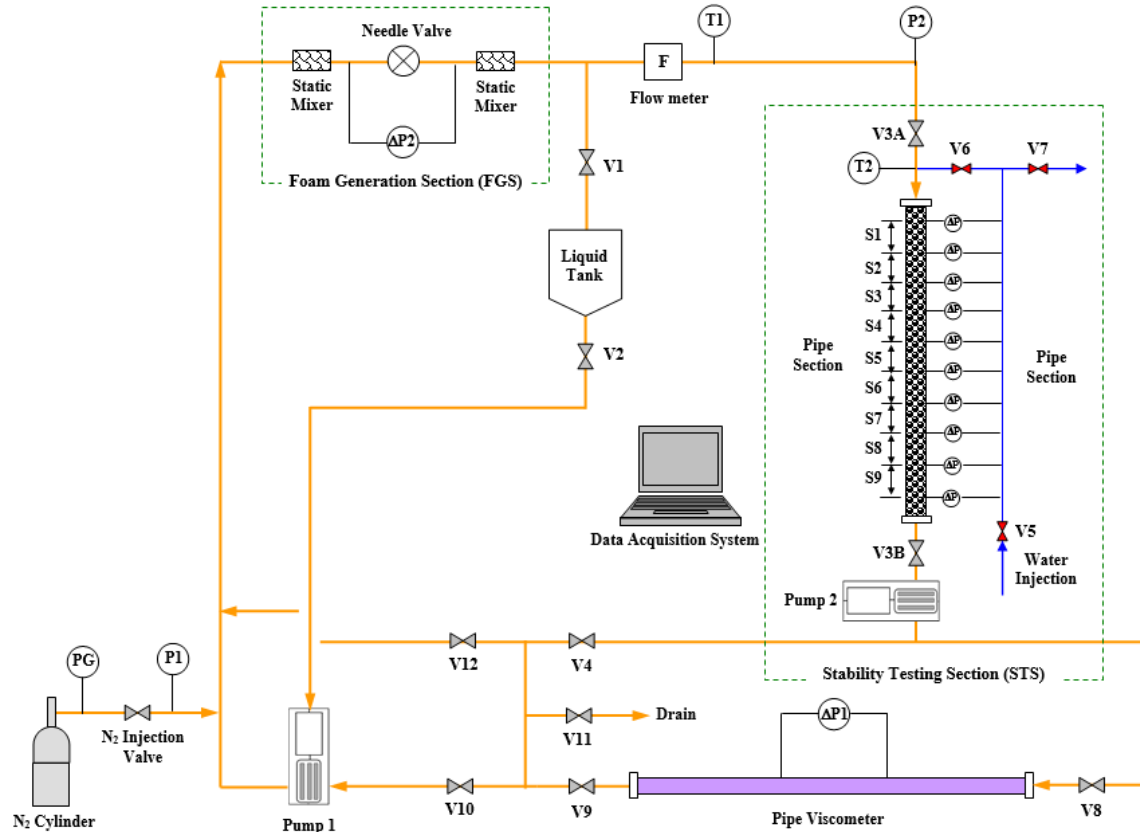


Figure 4.1. Experimental Setup

4.2. Test Procedure

This section includes the procedure used to prepare the base fluid and perform the foam stability test.

4.2.1. Base Fluid Preparation

The surfactant solution was prepared by dissolving the 40 ml of surfactant in the 2 L of tap water and mixing the solution with an agitator. All the solutions were mixed with surfactant at 2% (v/v) which according to preliminary studies (Govindu 2019; Akhtar et al. 2018) is higher than the CMC of the surfactant. Clay was added to the surfactant solution during base fluid preparation while

mixing the solution to disperse clay particles. The rheology of the base fluid was measured using the standard model Fann 35 and changing the speed from 3 to 600 RPM.

4.2.2. Rheology and Stability

The procedure for measuring the rheology and stability of foam involves eight steps. These steps are discussed in this section.

Step 1. Flow Loop Filling: The liquid tank was filled with the base fluid to 1000 ml volume.

The injection valve V_2 is opened for fluid to flow from the tank. During fluid flow from the tank, the fluid was in constant agitation to ensure the homogeneity of the fluid. The return valve V_1 was in a fully open position to allow the fluid to flow into the set-up. To fill up the vertical test sections, the other valves (V_{3A} , V_{3B} , V_4 , and V_{12}) were also in fully open positions.

Step 2. Fluid Circulation: When the set-up was filled up the base fluid, the injection valve V_2 was shut. The fluid was circulated through the flow loop in the vertical test section, pipe viscometer, and FGS. The needle valve across the FGS was in a fully open position.

Step 3. Pressure Balance: The pressure transmitters in the vertical test section were filled with water on the low side by opening valves V_5 and V_7 and then closing the valves afterward. To avoid the u-tube effect in the capillary tube, pressure equalization was obtained by filling the high side of the pressure transmitters with the base fluid in the system. The capillary tube pressure equalization valve (V_6) was opened to equalize the pressure.

Step 4. Nitrogen Injection: The desired pressure for the experiment was up to 1500 psi. Nitrogen gas was injected in increments while the base liquid was circulating at the

maximum flow rate of 2 L/min. The pressure was monitored until the pressure was obtained.

Step 5. Foam Generation: For the generation of foam, the pressure differential required was 0.15 MPa. The needle valve across the FGS was throttled until this differential pressure was obtained.

Step 6. Foam Quality Adjustment: The quality of the foam was adjusted by draining some of the fluid in the system by opening the drain valve (V11). The desired quality of the foam was maintained by draining the fluid and injecting nitrogen while monitoring the foam quality. The foam quality was measured by the hydrostatic pressure profile of the foam in the stability cell. This process continues until the final foam quality was reached.

Step 7. Foam Rheology Test: The rheology of the foam was determined by flowing the foam through the pipe viscometer at varying flowrate. The pressure differential was measured at these flow rates. The foam flow rate was increased to the maximum in between rheology measurements to regenerate the foam. The Figure 4.2 shows the varying flowrate and the change of differential pressure with the flowrate.

Step 8. Measuring Drainage: The measurement of the foam drainage was in the vertical test section (stability cell). The foam circulated at maximum pump rate for 10 minutes and the inlet and outlet valves of the vertical test section (V3A and V3B) were shut to trap the foam in the column. For two hours, the pressure variations of the foam column were recorded using ten differential pressure sensors.

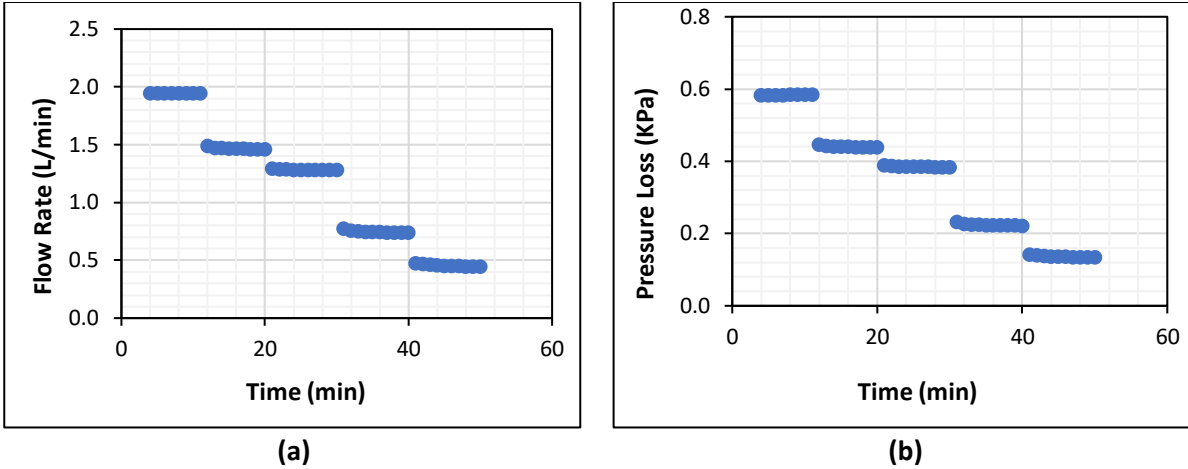


Figure 4.2. (a) Flowrate vs. time (b) Differential pressure variations with time

4.3. Experimental Scope and Test Materials

The experimental scope for the salt, clay and oil would be discussed in this section. Each of these experiments were conducted at 40%, 50% and 60% quality. Each experiment involves foam rheology and drainage measurements.

4.3.1. Salt

Two technical grade salts that are used in oil field applications (NaCl and CaCl_2) were considered in this investigation. During the test, salt concentration was varied from 5 to 18% wt. (Table 4.1). The salt concentration of 7% for CaCl_2 was not included in the study as at this concentration there was no noticeable change observed in the drainage and rheology of foam.

Table 4.1. Experiment Matrix – Salt

Quality	NaCl	CaCl ₂
40%,50%,60%	5%	5%
40%,50%,60%	7%	-
40%,50%,60%	9%	9%
40%,50%,60%	14%	14%
40%,50%,60%	18%	18%

4.4.2. Clay

The effects of clay type were investigated using drainage experiments. The concentration of the clay was varied to observe the effect on the stability of aqueous foams (Table 4.2). Bentonite and Kaolinite were studied in varying concentration from (2.5% to 5%) on the stability of the foam. The rheology of the base fluid in the presence of clay was measured to determine the effect of clay on the rheology. The stability measurement was conducted by considering the half-life of the foam and drainage volume.

Table 4.2. Experiment Matrix – Clay

Quality	Bentonite	Kaolinite
40%,50%,60%	2.5%	2.5%
40%,50%,60%	5%	5%

4.4.2.1. Materials

The bentonite and kaolinite clays used were grey and cream-colored powders, respectively. The mineralogy of the clays is shown in Table 4.3. For these tests, the clay particles were sieved to a maximum size of 75 micrometers. Clay minerals can exist in different forms. The different minerals differ due to the arrangement, substitution, and composition (Anderson et al. 2010). Based on the structure of the clay, it can be classified as halloysite, smectite, illite, chlorite, vermiculite, kaolinite, attapulgite-palygorskite-sepiolite and mixed-layer minerals (Grim 1968). The most important swelling clay is the 2:1 smectite clays which has huge swelling abilities. Smectite has the tendency to swell macroscopically and are frequently encountered in the drilling process. The FTIR for the Bentonite and Kaolinite shown in Table 4.3 shows that the bentonite has a high smectite component compared to Kaolinite and it is expected to have a high swelling ability.

Table 4.3. FTIR Analysis for Bentonite and Kaolinite

Clay Minerals	Kaolinite (%)	Bentonite (%)
Quartz	0	1
Calcite	0	8
Dolomite	0	8
Illite	21	0
Smectite	10	37
Kaolinite	46	2
Chlorite	0	0
Pyrite	0	2
Orthoclase Feldspar	11	11
Ogliooclase Feldspar	9	2
Mixed Clays	0	27
Albite	0	0
Anhydrite	1	2
Siderite	0	0
Apatite	1	0
Aragonite	1	0

4.4.3. Oil

The effects of oil type on the stability of foam were investigated using drainage experiments (Table 4.4). The concentration of mineral oil was varied from 5% to 20% to observe its influence on the stability of aqueous foams. Two crude oils with different densities and viscosities (Table 4.5) were considered in this analysis to examine their effect on the stability of aqueous foam.

Table 4.4. Experimental matrix for oil contamination study

Quality	Mineral Oil Quantity	Heavy Crude Quantity	Light Crude Quantity
40%,50%,60%	5%	-	-
40%,50%,60%	10%	10%	10%
40%,50%,60%	20%	-	-

Table 4.5. Properties of crude oils used in the experiment

Quality	Mineral Oil	Heavy Crude	Light Crude
Viscosity (cP)	38.4	62.2	12.0
Density (g/cm ³)	0.82	0.93	0.85
API gravity	35	21.0	34.7

4.4. Data Analysis

Figure 4.3 shows the initial hydrostatic pressure profile in aqueous foam obtained from the differential pressure transmitters (with accuracy of $\pm 5\%$ of the measuring span) when the test section was shut-in. At the beginning of the test, the column was filled with uniform foam, which is shown in the figure as a linear pressure profile. As the test time proceeds, the pressure distribution changes from linear to non-linear as the foam separates into gas and liquid and drainage occurs. The difference in pressure in the two successive pressure measurements (ΔP_m) is used to determine the foam density profile in the vertical section. The foam quality is mathematically related to the densities of foam, gas phase, and liquid phases. This means that the density of all the fluid involved impacts the quality of the foam in the test section.

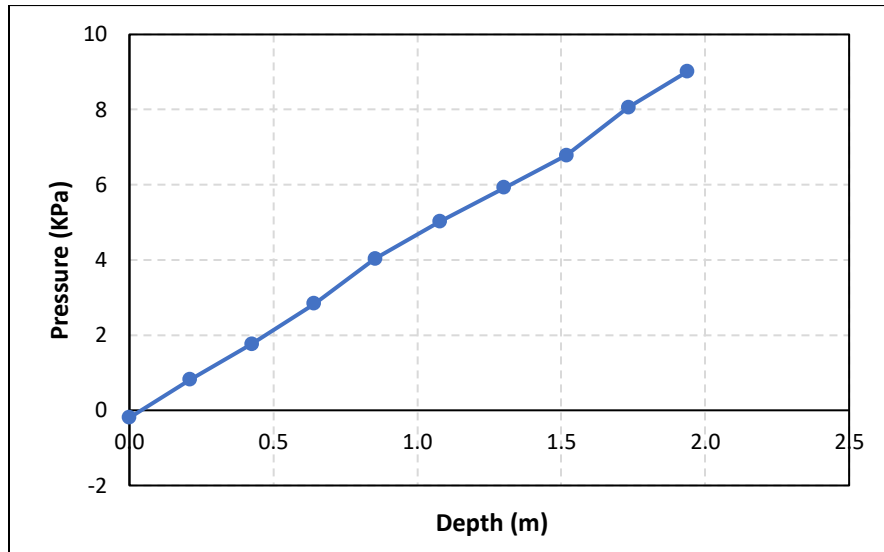


Figure 4.3. Pressure distribution in the vertical test section

Figure 4.4a shows the normalized foam density (the ratio of the density of foam at a given time to its initial density when the drainage measurement was started) for the nine segments of the vertical test section. The figure displays the density of the foam in each segment as a function of time. The

increase in density trend seen in the three curves indicated the bottom segments filling up with liquid. During the stability test, the top segments lose liquid, and this was detected by the pressures sensors as a reduction in pressure gradient. These curves show that the foam density in the bottom segments increased with time while the top segments demonstrated a reduction in fluid density. Later in the experiment, curve flattening was observed which implies that the segment was completely filled with liquid.

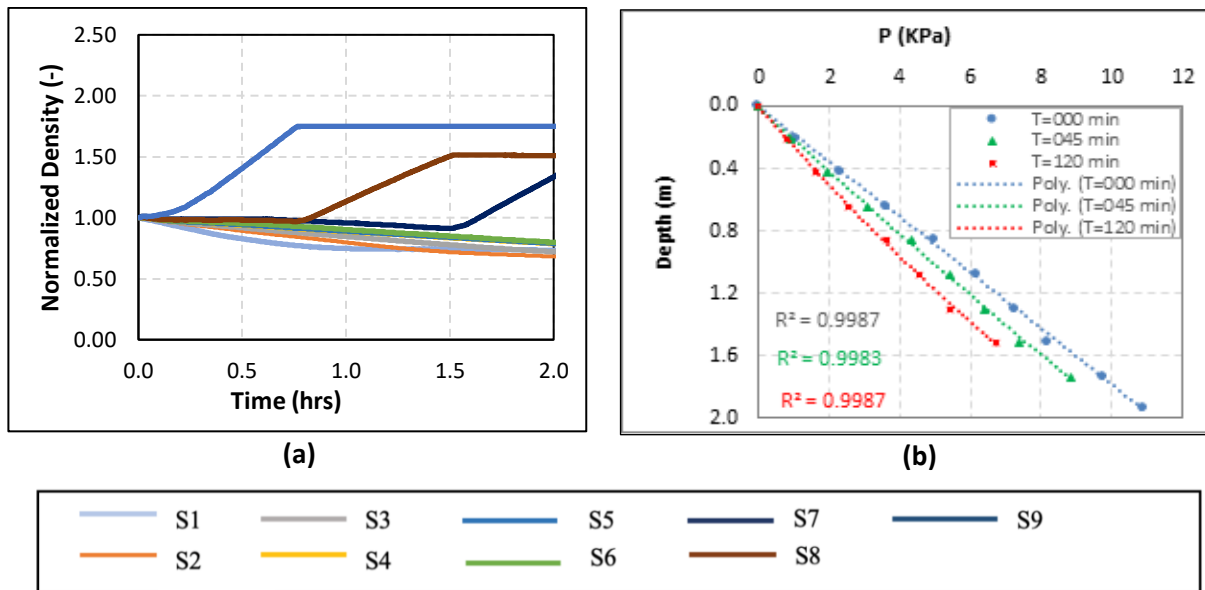


Figure 4.4. (a) Normalized density plot for the column sections (b) Pressure distribution at different times

Figure 4.4b displays the pressure profile in the foam column at different times. Initially, the pressure profile was linear. However, as time progressed, it became nonlinear. Hence, to analyze the hydrostatic pressure measurements, a curve fitting is performed using a second-order polynomial function. The polynomial equation is only valid when there is a smooth relationship between pressure and depth. Hence, it is not applicable for the filled-up segments because these segments show a linear pressure profile while the other part of the foam column displays a

nonlinear pressure distribution. Therefore, the measurements from liquid-filled segments were excluded from the data analysis. Based on this analysis, the average quality of foam in each segment is calculated as:

$$\Gamma = \frac{1-\text{slope}}{1-\left[\frac{MP}{RT}\right]} \quad (4.1)$$

$$\text{slope} = \rho_f g \quad (4.2)$$

M is the molar mass, P is the pressure (Psia), R is the gas constant, ρ_f is the foam density, g is the gas gravity and T is the temperature.

CHAPTER FIVE

RESULTS AND DISCUSSIONS

To understand the behavior of aqueous foam with varying pressure and in the presence of contaminants, this section discusses the behavior in the presence of salt (NaCl and CaCl₂), Oil (Mineral and Crude Oil), Clay (Bentonite and Kaolinite), and in relation with uncontaminated form. The contaminants are analyzed with varying concentrations and foam quality. The experiments were carried out at a fixed surfactant concentration of 2% vol which is above the surfactant CMC.

5.1. Aqueous Foam without Contaminants

5.1.1. Foam Rheology

The wall shear stress and nominal Newtonian shear rate ($8U/D$) are calculated from the pressure loss and flow rate measurements obtained from the 3.22 mm diameter pipe viscometer. The fluid behavior index, which describes the fluid's shear-thinning behavior, is represented by the slope of the logarithmic plots. The measured wall shear stress is compared (Figure 5.1) with the prediction of the model developed by Akhtar et al. (2018). The maximum discrepancy is 16%. The correlation was based on the experimental data. The method of foam generation used is the same foam generation technique utilized to generate foam in this study. The foam generation technique and degree of foam formation have been found to influence the rheological characteristics of the foam (Akhtar et al. 2018), as well as the foam structure and bubble dispersion. In the study by Akhtar et al. (2018), fully equilibrated foam (i.e., fully generated foam at its maximum viscosity) was generated using a needle valve in a closed-loop circulation system. Based on the technique of foam generation, the foam in this study is considered fully equilibrated foam. Foam is in

equilibrium when it has its highest energy. This foam is fully formed with high viscosity and stability.

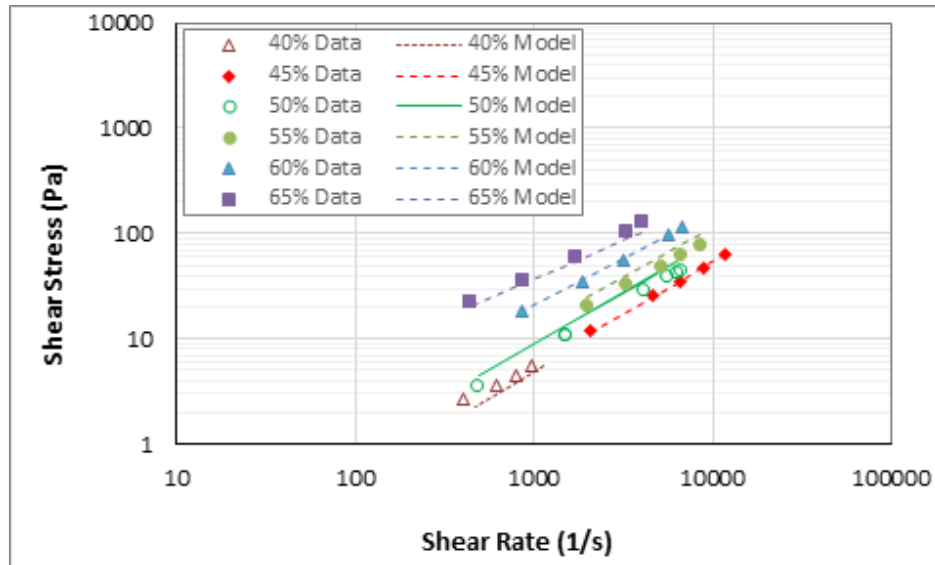


Figure 5.1 Comparison for predicted and measured rheogram of aqueous foam at 25°C and 6.89 MPa

Figure 5.2. shows that the fluid behavior index decreases with foam quality. This shows the shear-thinning behavior of foam as quality increases. The foams exhibited power-law fluid behavior. Since the fluid behavior index is less than 1, the foams are considered pseudoplastic or shear-thinning fluids. Figure 5.3 shows that the variation in flow behavior is minor at qualities less than 55% i.e., the foam behaves like bubbly liquids, but there is a drastic reduction in the fluid behavior index with the increase in foam quality, which is a non-Newtonian behavior and demonstrates the fluid's strong shear-thinning property and the development of bubble structure.

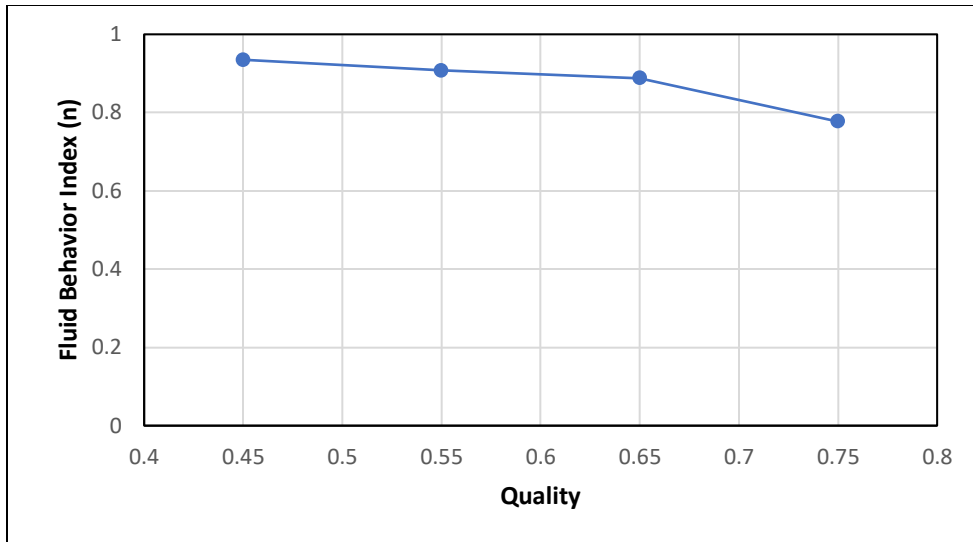


Figure 5.2: Power-law exponent

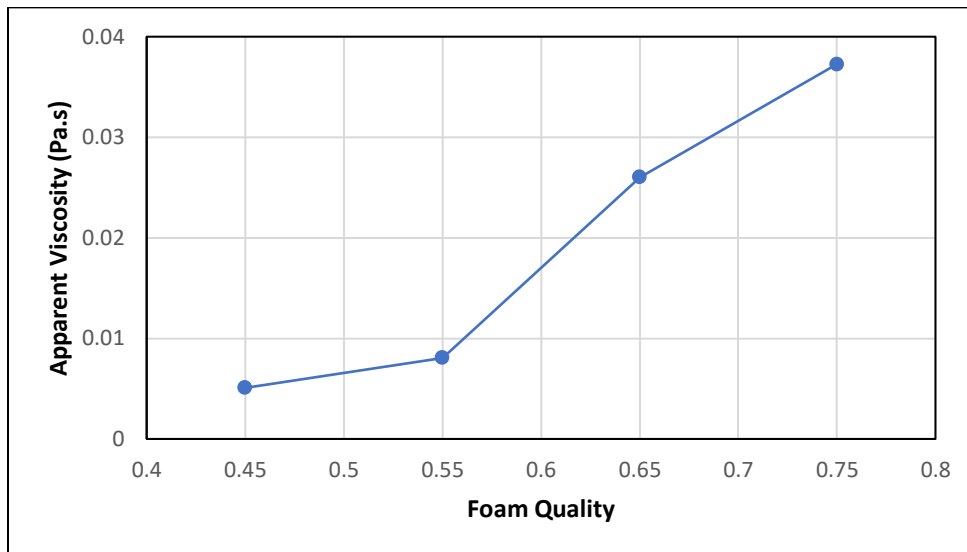
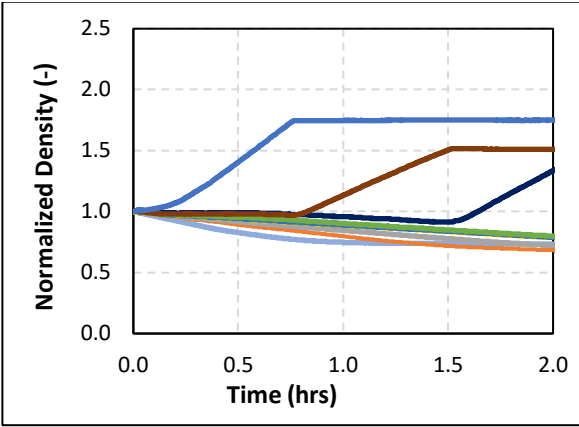
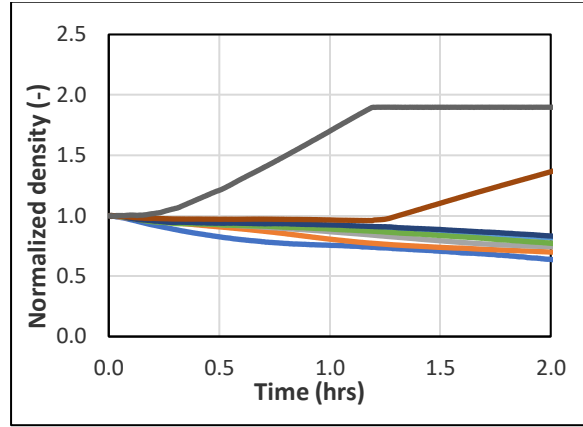


Figure 5.3. Apparent viscosity vs quality at 25°C and 6.89 MPa @ 5000 1/s

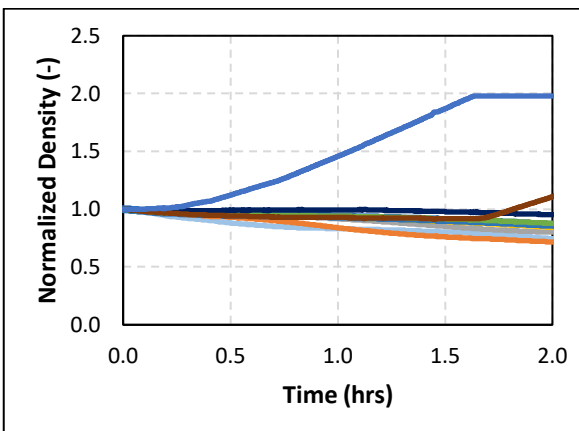
The apparent viscosity of the foam increased with foam quality (Figure 5.4). The increase was gradual below 55% viscosity. The viscosity increase became more drastic beyond 55% as observed from the large increase in the plot. This is because when foam quality increases above a critical value (in this case 55%), the foam starts to develop structure and becomes a shear-thinning fluid. For the foams considered in this study, with increasing quality, there is a reduction in the fluid behavior index and an increase in apparent viscosity.



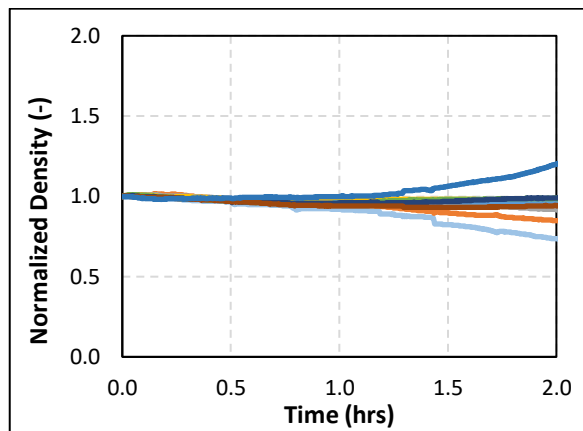
(a)



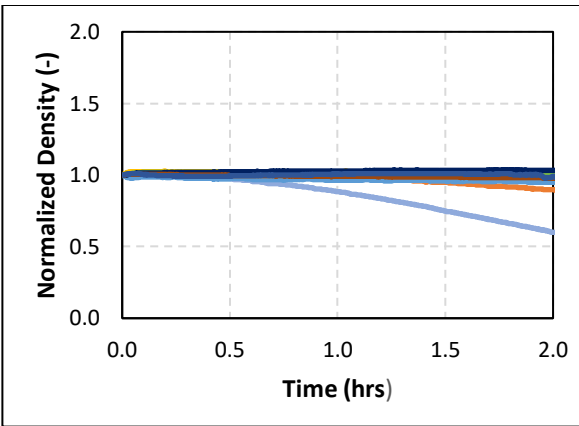
(b)



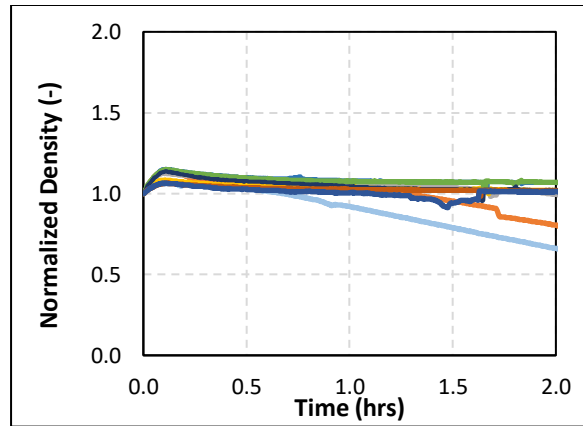
(c)



(d)



(e)



(f)



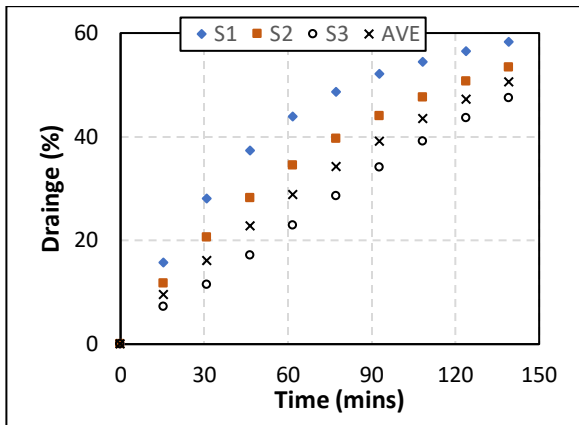
Figure 5.4. Normalized density curves a) 45% b) 50% c) 55% d) 60% e) 65% f) 70%

5.1.2. Drainage Measurement

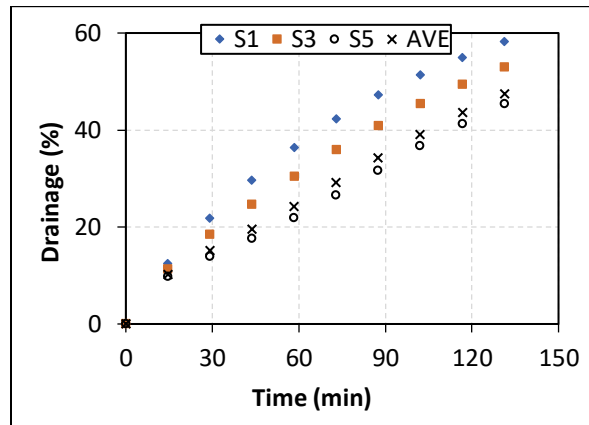
Figure 5.4 shows the average density of foam in each segment of the test section as a function of time. The density profile during the measurement period of 2 hours shows the point where the liquid starts to drain, this is indicated by an increase in the density of the fluid at that segment. The curve was flattened out when the segment was filled up with liquid. In the analysis of the results, the segments which were filled up with fluid are excluded. In Figure 5.4a, measurements for 45% quality foam are shown. The bottom three segments (S7 to S9) were the curves to flatten out which indicated that the segments were filled up with liquid. Measurements from these segments were removed from the analysis as they already contain liquid columns. The other segments that display a smooth density trend had homogenous foam. The measurements from these segments are included in the polynomial curve fitting analysis. Figures 5.4b and 5.4c demonstrate similar behavior (i.e., segments that were filled up with liquid columns).

Figure from 5.4d to 5.4f normalized densities of high-quality foams (60%, 65% and 70%). All segments show smooth density curves that have a consistent trend which means that they contain a homogenous foam. These segments were included in the analysis as they contained only foam and exhibit a nonlinear relationship. The trend observed is due to the high gas fraction in the foam which reduces the rate of drainage because of the liquid film thickness reduction and the formation of bubble structure. The top segments (S1 and S2) however exhibited a downward trend that shows that those sections were losing liquid and the density of the fluid was decreasing. This is because of the effect of gravity force which causes the liquid to drain from the top segments to the lower segments until it reaches the bottom of the column.

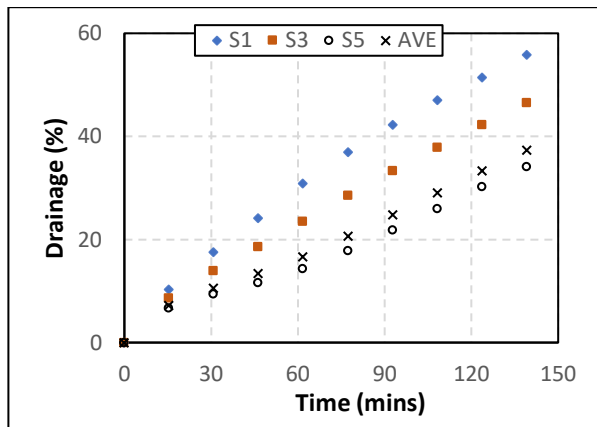
The drainage volume curves are consistent with the literature that shows three different drainage regimes. The first regime depicts a gradual increase in drainage rate followed by a rapid increase in drainage rate, i.e., the slope. The second regime shows a constant drainage rate, and the third regime shows a gradual reduction in drainage rate which approaches zero. Figure 5.5. presents drainage fraction (i.e., the ratio of the volume of drained liquid to the initial liquid volume) versus the time. The drainage fraction of the foam decreased with increasing foam quality. The plots are presented for each foam quality. At the start of the experiment, the drainage fraction is zero. As the experiment progressed, there was a gradual increase in the drainage fraction of foam which shows the draining of liquid out of the foam. After some time, the slope of the curve becomes constant, and the curve flattens demonstrating the end of gravity drainage as the foams in these segments become dry.



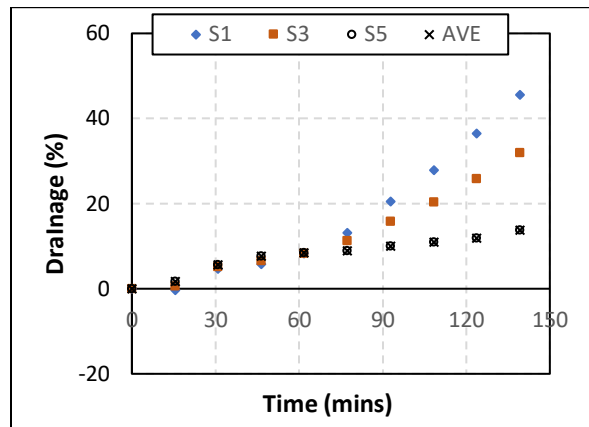
(a)



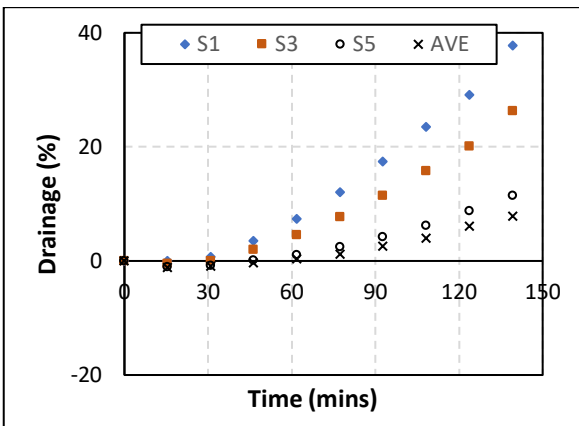
(b)



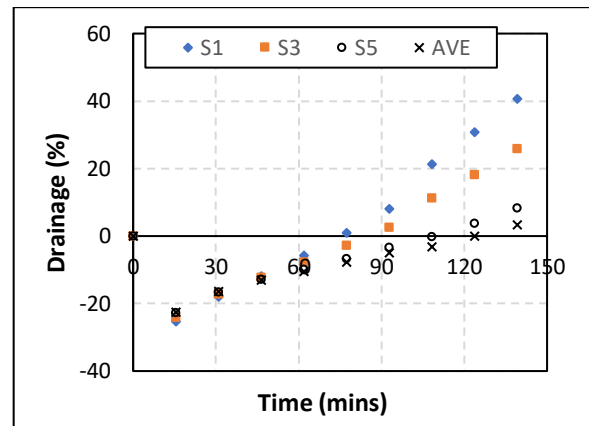
(c)



(d)



(e)



(f)

Figure 5.5. Drainage fraction versus time for aqueous foams a) 45% b) 50% c) 55% d) 60% e) 65% and f) 70%

The three curves shown in Figures 5.5a to 5.5d are for 40%, 45%, 50%, and 55% quality foams, respectively. For analysis, three segments in the upper part of the test section are considered. Lower segments are not presented here because some of them had liquid columns. The top-most segment (S1) has the highest drainage fraction i.e., it drains the most liquid. This is because the drainage fraction is the amount of liquid loss due to drainage relative to the volume of liquid present initially. In the top-most segment, there was only liquid loss and no gain during the experiment. The third segment (S3) has a lesser drainage fraction as compared to the top segment. The fifth segment (S5) has the least drainage volume because it was gaining liquid from the upper four segments (S1 to S4). The average drainage fraction is approximately the same as the third segment. The maximum drainage fraction was roughly 70% for 40% foam. The maximum drainage fraction was slightly reduced with foam quality.

Higher quality foams (Figure 5.5e and 5.5f) have different volume fraction behavior and the graph plotted shows the five segments. The upper three segments (S1-S5) have similar volume fraction behavior to the low-quality foams (40% to 55%). The top-most segment exhibited the highest drainage fraction. However, the two bottom segments (S7 and S9) displayed a different drainage fraction trend which shows liquid gain from the top segments. The negative drainage fraction indicates liquid gain due to drainage. The liquid gain occurred in the late stage of the experiment.

The result from the analysis shows that in high-quality foams, the drainage rate is low. This agrees with the literature that in the oil field, higher quality is more desirable as they have lower drainage as compared to low-quality foams. The reduced drainage of high-quality foams is because of the development of structure and film thinning which substantially reduce liquid drainage due to increased viscous resistance. The foam structure develops at high qualities and the plateau border at the junction of intersection between the bubbles restricts the flow of liquid in the foam.

This is a new method for determining the drainage volume of foam under high pressure which simulates field conditions. This method is different from the stability test currently conducted in the field which majorly utilizes a graduated cylinder to measure the liquid drainage of the foam. This test considers the drainage of each segment and how it affects the overall segment. The height of the graduated cylinder used for the analysis at the field site would affect the drainage volume and this is inconsistent.

5.2. Effect of Pressure on Drainage

The effect of pressure on foam drainage was studied at 100 psia, 700 psia, and 1400 psia. The drainage profile with the varying pressure is shown in Figure 5.6, the drainage curve for the 40% foam quality at 100 psia shows the highest drainage rate, and the highest drainage of about 90% was recorded at the pressure of 100 psia. The drainage curve at 700 psia is also shown in Figure 5.6a. The drainage rate increases steadily until the end of the two-hour drainage time. The maximum drainage volume recorded for the test pressure of 700 psia was 80%. The same trend was observed for the test at 1400 psia. The maximum drainage rate observed at the test pressure of 1400 psia was 63%.

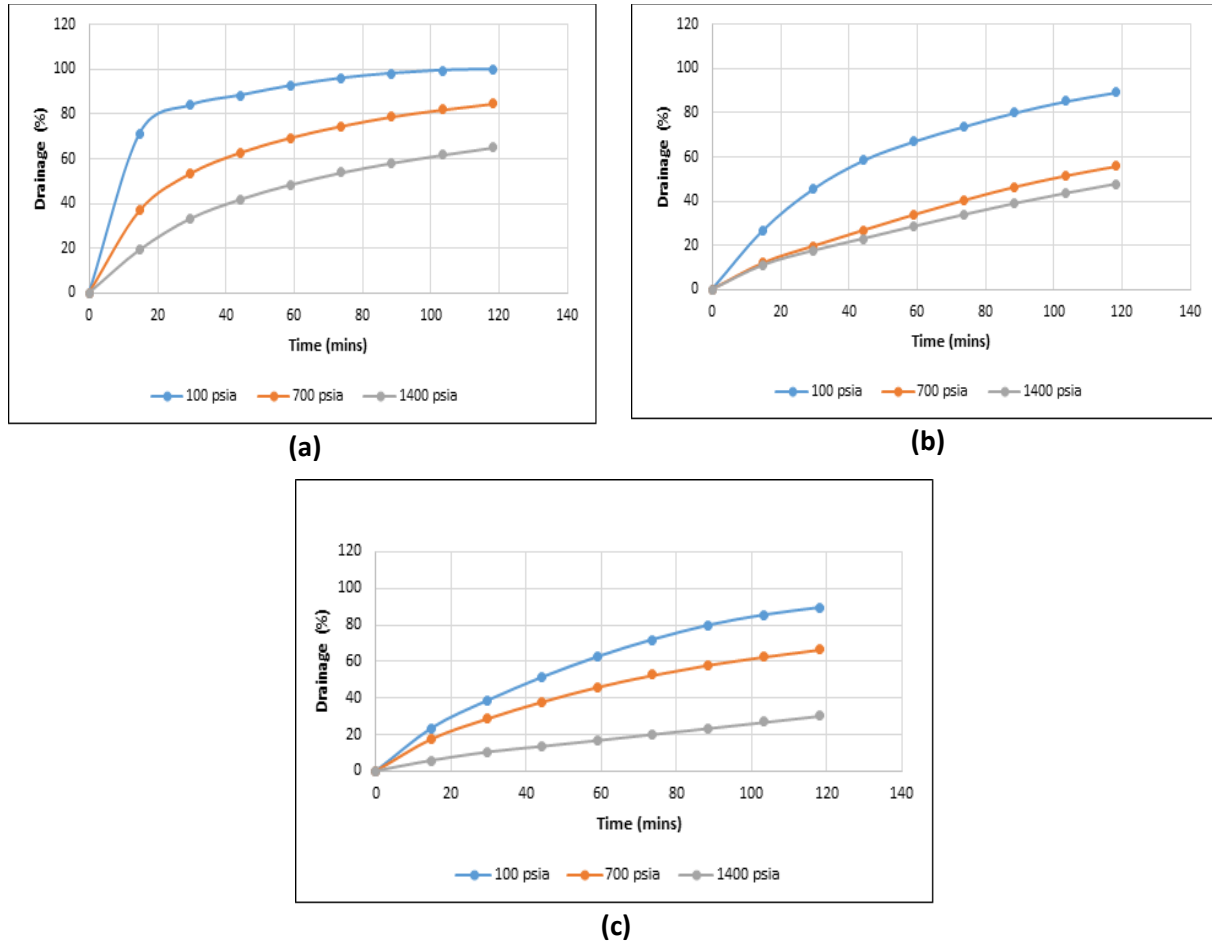


Figure 5.6. The effect of pressure on average drainage curves of different quality foams: a) 40%; b) 50%; and c) 60%

The results show the trend that the increase in pressure is inversely related to the drainage rate of the foam. The same trend was observed by the work of Maini and Ma (1986) and Rand and Kraynik (1983). The same trend was observed for the 50% and 60% quality foam (Figure 5.6b and 5.6c). The rate of drainage decreases with the increase of pressure. The drainage rate at 1400 psia appeared to be the lowest and the 100 psia is the largest.

Rand and Kraynik (1983) studied the effect of the generation pressure on the foam drainage half-life. The generation pressure was correlated with the foam cell size, and it was observed that the higher the form generation pressure, the smaller the cell size. Foams have been observed to

have lower drainage rate with smaller cell size. The smaller size of the foam cell implies more stable foam with a slower drainage rate.

The pressure in the system is increased by injecting more nitrogen gas into the existing foam. As the system pressure is increased, the gas viscosity in the test section increases.

The density and viscosity of the gas phase increases by changing the pressure of the system. This causes an increase in foam stability. Increasing pressure also increases the mobility of the surfactant molecules. This causes stabilization of foam due to the Marangoni convention which accelerates a move of liquid from areas with small surface tension to areas with high surface tension. This process stabilizes the foam film.

The stability of the foam depends on the physical parameters of the fluid which are pressure dependent. The parameters considered include\ the interfacial tension between the phases, the density, and viscosity of phases , and the mean bubble size of the foam.

5.3. Aqueous Foam with Salt

The effects of salt on surface tension, base fluid viscosity and density, and the drainage and flow behaviors of foam are investigated. Foam rheology measurements are presented in the Appendix B.1.

5.3.1. Effect of Mono and Divalent Salt on Surface Tension

The addition of salt has a profound effect on the surface tension of the foam. The presence of salt in the foam causes a decrease in the CMC of the surfactant. As previously discussed, (Section 2.5.1), the divalent salt CaCl_2 has a stronger effect on the reduction in the CMC compared to the NaCl salt. The surface tension measurements for the NaCl salt (Figure 5.7) shows that the surface

tension of the fluid decreased with salt concentration. The CaCl_2 salt also registers a decrease in surface tension with salt concentration. The decrease in surface tension due to the NaCl addition was slightly less than that of the CaCl_2 salt addition. According to Behera et al. (2014), as the valency or concentration of the ions is increased, a decrease in surface tension of the surfactant solution is observed. Marrucci (1967) discussed the dependences of the effectiveness of the coalescence prevention of inorganic electrolytes on the valency of the salt and the derivative (slope) of the surface tension vs concentration curve.

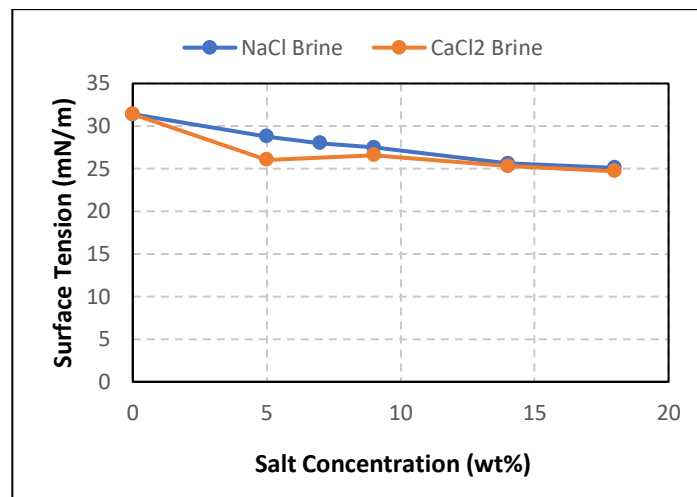


Figure 5.7. Surface tension measurement for NaCl and CaCl_2

5.3.2. Effect on Viscosity

The viscosity of the base fluid is increased when salt is added. Figures 5.8 and 5.9 depict the influence of salt type on viscosity and density for the two salts, respectively. Because of its increased valency, the CaCl_2 salt has a greater impact on the rise in the viscosity of the base fluid. One of the mechanisms that slow film coalescence is an increase in the viscosity of the base fluid. An increase in viscosity of the base fluid decreases the flow of the liquid surrounding the bubble, which can slow the coalescence rate of bubbles. Furthermore, the increase in viscosity results in greater viscous resistance which reduces the drainage of liquid in the foam structure.

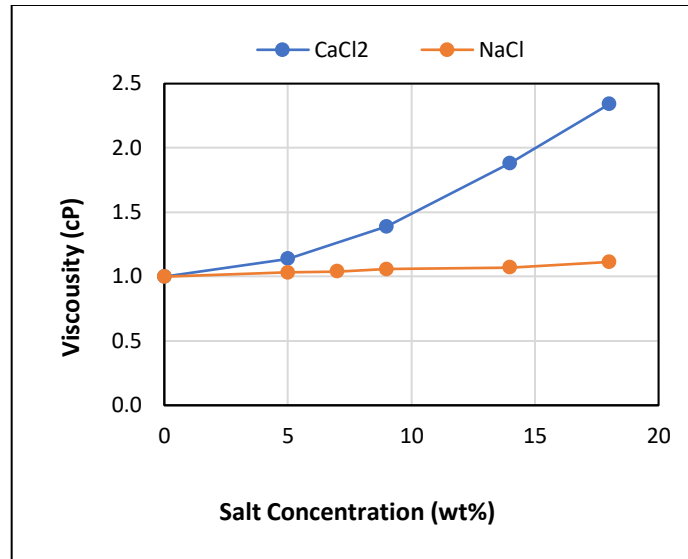


Figure 5.8. Viscosity changes with salt (NaCl and CaCl₂) concentration

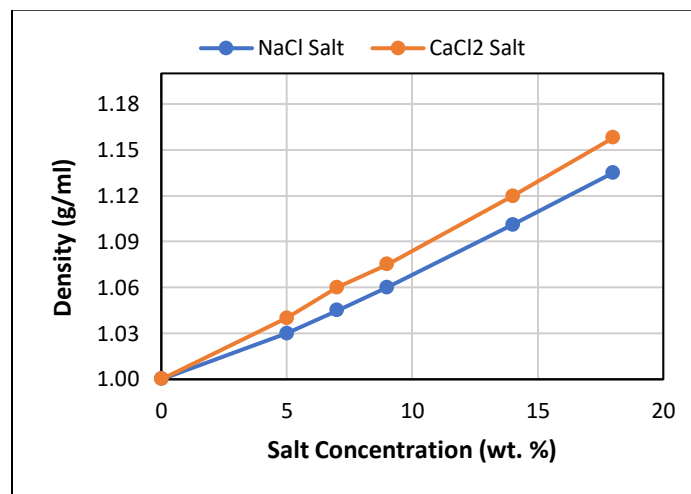
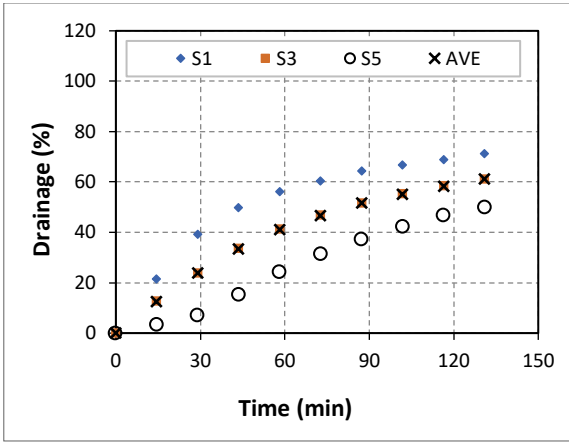


Figure 5.9. Density changes with NaCl and CaCl₂ concentration

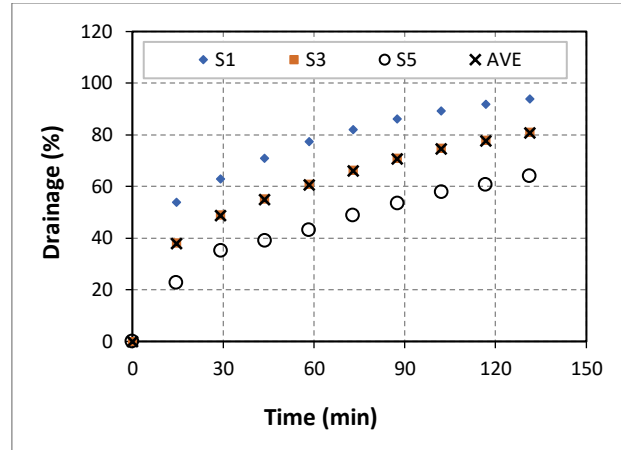
5.3.3. Effect of Salt Concentration on Foam Drainage

The experiments were performed at different salt concentrations (5%, 7%, 9%, 14% and 18%). The effects of salt concentration and valency were studied at a fixed surfactant concentration of 2% vol. The initial surfactant solution (Figure 5.10a) in the absence of salt can be seen to have an average drainage volume of 60% and an initial drainage rate of 0% at the start of the experiment, all the segment curves can be seen to converge at this start time which shows the initial stability

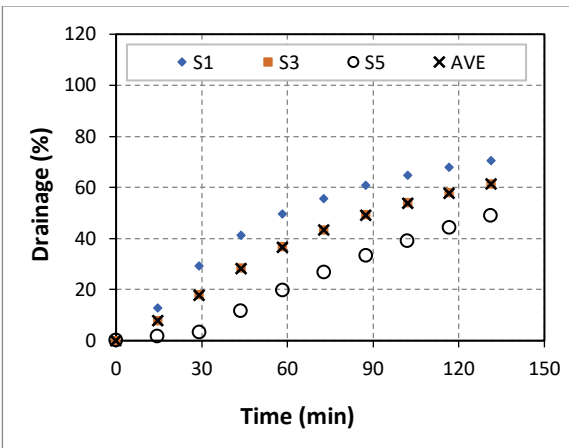
of the foam. However, as the experiment progresses, a separation in the curve can be seen to occur. The stability was measured over a period of 2 hours. The drainage fraction was seen to increase steadily during this period. The addition of salt and surfactant in the foam affects the drainage behavior via three factors (Ruckenstein and Bhakta 1996): the maximal disjoining force of foam, surface tension, and surface viscosity.



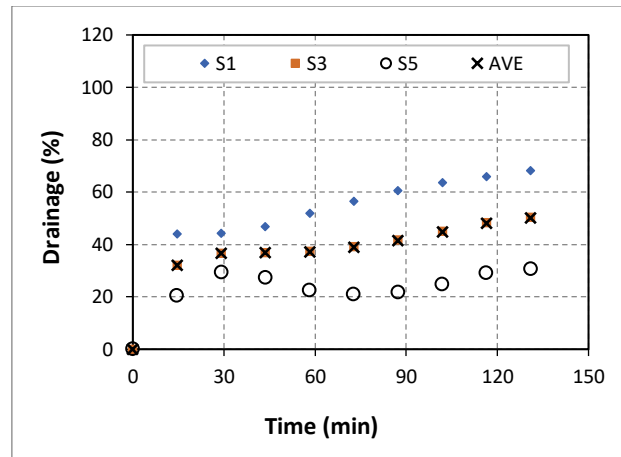
(a)



(b)



(c)



(d)

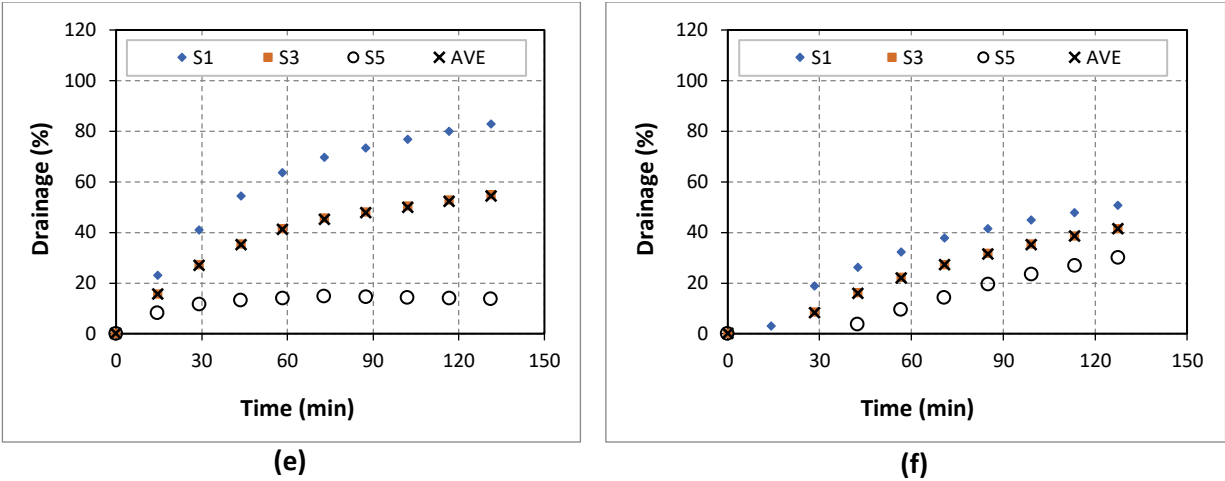


Figure 5.10: Effect of NaCl salt on the drainage volume of aqueous foam at 40% quality a.) 0% wt. b.) 5% wt. c.) 7% wt. d.) 9% wt. e.) 14% wt. f.) 18% wt.

The electrostatic repulsion between the molecules of the surfactant is decreased with an increase in salt concentration which causes adsorption of surfactant molecules to increase with salt concentration. In the presence of salt, the increase in adsorption of the surfactant molecules causes the foam lamellae to become rigid and reduce the film thinning rate (Rao et al. 1982). According to Ruckenstein and Bhakta (1996), the presence of NaCl salt in a surfactant solution has the following effects:

- i. Electrical double layer compression by increasing the ionic strength.
- ii. Increase in the binding of the counterions by reducing the degree of dissociation of the absorbed surfactant.

The attractive and repulsive surface forces determine the stability of a liquid layer. The DLVO theory is the most widely accepted theory of liquid film stability. The electrostatic double layer (EDL) and the Vander Waals forces are described by the balance of two separate forces. A liquid film is considered as stable if the electrostatic double layer is greater than the Vander Waals forces in the system. In addition to this, the hydrophobic forces have been observed to have an impact on

the stability of the liquid film. The magnitude of EDL is dependent upon the ions at the surface of two fluids in contact with overlapping double layers of the surface ions. The van der Waals forces are short ranged less than 10 nm (Isrealachvili 1991). The attractive forces of Vander Waals are therefore not considered in the stability of the salt liquid film as in comparison with the EDL at > 10 nm can be negligible especially in surfactant-free foam. The DLVO theory say that with increase in salt concentration, there is a decrease in surface potential and liquid film coalescence faster. This is however not the case in various conditions.

5.3.3.1. Monovalent Salt - NaCl

The drainage fraction of 40% quality foam at various salinities is presented in Figure 5.10. Measurements are presented for three of the upper segments (S1 to S5). Without the presence of salt, the average maximum drainage fraction (AMDF) was found to be 60% on average (Figure 5.10a). At 5% salinity, the AMDF of the foam increased as shown in Figure 5.10b. The increase in drainage indicates that the salt content causes the foam bubbles to coalesce at a faster pace. This is owing to the initial repulsive force of the electrical double layer. The ionic atmosphere between the surfaces has a thickness that decreases with an increase in the salt concentration (Giribabu et al. 2008). In the presence of ionic surfactants, the bubbles in the aqueous foam rest on the gas-liquid interface and are repelled by the double-layer force (Ghosh 2004). The liquid film thickness reduces with time, and this causes rupture due to van der Waals forces. This process is the coalescence of the foam bubbles which causes foam destabilization.

According to Giribabu et al. (2008), at a particular concentration, higher valency salt is more efficient in decreasing the thickness of the double-layer. Another factor that contributes to the decrease in double-layer repulsion is ion binding which decreases with surface potential.

When NaCl concentration was 7%, the drainage curve is similar to the drainage curve in the absence of salt (Figure 5.10c). The two counteracting forces that is the reduction in the repulsive forces and the coalescence threshold canceled each other and the drainage fraction remains the same.

At a higher salt concentration of 9%, there was a reduction in the AMDF of foam with an increase in salt concentration. This observation could be due to the increased adsorption of the surfactant molecules. The effect of the increased adsorption is stronger than the effect of reduction in double-layer force. At this concentration, the NaCl stabilizes the foam, and the rate of bubble coalescence is reduced (Figure 5.10d). Furthermore, when the concentration of NaCl is increased, it could cause a decrease in foam stability, which is shown as an increase in the drainage fraction. The drainage rate for this system is affected by the balance between reduced repulsive forces and enhanced surfactant adsorption (Figure 5.10e). These findings are consistent with (Giribabu et al. 2008).

The trend of change in drainage rate with increase in NaCl concentration is observed in Figures 5.11 and 5.12 for quality of 50% and 60% foam. The increase in salt concentration continually increases the adsorption of the surfactant molecule at the gas-liquid interface. The trend observed by changing the concentration of the NaCl salt from 5% - 18% is in agreement with the results

from (Liu et al. 2005). The trend they observed was an “W” shape curve with an increase in the NaCl concentration (Figure 5.13).

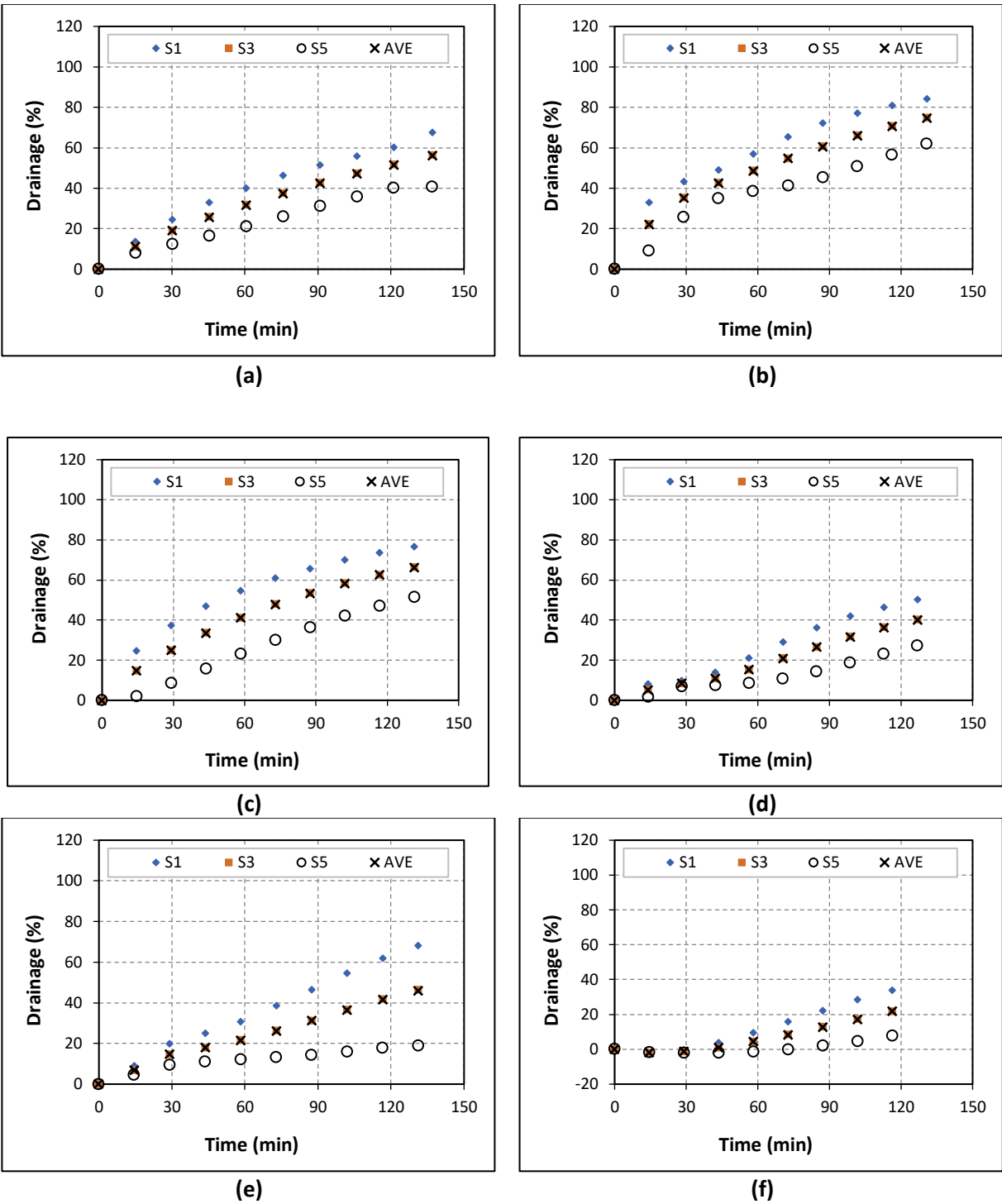
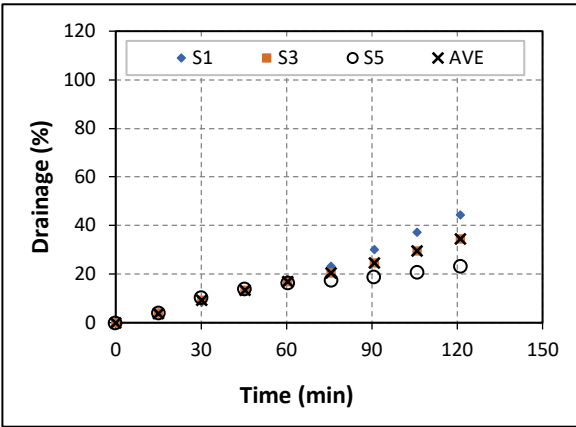
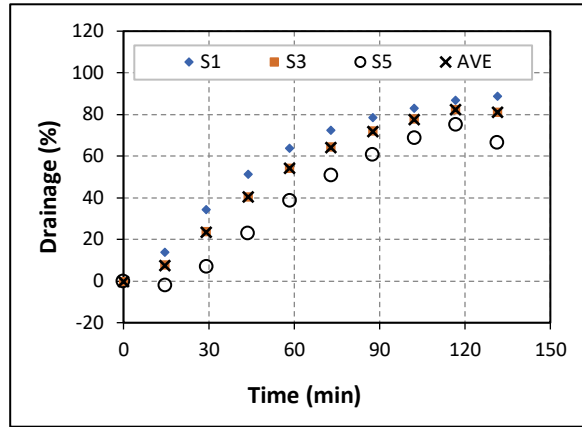


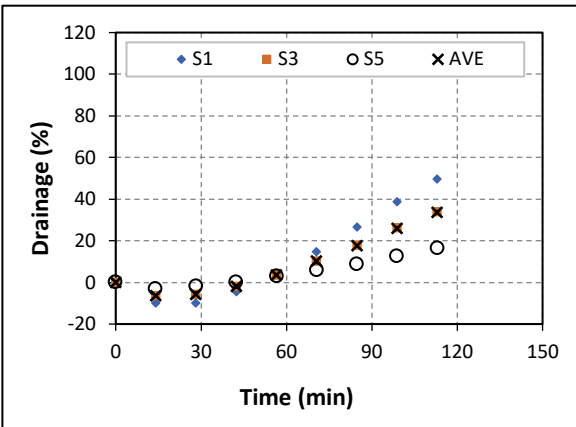
Figure 5.11. Effect of NaCl salt on the drainage volume of aqueous foam at 50% quality a.) 0% wt. b.) 5% wt. c.) 7% wt. d.) 9% wt. e.) 14% wt. f.) 18% wt.



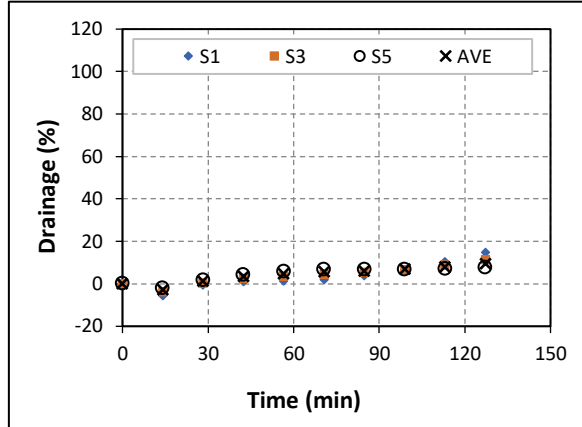
(a)



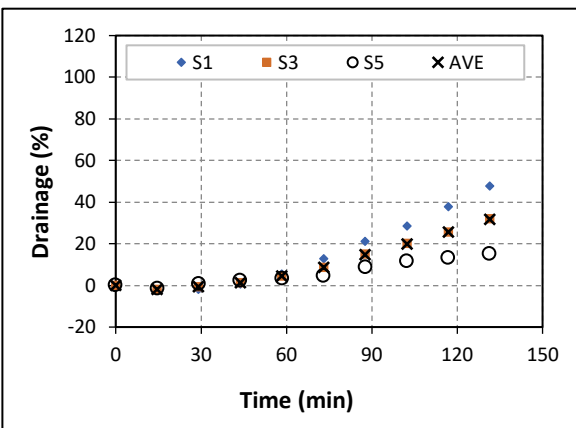
(b)



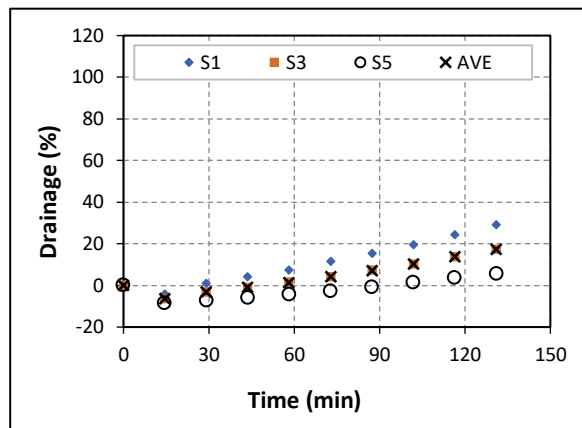
(c)



(d)



(e)



(f)

Figure 5.12. Effect of NaCl salt on the drainage volume of aqueous foam at 60% quality a.) 0% wt. b.) 5% wt. c.) 7% wt. d.) 9% wt. e.) 14% wt. f.) 18% wt.

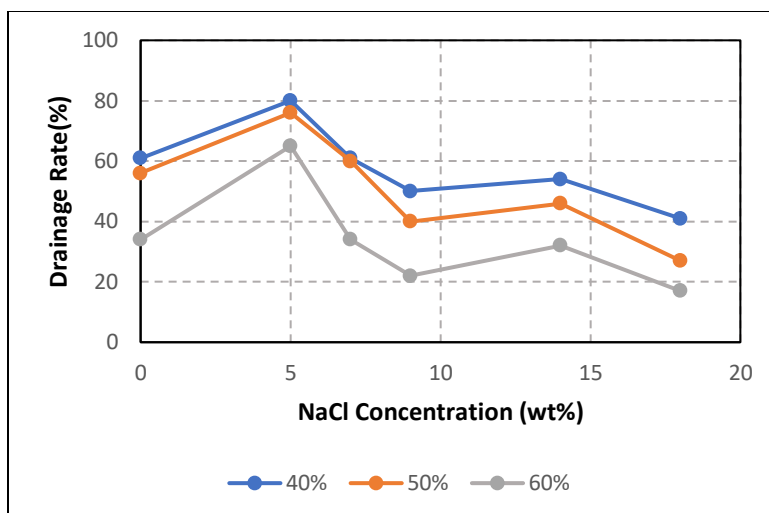
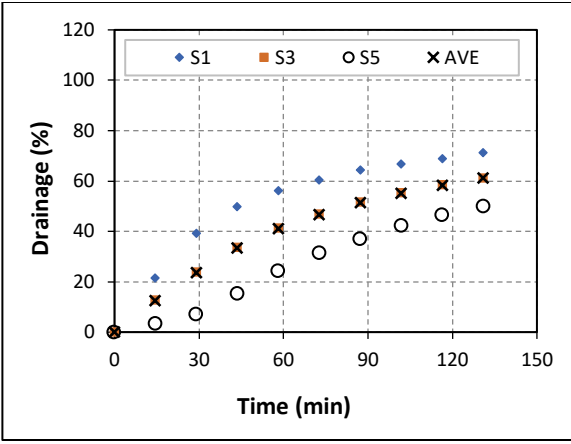


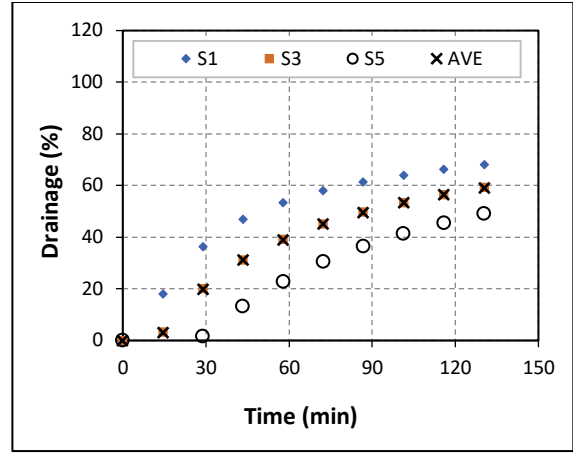
Figure 5.13: Effect of NaCl concentration on the AMDF of different quality foams

5.3.3.1. Divalent Salt - CaCl_2

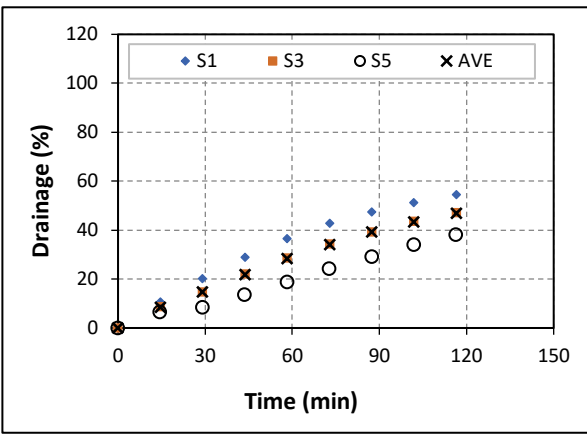
The valency of the salt is an important attribute in the stability system of the foam. The drainage fraction of 40% quality foam with CaCl_2 salt is shown in Figure 5.14. The average maximum drainage fraction (AMDF) was 60% when salt was not present. No noticeable change in the drainage was observed when the salt concentration was increased to 5%. Increasing the concentration further (9%) shows a significant reduction in the AMDF. At this point, the addition of CaCl_2 stabilized the foam and reduced drainage. Using higher salt concentrations of 14 wt. % and 18 wt. % resulted in an increase in the AMDF of foam as the reduction in the electrostatic double-layer becomes the dominant effect. The drainage fractions of 50% and 60% quality foams with CaCl_2 salt are presented in Figures 5.15 and 5.16.



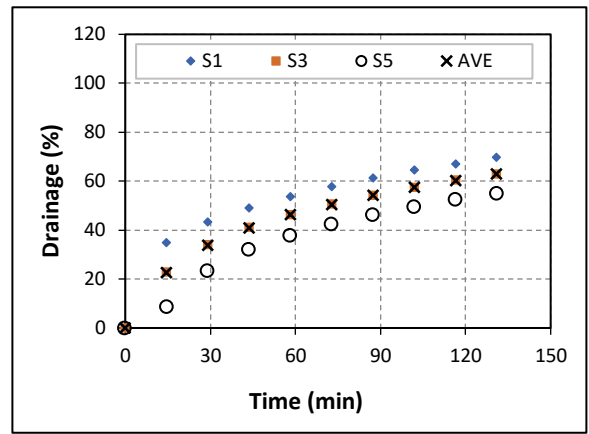
(a)



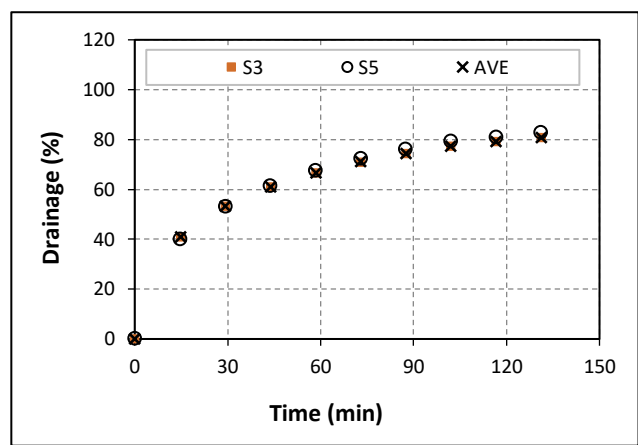
(b)



(c)

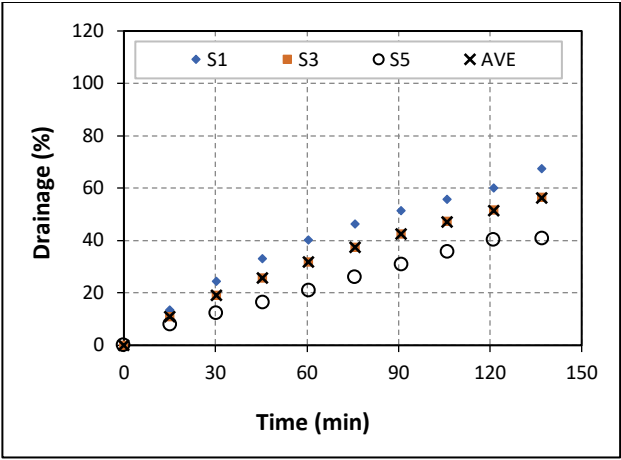


(d)

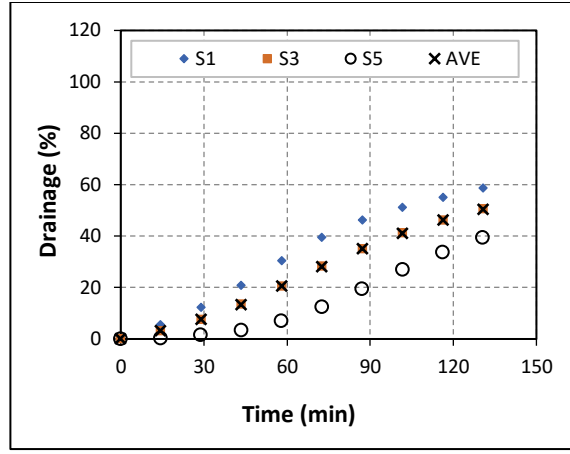


(e)

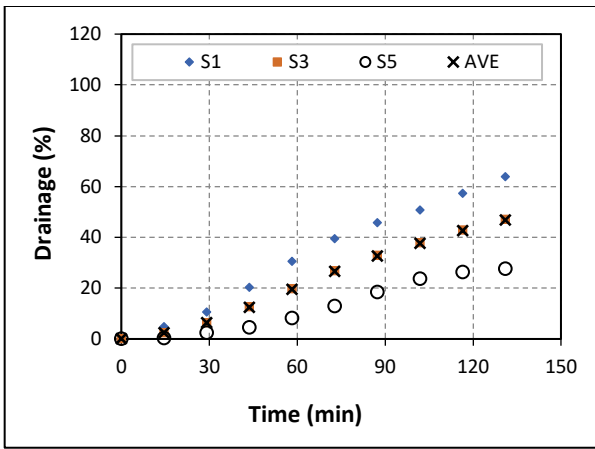
Figure 5.14. Effect of CaCl_2 salt on the drainage volume of aqueous foam at 40% Quality
a.) 0% wt. b.) 5% wt. c.) 9% wt. d.) 14% wt. e.) 18% wt.



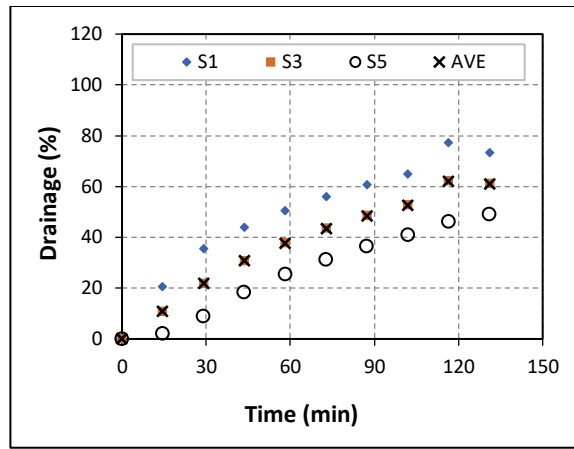
(a)



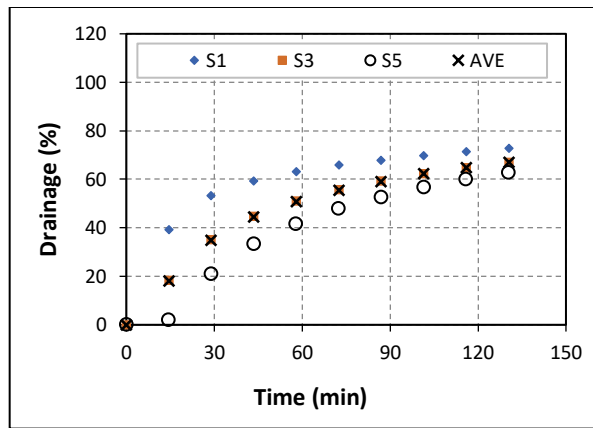
(b)



(c)



(d)



(e)

Figure 5.15. Effect of CaCl_2 salt on the drainage volume of aqueous foam at 50% Quality

a.) 0% wt. b.) 5% wt. c.) 9% wt. d.) 14% wt. e.) 18% wt.

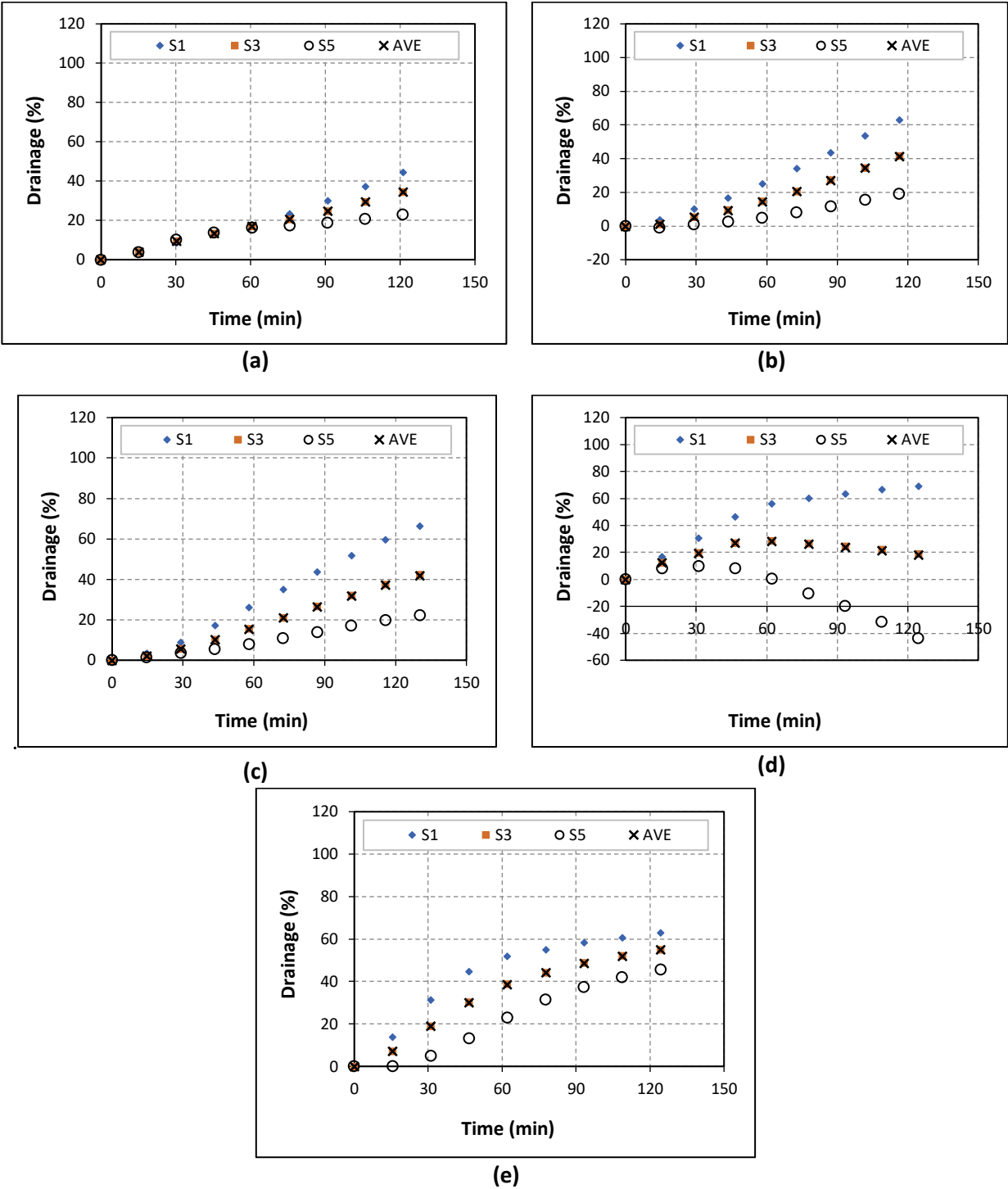


Figure 5.16. Effect of CaCl_2 salt on the drainage volume of aqueous foam at 60% Quality
 a.) 0% wt. b.) 5% wt. c.) 9% wt. d.) 14% wt. e.) 18% wt.

The effect of the CaCl_2 salt on the AMDF of 40% and 50% quality foams at various concentrations is shown in Figure 5.17. Without the presence of salt, the AMDF of 40% quality foam was 61%. The addition of a small amount of salt slightly reduced the AMDF of foam to 59%. The increase of the salt to 9% resulted in a further decrease in the AMDF of foam because of the electrostatic double-layer force that was able to overcome the Vander Waals forces in the system. However, it was observed that increasing the CaCl_2 concentration to 14wt.% increased the drainage rate of the foam. Increasing the salt concentration further can inhibit surfactant molecule adsorption and reduce bulk gas-liquid interface and bubble repulsion. The balance between the increase in adsorption and reduction in repulsive forces determines the drainage rate of foam. Increasing the salt concentration further increased drainage volume. The substantially higher drainage volume could be due to the effect of bindings of cation that quickens aggregation by decreasing the contact surface repulsion (Behera et al. 2014). The same effect was observed for the 50% and 60% quality foam (Figures 5.15 and 5.16).

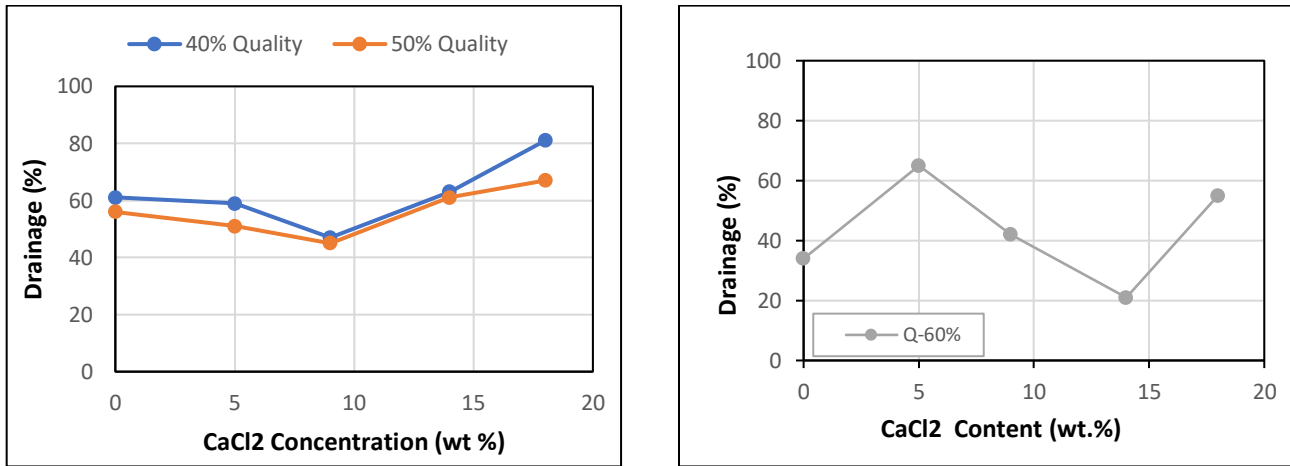


Figure 5.17. Effect of CaCl_2 concentration on the AMDF of (a) 40% and 50% quality foams (b) 60% quality foam

5.4. Aqueous Foam with Oil

The results of the analysis of the stability of the three oil types and varying oil concentrations. All drainage measurements are presented in this section.

5.4.1. Foam Generation Technique in the Presence of Crude Oil

According to Rojas et al. (2001), the method of introduction of oil into the system affects the stability behavior of foams. If high shear rate agitation is used, the oil tends to form emulsion in the foam lamellae. If low shear agitation is used, the oil tends to spread into the film. Foam with spread oil film is more unstable than oil with emulsified oil drops. In this work, only the effect of emulsified oil drops was considered.

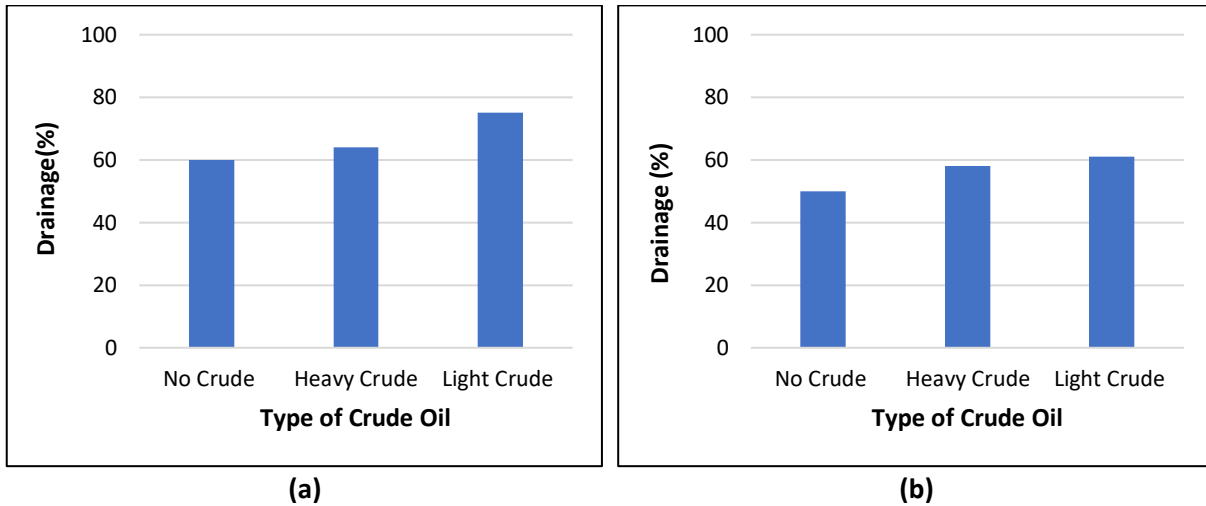
5.4.2. Effect Oil Type

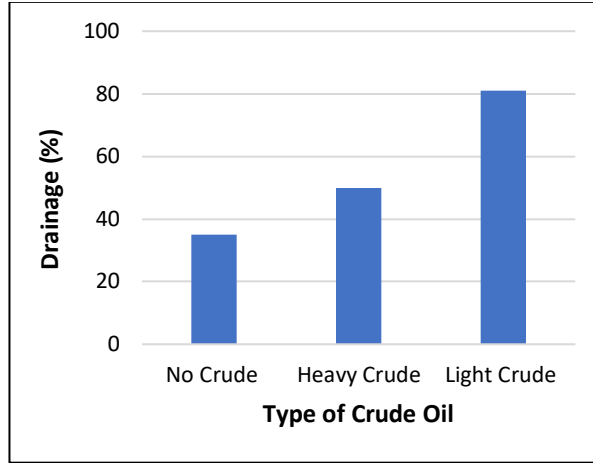
According to Simjoo et al. (2013), the first stage of foam decay is due to gravity. At this stage, all the oil types have the same behavior. The liquid drains out of the foam due to the force of gravity. The second stage of foam decay is influenced mainly by bubble coalescence. The type of oil influences the bubble coalescence. The influence of the oil type on the bubble coalescence is due to the length of the alkane. Alkanes with shorter chains have a high rate of coalescence and this results in a shorter half-life of foam. Oil with shorter alkanes chains i.e., low-density oils have a higher spreading and entering coefficient which means they have an increased rate of entering the foam film and spread over the gas-water interface. Shorter chain alkanes tend to solubilize in micelles.

5.4.3. Effect of Crude Oil Types

Two crude oils with noticeably different properties (Table 4.5) were considered in this investigation. The effect of crude oil on the crude oil is based on the presence of the base oil and the surface-active agents present in the crude oil. Crude oil being a fluid with various compositions can have agents that either stabilize or destabilize the crude oil. Some of these materials could be sulphur, nitrogen, and metals. The work done is based on particular crude oil composition.

According to Andrianov et al. (2012), the low viscosity oils cause higher destabilization of the aqueous foam. In this study (Figure 5.18a), the light crude increased the AMDF of 40% quality foam from 60% to 75% and the heavier crude increased the AMDF from 60% to 65%. Light crude oil results in a higher rate of destabilization than heavy crude oil. The same trend was observed for 50% and 60% quality foams.





(c)

Figure 5.18. Effect of crude oil type on AMDF of different quality foams: (a) 40%, (b) 50%, and (c) 60%

In Figure 5.18b, the drainage fraction of 50% quality increased from 55% to 60% with the addition of light crude oil whereas it increased from 55% to 58% for heavy crude oil. The drainage fraction of 60% quality increased from 38% to 80% with the addition of light crude oil and from 38% to 50% with the introduction of heavy crude (Figure 5.18c). At 60% quality, the light crude oil was observed to cause significant destabilization in the foam stability. This result agrees with the findings of Andrianov et al. (2012). Highly viscous oil tends to stay in the skeleton of lamellae and the plateau border even after most of the foam film is broken. In the absence of oil in the system, the foam eventually collapses due to the liquid drainage which causes thinning of the foam film. The high viscosity of crude oil can offset the effect by limiting liquid drainage due to its increased resistance to flow. On the other hand, light crude oil drains out of the foam film quickly resulting in a faster foam thinning effect.

According to Simjoo et al. (2013), at the initial stage of drainage, the drainage rate of the foam is dependent on the gravity drainage of the liquid. This is evident in Figure 5.19a and 5.19b for the

40% and 50% quality at below 30 mins. The foam decay could be governed by gravity drainage at this stage. This involves the flow of liquid down through the foam network structure due to the density difference between the two phases. The segregation continues until the surface tension cannot be handled by the thinning gas bubble walls (films).

At 40% quality, the drainage rate at below 30 mins was 25% for the three cases considered: foam without oil, foam with 10% heavy crude oil, and foam with 10% light crude oil. This stage was characterized by gravity drainage and the oil type does not have a significant effect. After 30 minutes, the foam decay was dominated by bubble coalescence. The decay process involves the breaking of the films and the merging of small bubbles into larger ones. The stability of the foam depends on the size of the bubbles. Smaller size bubbles create foams with increased stability (Rand and Kraynik 1983). The viscosity of the oil affects the bubble coalescence. The higher the oil viscosity, the lower the rate of bubble coalescence; and therefore, the rate of drainage reduces. Foams containing heavy crude oil have limited drainage due to the reduction in bubble coalescence by the heavy oil coating on the film surrounding bubbles. The heavy oil coating reduces film thinning and bubble coalescence.

A similar effect was observed when 50% quality foam was tested. Below 30 mins, the decay was dominated by the gravity flow and all the foam cases had approximately 20% drainage fraction at 30 mins. After 30 mins, the decay process was dominated by the bubble coalescence. However, this theory of constant drainage rate due to gravity flow breaks down at 60% quality (Figure 5.19c). This is because 60% quality foam has a lesser quantity of liquid and more gas volume than 40% and 50% quality foams. At higher foam quality, foam drainage is less dependent on gravity

drainage at any time and the bubble coalescence and film thinning take a more dominant role. The structure of foam changes as the quality increases from spherical to polyhedral (Davis 2013). This change in foam structure and behavior causes a variation of the foam behavior compared to the other cases. The light crude oil changes the rate of foam drainage more than the heavy crude oil. These observations agree with the findings of Simjoo et al. (2013) that indicated the impact of oil type on the foam drainage.

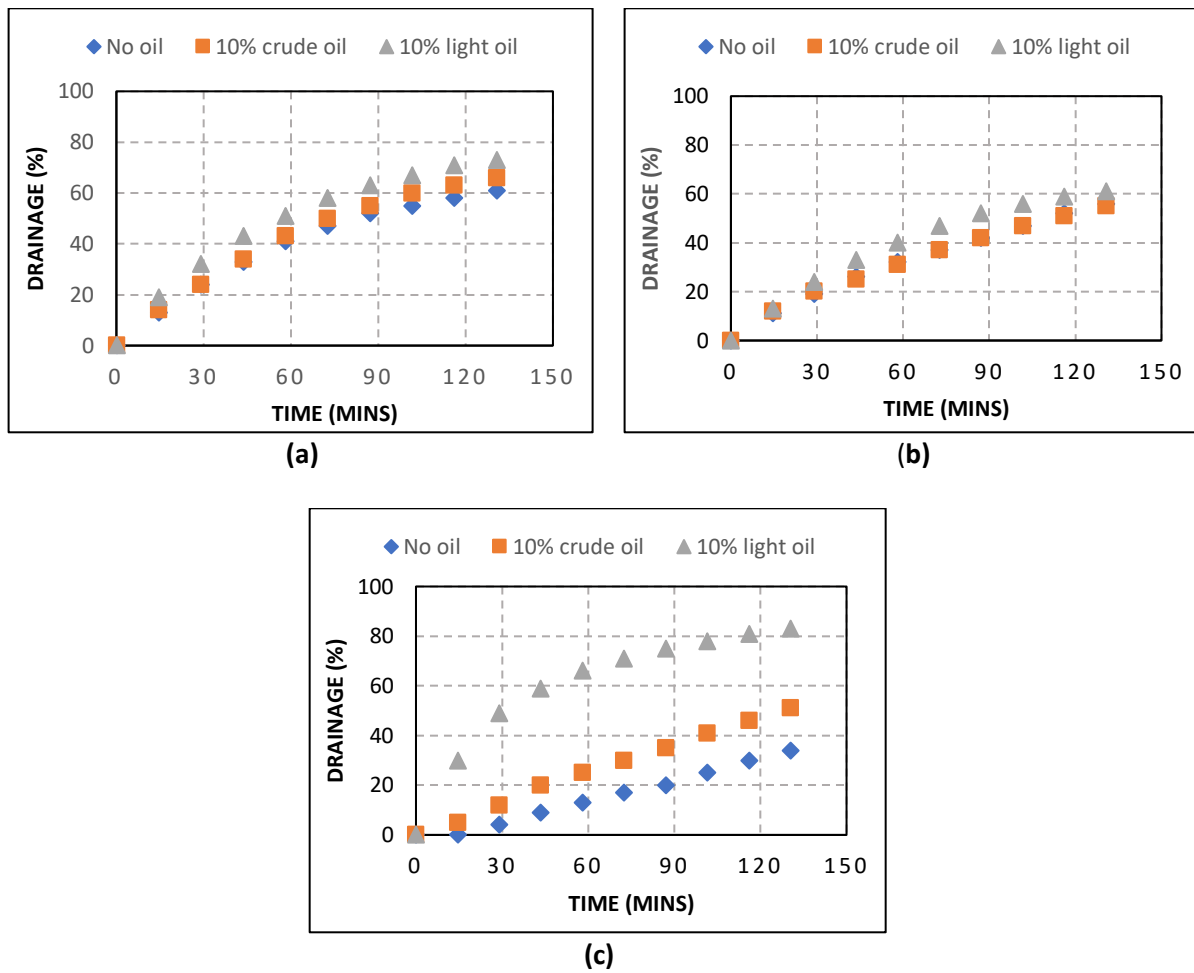
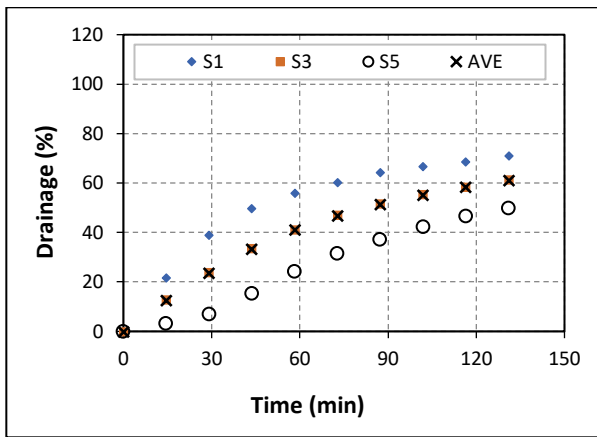


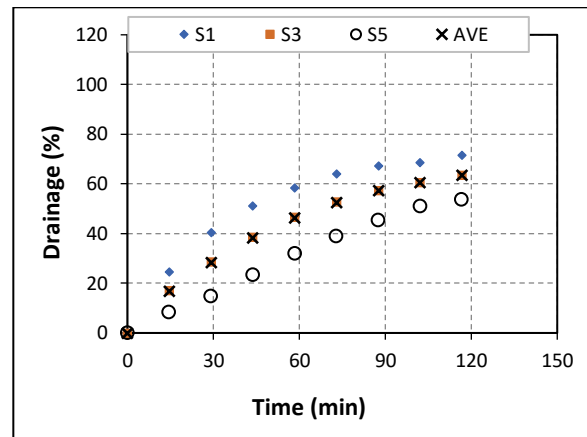
Figure 5.19. Fractional drainage vs. time for different quality foams: (a) 40%, (b) 50%, and (c) 60%

5.4.3. Effect of Mineral Oil

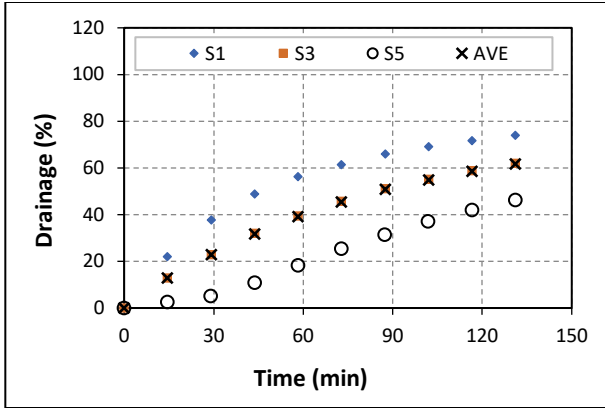
Extensive drainage experiments were conducted to determine the effect of mineral oil on the stability of aqueous foams. The concentration of mineral oil in the base fluid was varied from 5 to 20% by volume. According to Rojas et al. (2001), below 10% concentration, crude oil contamination does not affect the stability of the foam. The average maximum drainage fraction (AMDF) of 40% quality foam (Figure 5.21a) in the absence of oil was 60%. After introducing 5% mineral oil (Figure 5.21b), the AMDF of the foam didn't show a noticeable difference. The AMDF of the foam at 10% mineral concentration (Figure 5.20c) was also more or less the same as that observed with 5% mineral oil. This agrees with the work by Rojas et al. (2001). Despite this, adding 20% mineral oil (Figure 5.20d) increased the stability of the foam as indicated by the reduction of AMDF of the foam from 60% to 50%. This shows the increase in the stability of foam to the concentration of mineral oil. The 50% quality foam (Figure 5.21) exhibited mostly the same behavior as the 40% quality foam. The AMDF of the foam was maximized at a 5% mineral oil concentration.



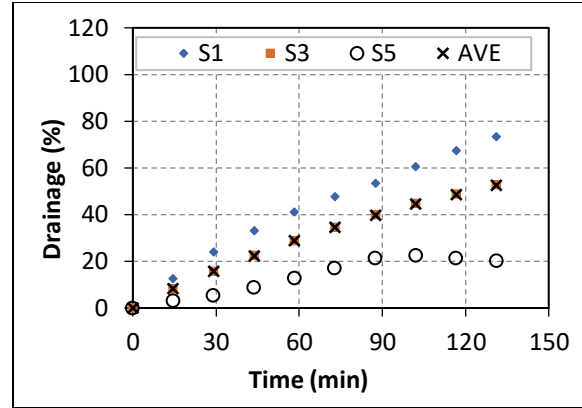
(a)



(b)

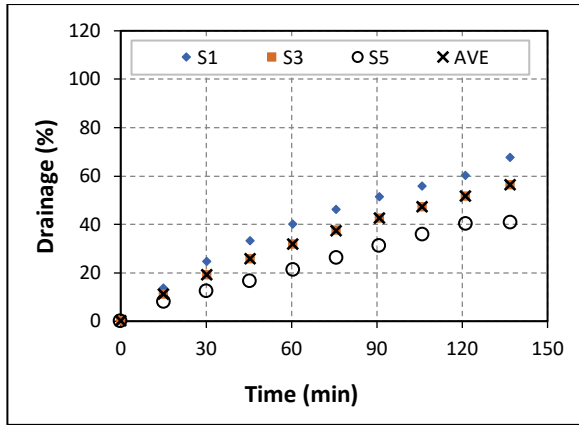


(c)

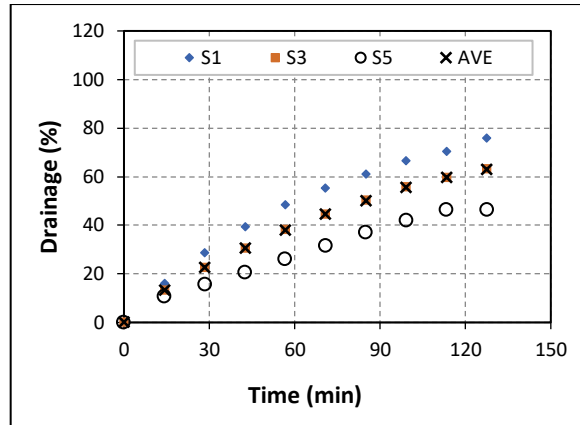


(d)

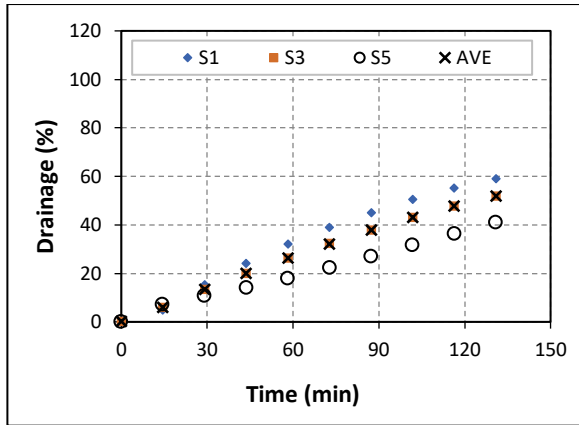
Figure 5.20. Fractional drainage vs. time for 40% quality foam at different mineral oil concentration: (a) No Oil, (b) 5%, (c) 10%, and (d) 20%



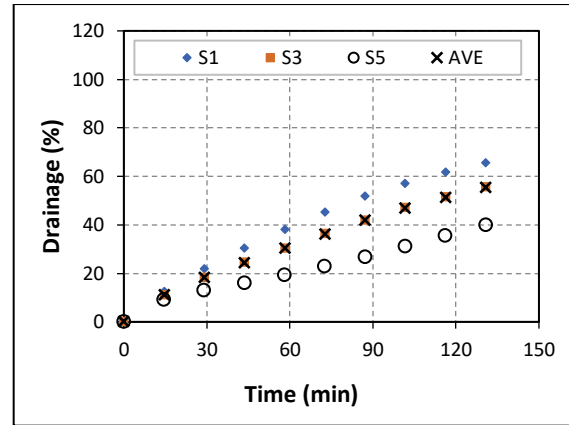
(a)



(b)



(c)



(d)

Figure 5.21. Fractional drainage vs. time for 50% quality foam at different mineral oil concentration: (a) No Oil, (b) 5%, (c) 10%, and (d) 20%

The AMDF of 60% quality foam was 35% in the absence of oil (Figure 5.22a). At 5% mineral oil concentration, the AMDF increased to 40% (Figure 5.22b). The AMDF further increased to 50% at a mineral oil concentration of 10% (Figure 5.22c). Further increase in the oil concentration increased the AMDF to 60% (Figure 5.22d). The behavior of 60% quality foam differs from those of 40% and 50% quality foams. The addition of mineral oil influenced the stability of foams. This shows that higher-quality foams are more sensitive to oil contaminants.

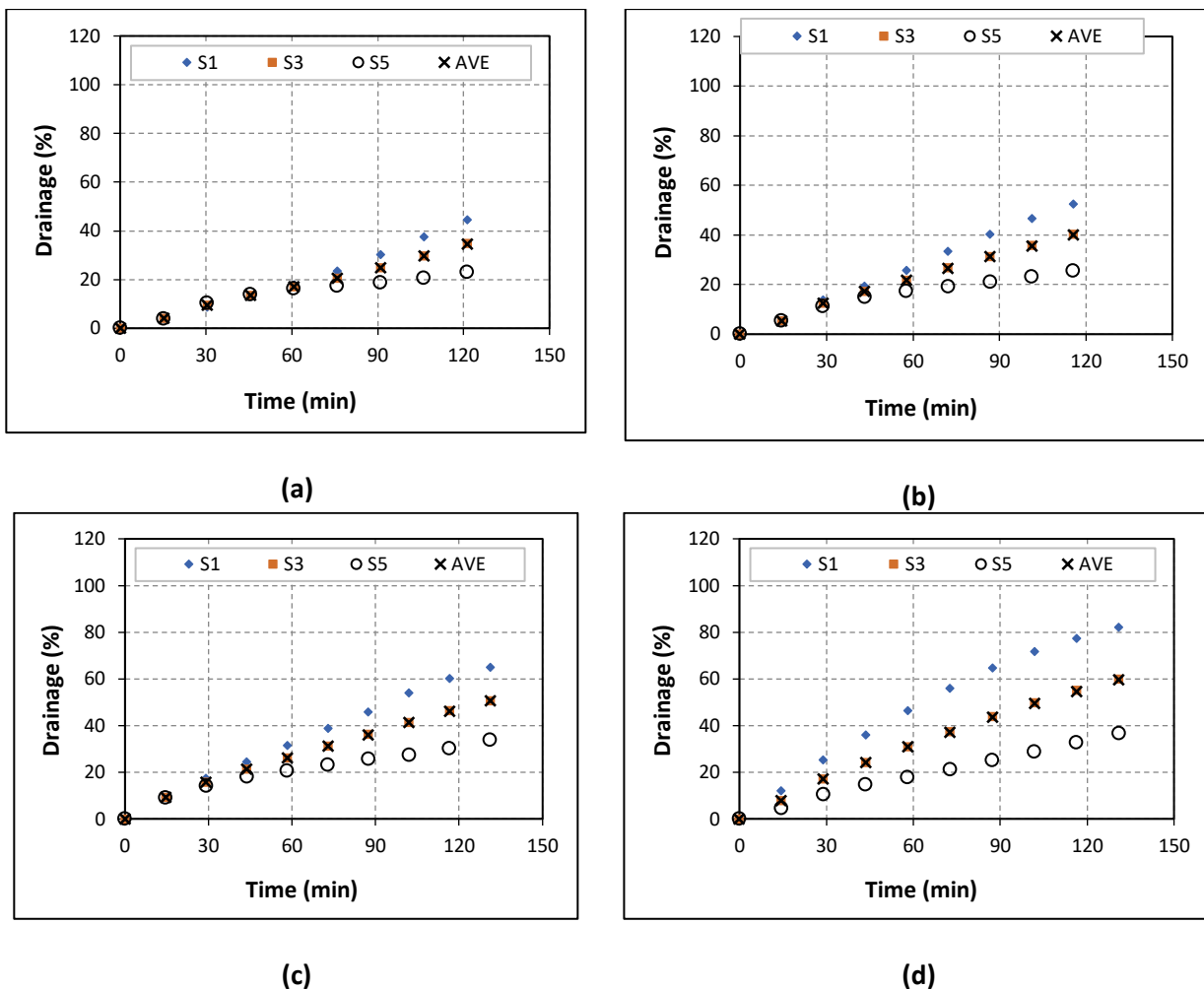


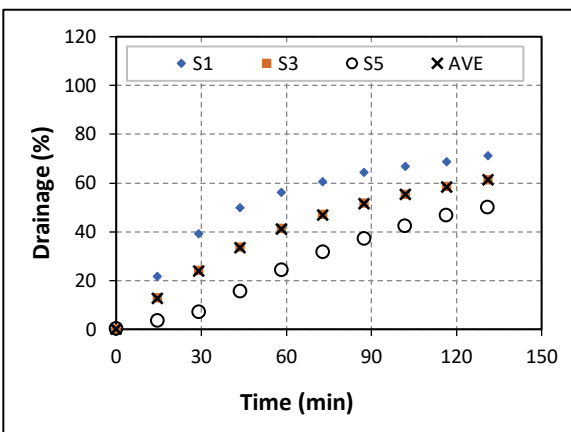
Figure 5.22. Drainage rate at 60% Quality (a) No Oil (b) 5% (c) 10% (d) 20%

5.5. Aqueous Foam with Clay

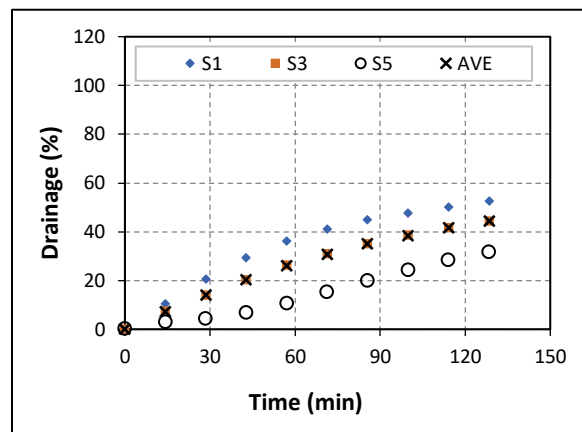
To investigate the drainage behavior of aqueous foam in the presence of clays, drainage experiments were conducted with foams containing bentonite and kaolinite. The effect of clay is analyzed by varying clay concentration and foam quality. The experiments were carried out at a fixed surfactant concentration of 2% vol which is above the surfactant CMC.

5.5.1. Effect of Bentonite

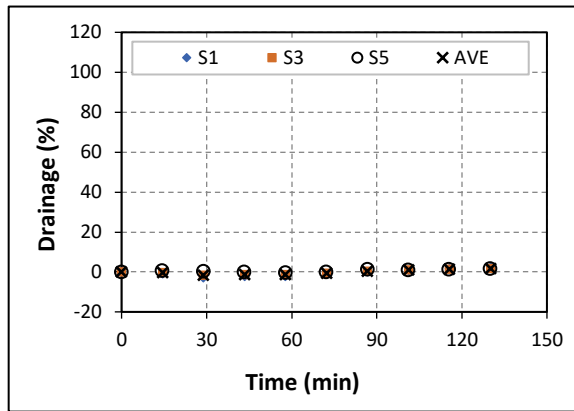
At 40% quality, the foam drainage increased with the concentration of bentonite (Figure 5.23). The AMDF of the aqueous foam in the absence of bentonite was 60%. As the bentonite concentration was increased to 2.5% w/w, the AMDF of 40% quality foam decreased to 42% (Figure 5.23b). And as more bentonite was added (5% w/w) the drainage rate further decreased to approximately 0% (Figure 5.23c). Overall, the addition of bentonite stabilized the foam. This observation agrees with the findings of Zhang et al. (2008).



(a)



(b)



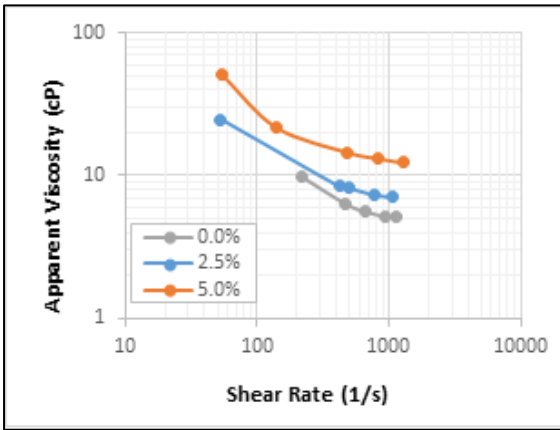
(c)

Figure 5.23. Drainage rate at 40% quality foam with different bentonite concentrations: (a) 0.0%, (b) 2.5%, and (c) 5.0%

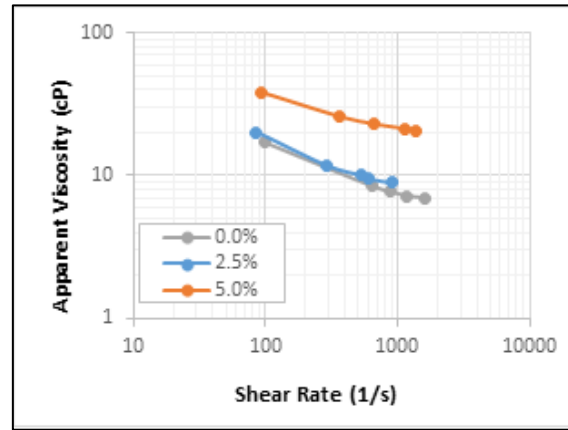
The possible explanations for the improvement of foam stability due to bentonite addition could be clay flocculation and/or an increase in viscosity of the base fluid. The absorption of surfactant by clay particles is due more to the hydrophobic interactions between them than electrostatic interaction. The increase in the clay concentration causes an increase in the rate of flocculation of the particles in the foam. The base fluid viscosity/rheology influences the stability of foam (Chen et al. 2005; Ibizugbe 2012; Sherif et al. 2016). Base liquid with low viscosity creates unstable foam in which the liquid drains quickly with limited viscous resistance in the foam network. The viscosity of the base fluid can be improved by adding viscosifiers such as clay and polymer. The viscosity of the base fluid was increased substantially with the addition of bentonite (Table 5.1). Furthermore, the addition of bentonite to the base fluid influences not only the drainage but also the rheology of foam. The increase in the shear stress and demonstrate that the increase in viscosity of the foam with increasing bentonite concentration (Figure 5.24). The same trend of reduction in foam drainage was observed for the 50% and 60% quality foams (Appendix A.1). Irrespective of the foam quality, bentonite clay stabilizes the aqueous foam.

Table 5.1: Rheology measurements of base fluids with bentonite

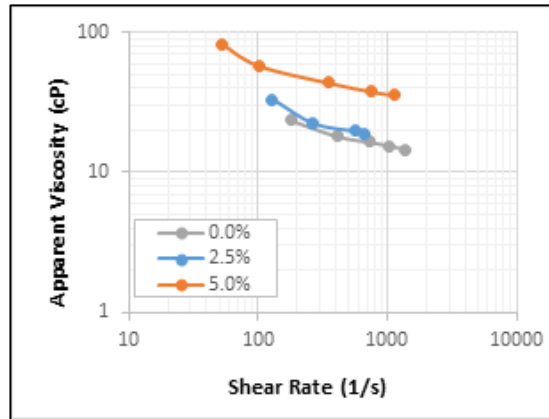
Rotational speeds (RPM)	Viscometer Readings		
	No Bentonite	2.5% Bentonite	5% Bentonite
3	0.1	0.2	0.4
6	0.4	0.8	1.2
100	0.7	1.2	5
200	0.9	2	8
300	1.2	2.6	9.2
600	2.2	4.6	16.4



(a)



(b)

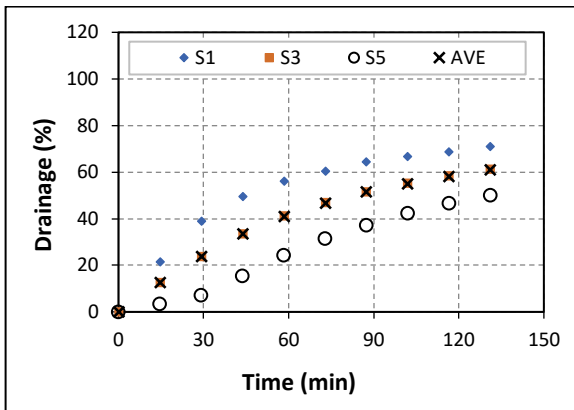


(c)

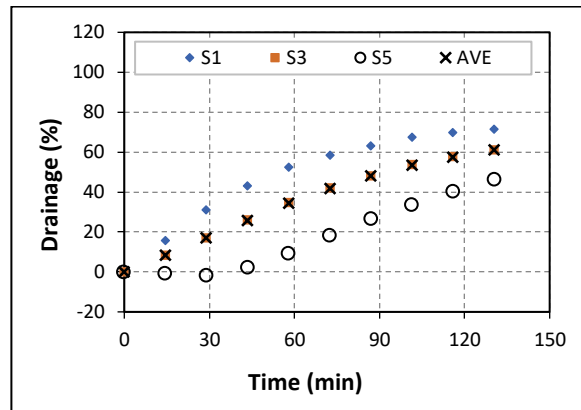
Figure 5.24: Rheology of bentonite containing foam at different qualities: a) 40%, b) 50%, and c) 60%

5.5.2. Effect of Kaolinite

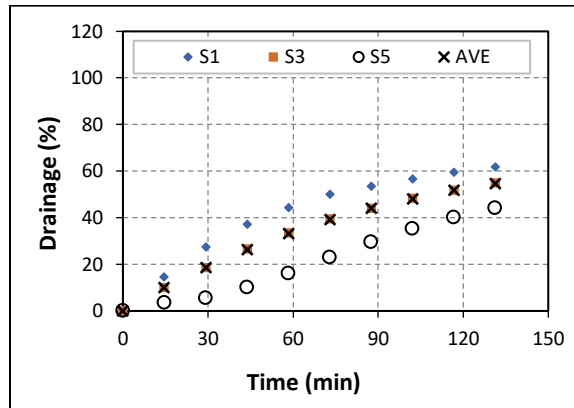
The stability behavior of aqueous foam in the presence of kaolinite was found different from that with bentonite. At 40% quality, the addition of 2.5% kaolinite had a limited effect on the drainage of foam (Figure 5.25). The drainage fraction follows the same trend in both cases and the AMDF was 60% in both cases. Similar results were obtained for other quality foams and the result is presented in Appendix A1. Base fluid viscosity is expected to improve foam stability. However, the addition of 2.5% kaolinite had little effect on the base fluid rheological properties (Table 5.2). The viscosity change due to kaolinite was minor. Besides this, little change in the rheology of foam was observed with the addition of 2.5% Kaolinite (Figure 5.25b). After adding 5% kaolinite, the drainage of the foam showed a noticeable difference (Figure 5.25c).



(a)



(b)

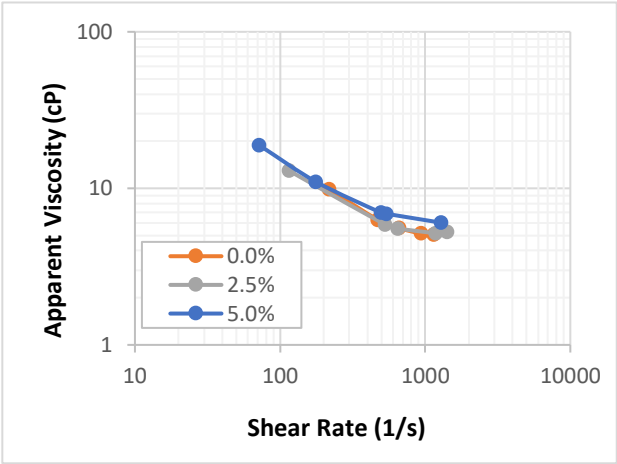


(c)

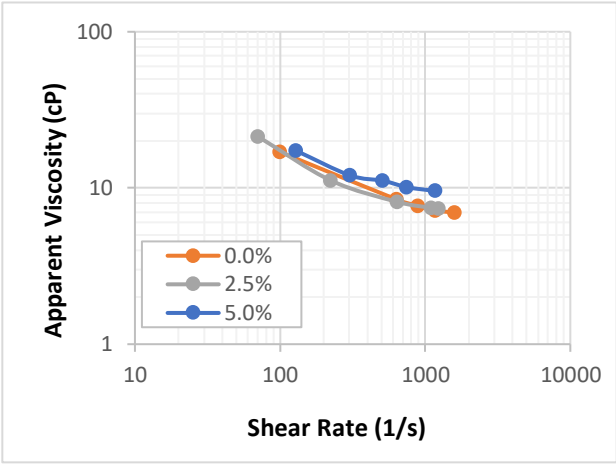
Figure 5.25. Drainage rate at 40% quality foam with different Kaolinite concentrations: (a) 0.0%, (b) 2.5%, and (c) 5%

Table 5.2: Rheology measurements of base fluids with Kaolinite

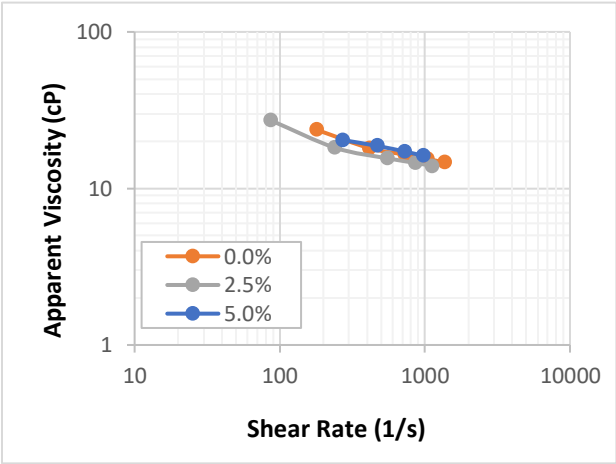
Rotational speeds (RPM)	Viscometer Readings		
	No Kaolinite	2.5% Kaolinite	5% Kaolinite
3	0.1	0.1	0.2
6	0.4	0.4	0.5
100	0.7	0.75	1
200	0.9	0.9	1.1
300	1.2	1.3	1.4
600	2.2	2.4	2.6



(a)



(b)



(c)

Figure 5.26. Rheology of kaolinite containing foam at different qualities: a) 40%, b) 50%, and c) 60%

The AMDF in the absence of kaolinite was 60% and it decreased to 53% in the presence of 5% kaolinite. Overall, kaolinite did not have a significant effect on the stability of aqueous foam like bentonite. Figure 5.27 further demonstrates this distinction. The behavior of the trend-line does not appear linear, and more experiments can be carried out between 0 and 2.5% and 2.5% and 5 wt.% to understand if the reduction in the drainage rate with bentonite increase is linear or not.

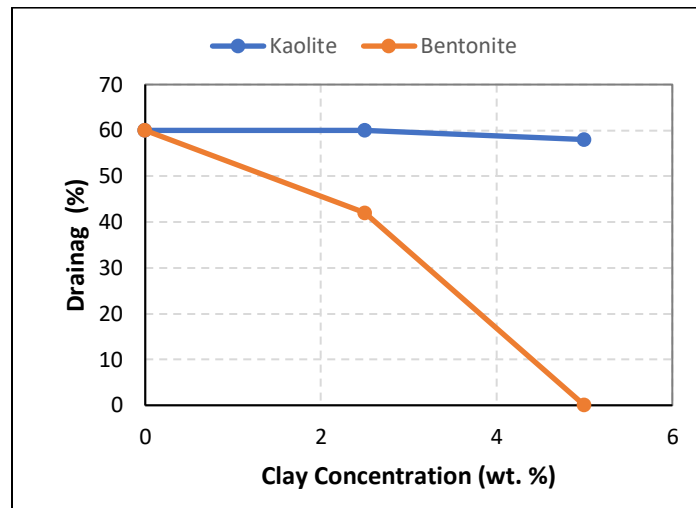


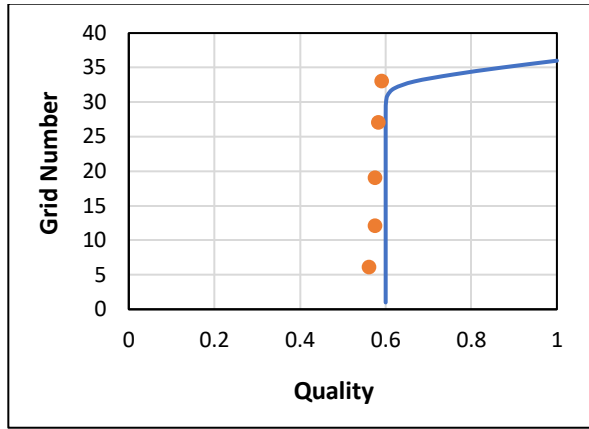
Figure 5.27. Drainage fraction versus clay concentration

5.6. Comparison of Model Predictions with Measurements

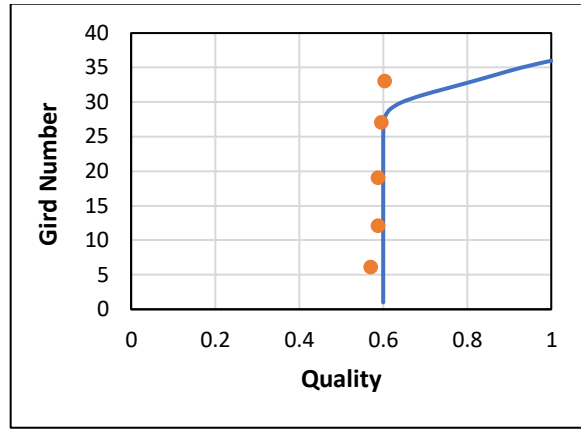
The results from the experiments are compared with predictions obtained from the numerical model. The numerical model considered in this work is the node-dominated drainage equation developed by Koehler et al (2000) and the numerical procedure and computer codes have been established by recent studies (Ibizugbe 2012; Govindu 2019). The comparison is performed for different foams qualities (40%, 50%, and 60%) and NaCl salt of concentrations (0% and 9%). The model predicts the quality profile in the foam column over two hours of the test run.

5.6.1. Aqueous Foam without Salt

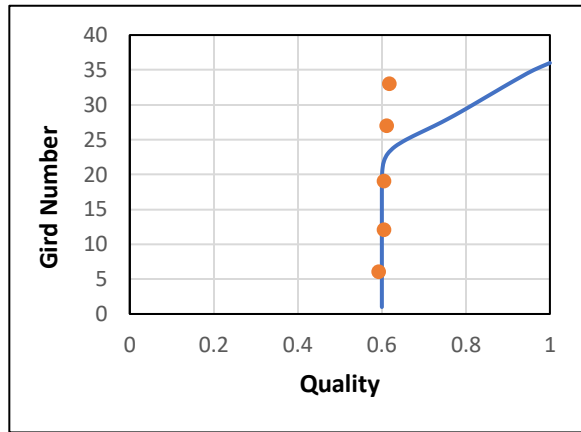
The model prediction obtained for the 0% salt content was compared with the experimental measurements to validate the model (Figure 5.28). Results show the quality profile in the foam column. At the early stage of time drainage (Figures 2.28a and 2.28b), there is a reasonable match between the model predictions and measurements. But at later times, there is a slight shift in the model prediction as compared to the measurements (Figures 2.28c, 2.28d, and 2.28e). The model assumes that the top of the foam column (grid 36) drains immediately after the start of the experiment and has a quality of 100% (i.e., totally gas at any computational time greater than zero). However, in reality, this is not the same observation as for high-quality foams, even at the top of the column, the foam quality gradually changes with time.



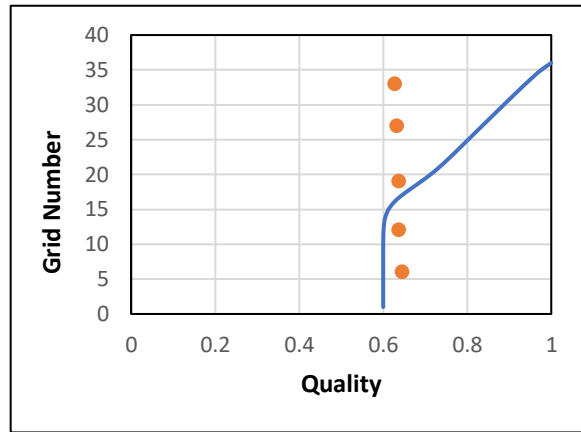
(a)



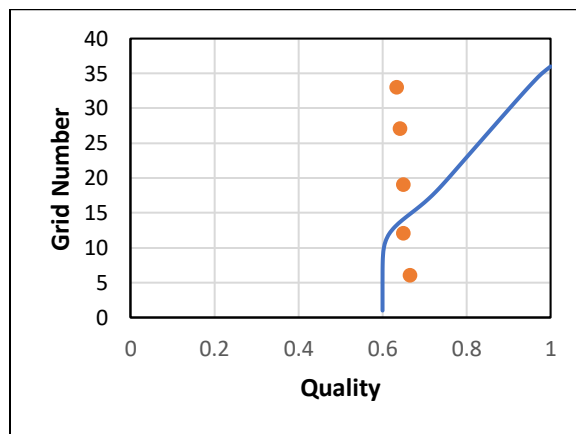
(b)



(c)



(d)



(e)



Figure 5.28. Quality profiles at 60% quality foam at 0% salt: (a) 15 minutes, (b) 30 minutes, (c) 60 minutes, (d) 100 minutes, and (e) 120 minutes

5.6.2. Aqueous Foam with 9% Salt

To validate the drainage model, the model prediction for quality profile is obtained for the 9% salt (NaCl) compared with measured data in Figure 5.29. The discrepancies between the model predictions and measurements observed in the 0% salt foam are observed in the 9% salt-containing foams. The drainage was slower in the 9% salt-containing foam as compared to the foam without salt contamination. The model predictions are reasonable in the early time of the drainage process.

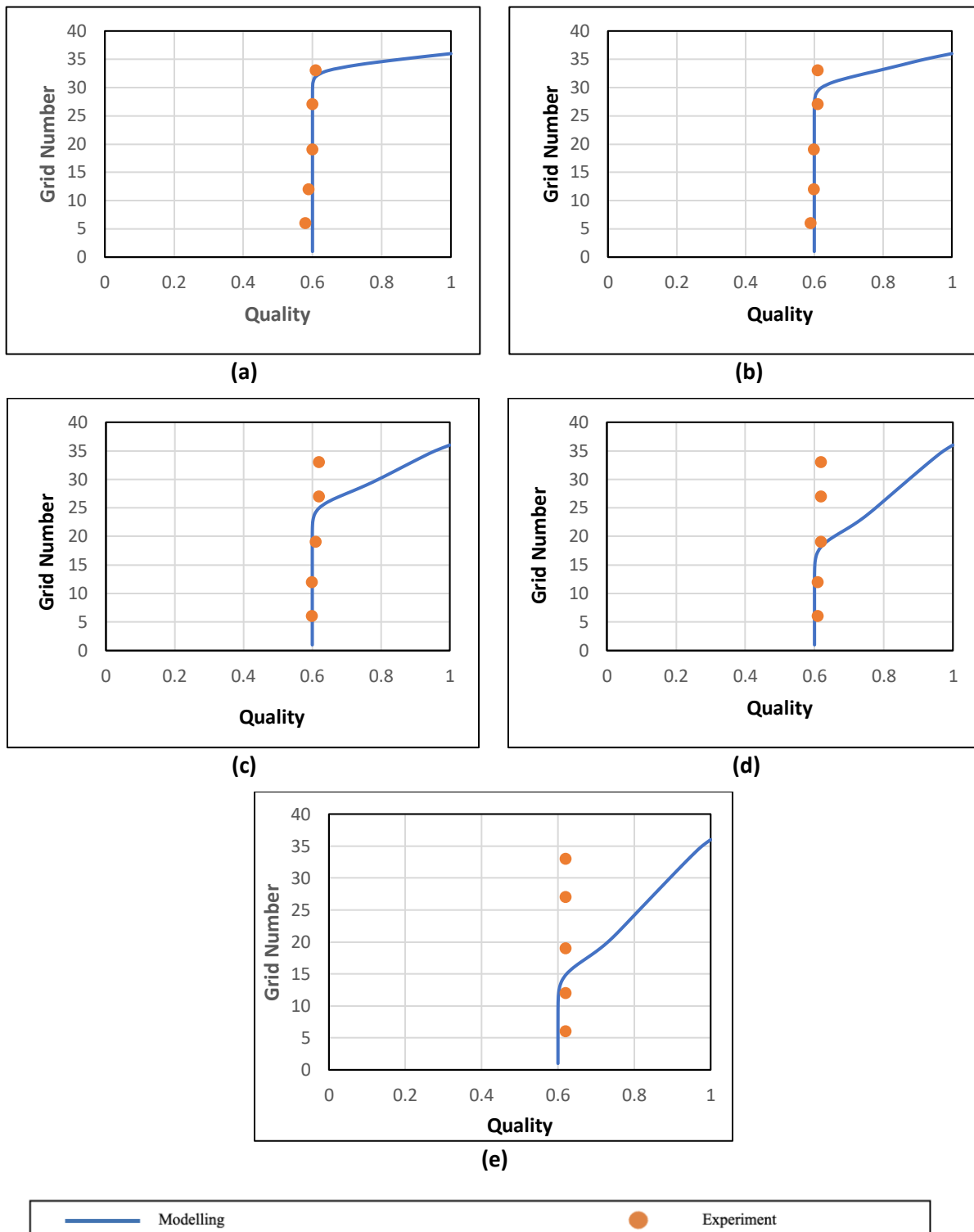


Figure 5.29. Quality profiles at 60% quality foam at 9% salt: (a) 15 minutes, (b) 30 minutes, (c) 60 minutes, (d) 100 minutes, and (e) 120 minutes

CHAPTER SIX

CONCLUSIONS AND RECOMMENDATIONS

The conclusions and recommendations for this work is broken into section depending on the type of contaminant present.

6.1. Conclusions

6.1.1. Aqueous Foam without Contaminant

- At a critical foam quality of 55%, there is a change in the behavior of foam due to the development of foam structure. The structure development was manifested by the reduction in foam behavior index and a sharp increase in apparent viscosity.
- Higher quality foams are more stable as compared to foam with lower qualities. This is shown from the normalized density plot for the 120 mins of which the test was analyzed. The higher the quality of foam, the more resistant the foam is to drainage and coalescence.
- Drainage measurements from the various foam qualities show that the foam at high qualities has a minimal drainage volume as compared to foams at high qualities.

6.1.2. Aqueous Foam with Salt

- Even though the addition of NaCl has minimal effects on the viscosity and density of the base liquid (surfactant solutions), it resulted in the thickening of aqueous foams.
- Foam drainage is affected by the type of salt and its concentration. The effect of salt concentration on drainage is mixed, it shows both increasing and decreasing trends of drainage with salt concentration depending on the concentration range.

6.1.3. Aqueous Foam with Oil

- The properties of the oil such as viscosity and composition affect the degree of change of the foam drainage rate at the same concentration. Higher viscous oil has a more stabilizing effect than less viscous oil.
- The contaminant in the crude oil decreases foam stability by increasing liquid drainage. The effect is due to the specific composition of the crude oil considered.
- The effect of mineral oil on foam stability is limited in smaller concentrations (less than 10%).

6.1.4. Aqueous Foam with Clay

- The presence of a small amount (up to 5%) of active clay such as bentonite can affect the drainage and rheology of foam and its base liquid rheological properties.
Bentonite strongly increased the viscosity of the base fluid and subsequently improves foam stability more than kaolinite. At the same concentration, kaolinite has a smaller thickening effect and the subsequently minimal impact in improving the stability of foam.

6.2. Recommendations

Based on the outcomes of the current study the following recommendations are made:

- It would be insightful to see the effect of all the contaminants combined and how they affect the drainage behavior of aqueous foams.
- This study was done considering a single diameter of the drainage section. There might be a change in drainage rate that might occur with varying the section diameter.

- The inclination considered is a 90-degree section which implies we are simulating a vertical well. Most of the oil wells drilled now are highly inclined and even horizontal wells. The effect of inclination would have on the drainage rate would be very insightful and practical.

NOMENCLATURE

AlCl_3 = Aluminum Chloride

CaCl_2 = Calcium Chloride

CMC = Critical Micelle Concentration

cP = centipoise

CTAB = Cetyltrimethylammonium Bromide; Hexadecyltrimethylammonium Bromide

EDL = Electrostatic Double Layer

EOR = Enhanced Oil Recovery

FGS = Foam Generation Section

FTIR = Fourier Transform Infrared Spectroscopy

K = Flow Consistency Index

KCl = Potassium Chloride

m = Mass (g)

M = Molar Mass kg/mol

MgCl_2 = Magnesium Chloride

mm = millimeter

NaCl = Sodium Chloride

nm = nanometer

P = Pressure (pa)

PB = Plateau Border

R = Gas Constant 8.314 J/mol.K

RPM = Revolutions per Minute

Sec = section

SDS - Sodium dodecyl sulfate

SDBS - Sodium Dodecylbenzene Sulfonate

T = Temperature (K)

V = Volume

wt. = weight

Γ = Foam Quality

ρ = Density (g/cm^3)

SUBSCRIPTS

f – Foam

g – Gas

L – Liquid

w – Water

REFERENCES

- Ahmed, R., Ergun, K., Arild, S. 2003. Critical Review of Drilling Foam Rheology. Annual Transactions of the Nordic Rheology Society 11: 1-10.
- Ahmed, S., Sri, H. A., Hashmet, M.R. 2019. CO₂ Foam as an Improved Fracturing Fluid System for Unconventional Reservoir. Exploitation of Unconventional Oil and Gas Resources - Hydraulic Fracturing and Other Recovery and Assessment Techniques.
- Akhtar, T.F., Ahmed, R., Elgaddafi, R., Shah, S., Amani, M. 2018. Rheological behavior of aqueous foams at high pressure. J. Pet. Sci. Eng. 162: 214-224.
- Alargova, Rossitza G., Devdutta Warhadpande, V. N. Paunov and O. Velev. (2004) Foam superstabilization by polymer microrods. Langmuir: the ACS journal of surfaces and colloids 20, 10371-10374.
- Andrianov, A., Farajzadeh, R., Mahmoodi Nick, M., Talanana, M., Zitha, P.L.J. 2012. Immiscible foam for enhancing oil recovery: Bulk and porous media experiments. Industrial and Engineering Chemistry Research 51, 2214–2226.
- Angarska, J. K., Tachev, K. D., Ivanov, I. B., Mehreteab, A., and Brose, G. 1997. Effect of magnesium ions on the properties of foam films stabilized with sodium dodecyl sulfate. Journal of Colloid and Interface Science, 195(2), 316–328.
- Argillier, J.F., Saintpere, S., Herzhaft, B., Toure, A. 1998. Stability and Flowing Properties of Aqueous Foams for Underbalanced Drilling. Paper Presented at SPE Annual Technical Conference and Exhibition, New Orleans, Louisiana, 27-30 September.
- Arnaudov, L., Denkov, N. D., Surcheva, I., Durbut, P., Broze, G., Mehreteab, A. 2001. Role of interfacial properties. Langmuir, 17(22), 6999–7010.

- Aveyard, R., Binks, B.P., Fletcher, P.D.I., Peck, T.G., Garrett, P.R. 1993. Entry and spreading of alkane drops at the air/surfactant solution interface in relation to foam and soap film stability. *Journal of the Chemical Society, Faraday Transactions* 89, 4313–4321.
- Basheva, E. S., Stoyanov, S., Denkov, N. D., Kasuga, K., Satoh, N., Tsujii, K. 2001. Foam boosting by amphiphilic molecules in the presence of silicone oil. *Langmuir*, 17(4), 969–979.
- Behera, M. R., Varade, S. R., Ghosh, P., Paul, P., Negi, A. S. 2014. Foaming in micellar solutions: Effects of surfactant, salt, and oil concentrations. *Industrial and Engineering Chemistry Research*, 53(48), 18497–18507.
- Beyer, K., Leine, D., Blume, A. 2006. The demicellization of alkyltrimethylammonium bromides in 0.1 M sodium chloride solution studied by isothermal titration calorimetry. 49, 31–39.
- Bhakta, A., and Ruckenstein, E. 1995a. Drainage of a Standing Foam. *Langmuir* 11(5), 1486–1492.
- Bhakta, A., and Ruckenstein, E. 1995b. Modeling of the Generation and Collapse of Aqueous Foams. *Langmuir* 12(12): 3089-3099.
- Bhakta, A., and Ruckenstein, E. 1997. Drainage and Coalescence in Standing Foams. *Journal of Colloid and Interface Science* 201(191), 184–201.
- Binks, B. P. 2002. Particles as surfactants-similarities and differences. *Current Opinion in Colloid & Interface Science* 7, 21-41.
- Blackwell, B.F., Sobolik, K.B. 1987. An Experimental Investigation of Pressure Drop of Aqueous Foam in Laminar Tube Flow. Sandia Report, No. SAND-85-1921. Sandia National Laboratories, Albuquerque, NM, USA.

- Bonilla, L.F., Shah, N.S., 2000. Experimental Investigation on the Rheology of Foams. Paper presented SPE/CERI Gas Technology Symposium, Calgary, Alberta, Canada, 3-5 April.
- Bournival, G. 2014. Stabilisation of Bubbles and Froths with Colloidal Particles and Inorganic Electrolytes. Ph.D. Thesis, The University of Newcastle, Australia.
- Bott, R., and Wolff, T. 1997. Micellization of cetyltrimethylammonium bromide in the presence of 9-anthryl alkanols. *Colloid and Polymer Science*, 275(9), 850–859.
- Carale, T. R., Pham, Q. T., Blankschtein, D. 1994. Salt Effects on Intramicellar Interactions and Micellization of Nonionic Surfactants in Aqueous Solutions. *Langmuir*, 10(1), 109.
- Chen, Z., Ahmed, R.M., Miska, S.Z., Takach, N.E., Yu, M., Pickell, M.B. 2005. Rheology Characterization of Polymer Drilling Foams Using a Novel Apparatus. *Annual Transactions of the Nordic Rheology Society* 13, 111–120.
- Chen, S., Liu, H., Yang, J., Zhou, Y., Zhang, J. 2019. Bulk foam stability and rheological behavior of aqueous foams prepared by clay particles and alpha olefin sulfonate. *Journal of Molecular Liquids*, 291, 111250.
- Craig, V. S. J., Ninham, B. W., and Pashley, R. M. 1993. The effect of electrolytes on bubble coalescence in water. *Journal of Physical Chemistry*, 97(39), 10192–10197.
- David, A., Marsden, S.S., 1969. The Rheology of Foam. SPE 2544-MS, Presented at 44th Annual Fall Meeting of the Society of Petroleum Engineers of AIME, Denver, Colo., Sept. 28 – Oct. 1.
- Davis, M. 2013. Basic Physics of Foam Stability and Collapse.
- De Vries, A. J., 1958. Foam stability. Part I. Structure and stability of foams. *Recueil Des Travaux Chimiques Des Pays-Bas* 77(1), 81–91.

- Denkov, N. D., Marinova, K., Tcholakova, S., Dentelle, M. 2002. Mechanism of Foam Destruction By Emulsions of PDMS-Silica Mixtures. Proceedings 3rd World Congress on Emulsions, 24–27.
- Denkov, N.D., Marinova, K.G. 2000. Antifoaming Action of Oils. In Proceedings of 3rd Eurofoam Conference. p. 199.
- Dong, B., Zhang, J., Zheng, L., Wang, S., Li, X., Inoue, T. 2008. Salt-induced viscoelastic wormlike micelles formed in surface-active ionic liquid aqueous solution. *Journal of Colloid and Interface Science*, 319(1), 338–343.
- Engelsen, C.W. den, Isarin, J.C., Goojier, H., Warmoeskerken, M. G., Wassink Groot, J. 2002. Bubble Size Distribution of Foam. *AUTEX Research Journal* 2(1): 14–27.
- Eren, T. 2004. Foam Characterization: Bubble Size and Texture Effects, MS Thesis, Middle East Technical University, Turkey.
- Falls A.H, Musters J.J, Ratulowski J. 1989 The apparent viscosity of foams in homogeneous bead packs. *SPE Reservoir Eng* 4(5):155–164.
- Fang, L., Gan-Zuo, L., Han-Qing, W., and Xue, Q. J. 1997. Studies on cetyltrimethylammonium bromide (CTAB) micellar solution and CTAB reversed microemulsion by ESR. *Colloids and Surfaces A: Physicochemical and Engineering Aspects*, 127(1–3), 89-96
- Farajzadeh R, Andrianov A, and Bruining H, Zitha P. 2009. Comparative study of CO₂ and N₂ foams in porous media at low and high pressure-temperatures. *Ind Eng Chem Res* 48(9), 4542–4552.

- Farzaneh, S.A., Sohrabi, M. 2013. A Review of the Status of Foam Applications in Enhanced Oil Recovery. Paper presented at EAGE Annual Conference and Exhibition, London, UK., 10-13 June.
- Gallego-Juárez, J. A., Rodríguez, G., Riera, E., Cardoni, A. 2015. Ultrasonic defoaming and debubbling in food processing and other applications. *Power Ultrasonics: Applications of High-Intensity Ultrasound*, 793–814.
- Garrett, P.R. 1993. Recent Developments in the Understanding of Foam Generation and Stability. *Chemical Engineering Science* 48(2), 367-392.
- Ghosh, P. 2004. Coalescence of air bubbles at air-water interface. *Chemical Engineering Research and Design*, 82(7), 849–854.
- Giribabu, K., Reddy, M. L. N., Ghosh, P. 2008. Coalescence of air bubbles in surfactant solutions: Role of salts containing mono-, di-, and trivalent ions. *Chemical Engineering Communications*, 195(3), 336–351.
- Govindu, A. 2019. Drainage Behavior of Aqueous, Polymeric, and Oil-Based Nitrogen Foams: Theoretical and Experimental Investigation. Ph.D. Thesis, University of Oklahoma, Norman, Oklahoma.
- Govindu, A., Ahmed, R., Shah, S., Amani, M. 2019. Stability of foams in pipe and annulus. *Journal of Petroleum Science and Engineering* 180: 594 - 604.
- Gonzenbach, T., Andre, R. Studart, Elena Tervoort, and Ludwig J. G. 2006. Stabilization of Foams with Inorganic Colloidal Particles. *Langmuir* 22, 10983-10988.
- Haas, P.A., Johnson, H.F. 1967. A Model and Experimental Results for Drainage of Solution Between Foam Bubbles. *Industrial and Engineering Chemistry Fundamentals* 6(2): 225–233.

- Hadjiiski, A., Tcholakova, S., Denkov, N.D., Durbut, P., Broze, G., Mehreteab, A. 2001. Effect of Oily Additives on Foamability and Foam Stability. 2. Entry Barriers Langmuir 17 (22), 7011-7021.
- Harris, P.C., Health, S.J. 1996. High-Quality Foam Fracturing Fluids. Paper presented at SPE Gas Technology Symposium held In Calgary, Alberta, Canada, April 28 - May 1.
- Hirt, Douglas E., Robert K. Prud'homme, Ludwig Rebenfeld. 1987. Characterization of Foam Cell Size and Foam Quality Using Factorial Design Analyses. Journal of Dispersion Science and Technology 8(1): 55–73.
- Ibizugbe, N. O. 2012. Drainage Behavior of Oil-Based Drilling Foam Under Ambient Condition. MS-Thesis, University of Oklahoma.
- Isrealachvili, J.N. 1997. Intermolecular and Surface Forces. pp 276 - 281.
- Iyota, H., Krastev, R. 2009. Miscibility of sodium chloride and sodium dodecyl sulfate in the adsorbed film and aggregate. Colloid and Polymer Science, 287(4), 425–433.
- Koczo, K., Lobo, L. A., Wasan, D. T. 1992. Effect of oil on foam stability: Aqueous foams stabilized by emulsions. Journal of Colloid And Interface Science, 150(2), 492–506.
- Koehler, S. A., Hilgenfeldt .S., Stone H .A.1999. Liquid Flow through Aqueous Foams: The Node-Dominated Foam Drainage Equation, Phys. Rev. Lett. 82, 4232.
- Koehler, S. A., Hilgenfeldt, S., Stone, H. A. 2000. Generalized view of foam drainage: Experiment and theory. Langmuir 16(15): 6327–6341.
- Kralchevsky, P. A., Danov, K. D., Broze, G., Mehreteab, A. 1999. Thermodynamics of ionic surfactant adsorption with account for the counterion binding: Effect of salts of various valency. Langmuir, 15(7), 2351–2365.

- Kuhlman, M. I. 1990. Visualizing the Effect of Light Oil on CO₂ Foams. *J Pet Technology* 42 (1990): 902–908.
- Kumar, M. K., Ghosh, P. 2006. Coalescence of air bubbles in aqueous solutions of ionic surfactants in presence of inorganic salt. *Chemical Engineering Research and Design*, 84(8 A), 703–710.
- Leonard, R. A., Lemlich, R. 1965. A study of interstitial liquid flow in foam. Part I. Theoretical model and application to foam fractionation. *AIChE Journal* 11(1): 18–25.
- Lessard, R.R., Zieminski, S.A. 1971. Bubble Coalescence and Gas Transfer in Aqueous Electrolytic Solutions. *Ind. Eng. Chem. Fundamen.* Vol. 10, 2, 260–269.
- Levine, S., Bowen, B. D., and Partridge, S. J. 1989. Stabilization of Emulsions by Fine Particles I. Partitioning of Particles between Continuous Phase and Oil/Water. *Interface Colloids & Surfaces* 38(2): 325–343.
- Li, D., Slattery, J. C. 1988. Experimental support for analyses of coalescence. *AIChE Journal*, 34(5), 862–864.
- Li, Y., Kuru, E. 2004. Optimization of hole cleaning in vertical wells using foam. Paper Presented at SPE International Thermal Operations and Heavy Oil Symposium and Western Regional Meeting, Bakersfield, California, U.S.A., 16–18 March. SPE 86927-MS.
- Li, Y., Kuru, E. 2009. Optimization of hole cleaning in vertical wells using foam. *Energy Sources, Part A: Recovery, Utilization and Environmental Effects* 31(1): 1–16.
- Liu, Y., Grigg, R. B., Bai, B. 2005. Salinity, pH, and surfactant concentration effects on CO₂-foam. *Proceedings - SPE International Symposium on Oilfield Chemistry*, 307–317.
- Lu, J., Corvalan, C. M. 2012. Coalescence of viscous drops with surfactants. *Chemical Engineering Science*, 78, 9–13.

- Maini, Brij B., Vincent Ma. 1986. Laboratory Evaluation Of Foaming Agents For High-Temperature Applications - I. Measurements Of Foam Stability at Elevated Temperatures And Pressures, *Journal of Canadian Petroleum Technology* 25(6): 85-89.
- Marčelja, S. 2006. Selective coalescence of bubbles in simple electrolytes. *Journal of Physical Chemistry B*, 110(26), 13062–13067.
- Martins, A. L., Lourenço, A. M. F., De Sá, C. H. M. 2000. Foam Properties Requirements for Proper Hole Cleaning While Drilling Horizontal Wells in Underbalanced Conditions. SPE - Asia Pacific Oil and Gas Conference, 247–257.
- Martins, A. L., Lourenço, A. M. F., De Sá, C. H. M. 2000. Foam Properties Requirements for Proper Hole Cleaning While Drilling Horizontal Wells in Underbalanced Conditions. Paper presented at SPE - Asia Pacific Oil and Gas Conference, Brisbane, Australia, 16–18 October.
- Nikolov, A.D., Wasan, D.T., Huang, D.W., Edwards, D.A. 1986. The effect of oil on foam stability: Mechanisms and implications for oil displacement by foam in porous media. In *Proceedings - SPE Annual Technical Conference and Exhibition*.
- Novosad, J.J., Mannhardt, K. 1989. The Interaction Between Foam And Crude Oils. Paper presented at the Annual Technical Meeting.
- Oh, S. G., Shah, D. O. 1993. Effect of counterions on the interfacial tension and emulsion droplet size in the oil/water/dodecyl sulfate system. *Journal of Physical Chemistry*, 97(2), 284–286.
- Okpobiri, G.A, Ikoku, C.U. 1986. Volumetric Requirements for Foam and Mist Drilling Operations. *SPE Drilling Engineering*, 1(1), 71–88.
- Pickering, S. U. 1907. Pickering: emulsions. *J. Chem. Soc. Trans.* 91 (23), 2001–202.

- Pugh, R.J., 1996. Foaming, foam films, antifoaming and defoaming. *Advances in Colloid and Interface Science*, 64, 67-142.
- Princen, H.M., Goddard, E.D. 1972. The effect of mineral oil on the surface properties of binary surfactant systems. *Journal of Colloid and Interface Science* 38, 523–534.
- Qazi, M. J., Schlegel, S. J., Backus, E. H. G., Bonn, M., Bonn, D. 2020. Dynamic Surface Tension of Surfactants in the Presence of High Salt Concentrations.
- Ramani, M. V., Gandhi, K.S., Kljmar, R. 1993. A Model for Static Foam Drainage. *Chemical Engineering Science*, 48(3), 455-465.
- Ramsden, W. 1903. Separation of solids in the surface-layers of solutions and ‘suspensions’ (observations on surface-membranes, bubbles, emulsions, and mechanical coagulation). - Preliminary account *Proc. R. Soc. Lond.* 72, 156–164.
- Rand, P.B., Kraynik, A.M. 1983. Drainage of Aqueous Foams: Generation-Pressure and Cell-Size Effects. *Society of Petroleum Engineers journal* 23(1), 152–154.
- Rao, A.A., Wasan, D.T., Manev, E. D. 1982. Foam Stability – Effect of Surfactant Composition on the Drainage of Microscopic Aqueous Films. *Chemical Engineering Communications*, 15(1-4), 63 – 81.
- Rehm, B., Paknejad, A. 2012. Foam Drilling. In *Underbalanced Drilling: Limits and Extremes*. pp. 197 – 233
- Rojas, Y., Kakadjian, S., Aponte, A., Marquez, R., G. Sanchez. 2001. Stability and Rheological Behavior of Aqueous Foams for Underbalanced Drilling. Paper presented at SPE International Symposium on Oilfield Chemistry. pp. 219 - 229.
- Ruckenstein, E., Bhakta, A. 1996. Effect of Surfactant and Salt Concentrations on the Surfactants. *Langmuir* 12, 4134–4144.

- Saint-Jalmes, A., Langevin, D. 2002. Time Evolution of Aqueous Foams : Drainage and Coarsening. *Journal of Physics: Condensed Matter* 14(40), 9397–9412.
- Saint-Jalmes, A. 2006. Physical Chemistry in Foam Drainage and Coarsening. *Soft Matter* 2(10), 836-849.
- Sani, M., Mohanty, K.K. (2009). Incorporation of clay nano-particles in aqueous foams. *Colloids and Surfaces A: Physicochemical and Engineering Aspects*. 340.
- Sherif, T., Ahmed, R., Shah, S., Amani, M. 2016. Rheological correlations for oil-based drilling foams. *Journal of Natural Gas Science and Engineering*, 35, 1249–1260.
- Sherif, T., Ahmed, R., Shah, S., Amani, M. 2016. Rheological Correlations for Oil-Based Drilling Foams. *Journal of Natural Gas Science and Engineering* 35, 1249–1260.
- Simjoo, M., Rezaei, T., Andrianov, A., Zitha, P. L. J. 2013. Foam stability in the presence of oil: Effect of surfactant concentration and oil type. *Colloids and Surfaces A: Physicochemical and Engineering Aspects*, 438, 148–158.
- Sinha, V., Ahmed, R., Akhtar, T., Shah, S., Amani, M. 2019. Rheology and hydraulics of polymer-based foams at elevated temperatures. *Journal of Petroleum Science and Engineering* 180, 330–346.
- Skauge, A., Solbakken, J., Ormehaug, P. A., Arra, M. G. 2020. Foam Generation, Propagation and Stability in Porous Medium. *Transport in Porous Media* 131(1), 5–21.
- Soleymani, M., Kamali, M. R., Saeedabadian, Y. 2013. Experimental Investigation of Physical and Chemical Properties of Drilling Foam and Increasing its Stability. *Iranian Journal of Chemistry and Chemical Engineering* 32(3), 127–132.
- Stefan, H., Denis, S., Anthony, S., Simon, C., Nicolas, P. 2005. The Physics of Foam Drainage. *European Detergents Conference*, pp. 191 - 206.

- Sunmonu, R. M., Onyekonwu, M. 2013. Enhanced oil recovery using foam injection; a mechanistic approach. Paper presented at Society of Petroleum Engineers - 37th Nigeria Annual Int. Conf. and Exhibition, 2, 1061–1073.
- Taiwo, O., Ogbonna, J. 2011. Foam Cementing Design and Application: A Cure for Low Gradient- Associated Problems in Deepwater Operations in the Gulf of Guinea. Paper presented at Society of Petroleum Engineers Nigeria Annual International Conference and Exhibition, Abuja, Nigeria, 30 July–3 August.
- Tuna. E. 2004. Foam Characterization: Bubble Size and Texture Effects.
- Varade, S. R., Ghosh, P. 2017. Foaming in aqueous solutions of zwitterionic surfactant: Effects of oil and salts. *Journal of Dispersion Science and Technology*, 38(12), 1770–1784.
- Warszyński, P., Lunkenheimer, K., Czichocki, G. 2002. Effect of counterions on the adsorption of ionic surfactants at fluid-fluid interfaces. *Langmuir*, 18(7), 2506–2514.
- Weaire, D., Phelan, R. 1996. The Physics of Foam. *Journal of Physics Condensed Matter* 8(47), 9519–9524.
- Yang, F., Liu, S., Xu, J. et al. 2006. Pickering Emulsions Stabilized Solely by Layered Double Hydroxides Particles: The Effect of Salt on Emulsion Formation and Stability. *J Colloid & Interface Sci* 302 (1), 159–169.
- Yu, L., Li, s., Stubbs, L. P., Hon C. L. 2021. Effects of Salinity and pH on the Stability of Clay-Stabilized Oil-in-Water Pickering Emulsions. *SPE J.* 26, 1402–1421.
- Zajac, J., Thompett, J. L., Partyka, S., 1996. Adsorption of Cationic Surfactants on a Hydrophilic Silica Surface at Low Surface Coverages: Effects of the Surfactant Alkyl Chain and Exchangeable Sodium Cations at the Silica Surface. *Langmuir* 12, 1357 - 1367

Zhang, S., Sun, D., Dong, X., Li, C., Xu, J. 2008. Aqueous foams stabilized with particles and nonionic surfactants. *Colloids and Surfaces A: Physicochemical and Engineering Aspects* 324(1–3), 1–8.

Appendix A: Drainage Measurements

A.1 Results for Clay Contaminated Foams

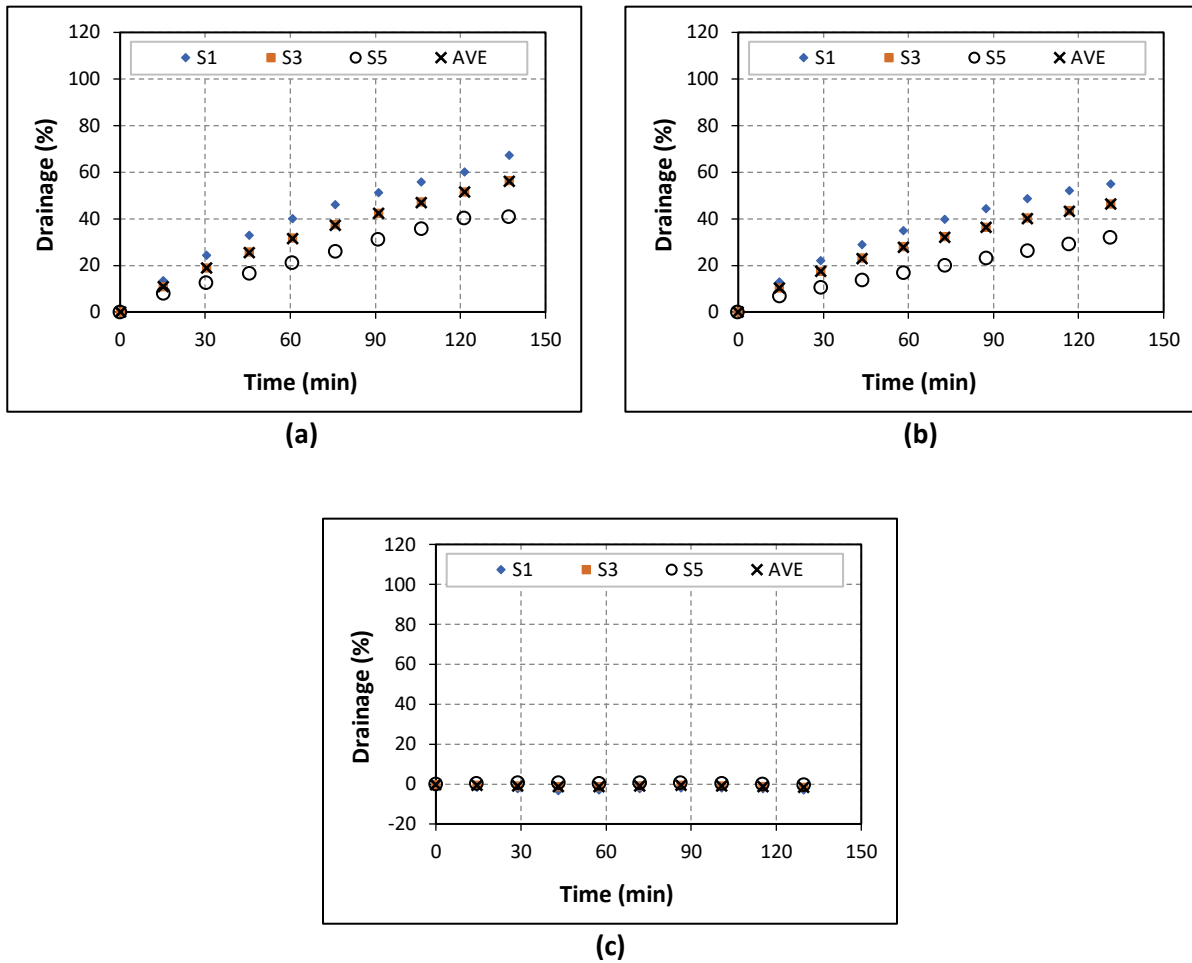
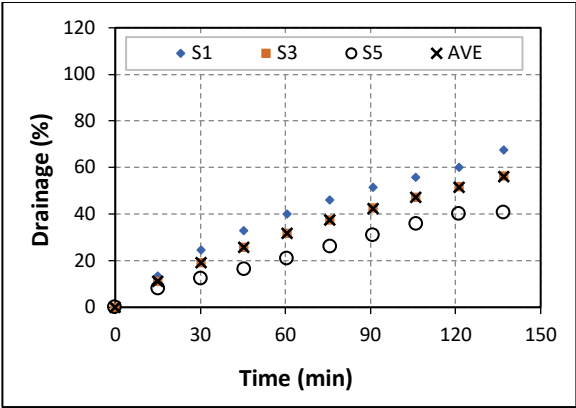
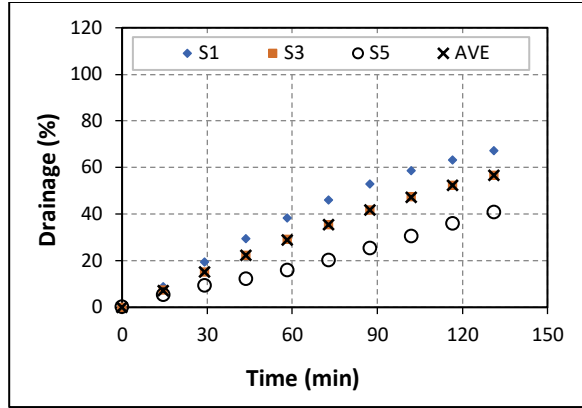


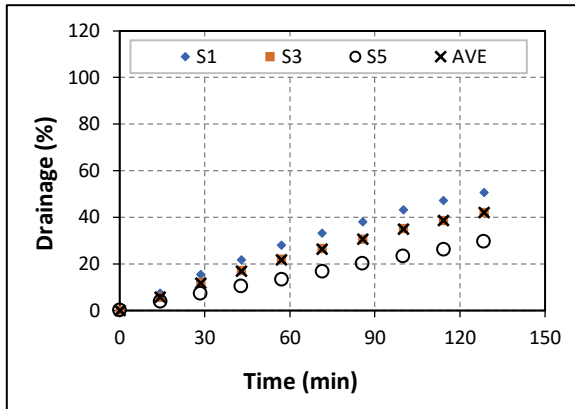
Figure A.1.1. Drainage fraction versus time at 50% Quality (a) No Bentonite (b) 2.5% Bentonite (c) 5% Bentonite



(a)

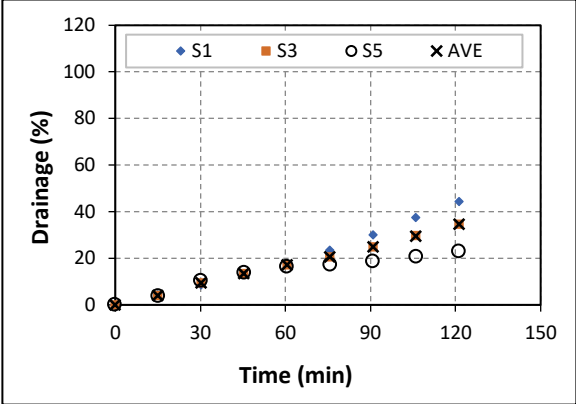


(b)

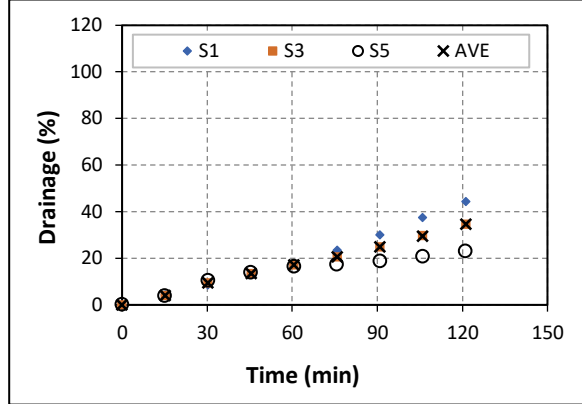


(c)

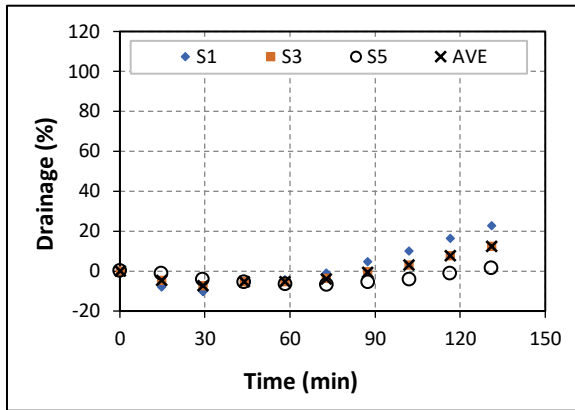
Figure A.1.2. Drainage rate at 50% Quality (a) No Kaolinite (b) 2.5% Kaolinite (c) 5% Kaolinite



(a)

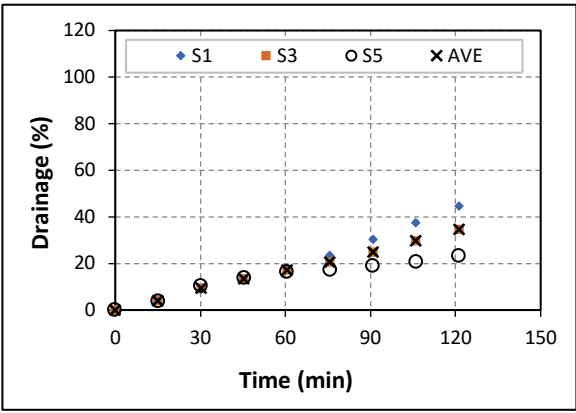


(b)

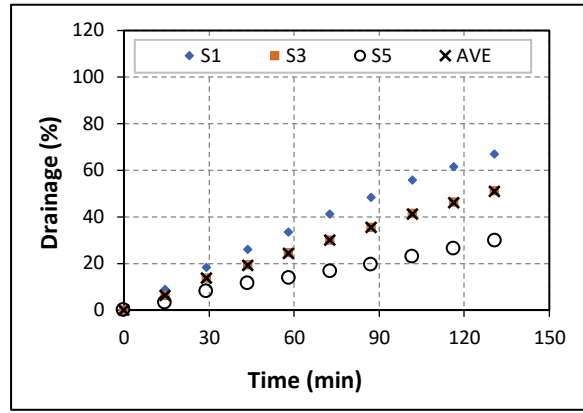


(c)

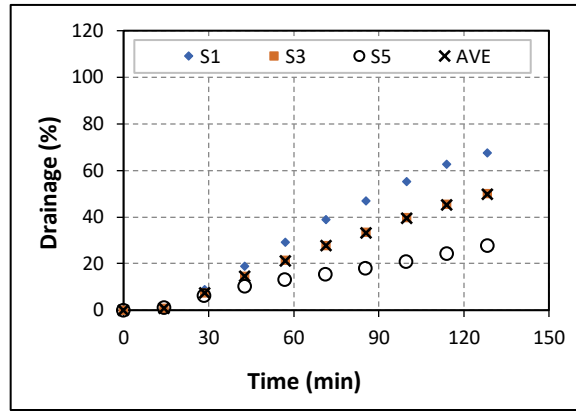
Figure A.1.3. Drainage rate at 60% Quality (a) No Bentonite (b) 2.5% Bentonite (c) 5% Bentonite



(a)



(b)



(c)

Figure A.1.4. Drainage rate at 60% Quality (a) No Kaolinite (b) 2.5% Kaolinite (c) 5% Kaolinite

Appendix B: Foam Rheology Measurements

B.1 Results for Salt Contaminated Foams

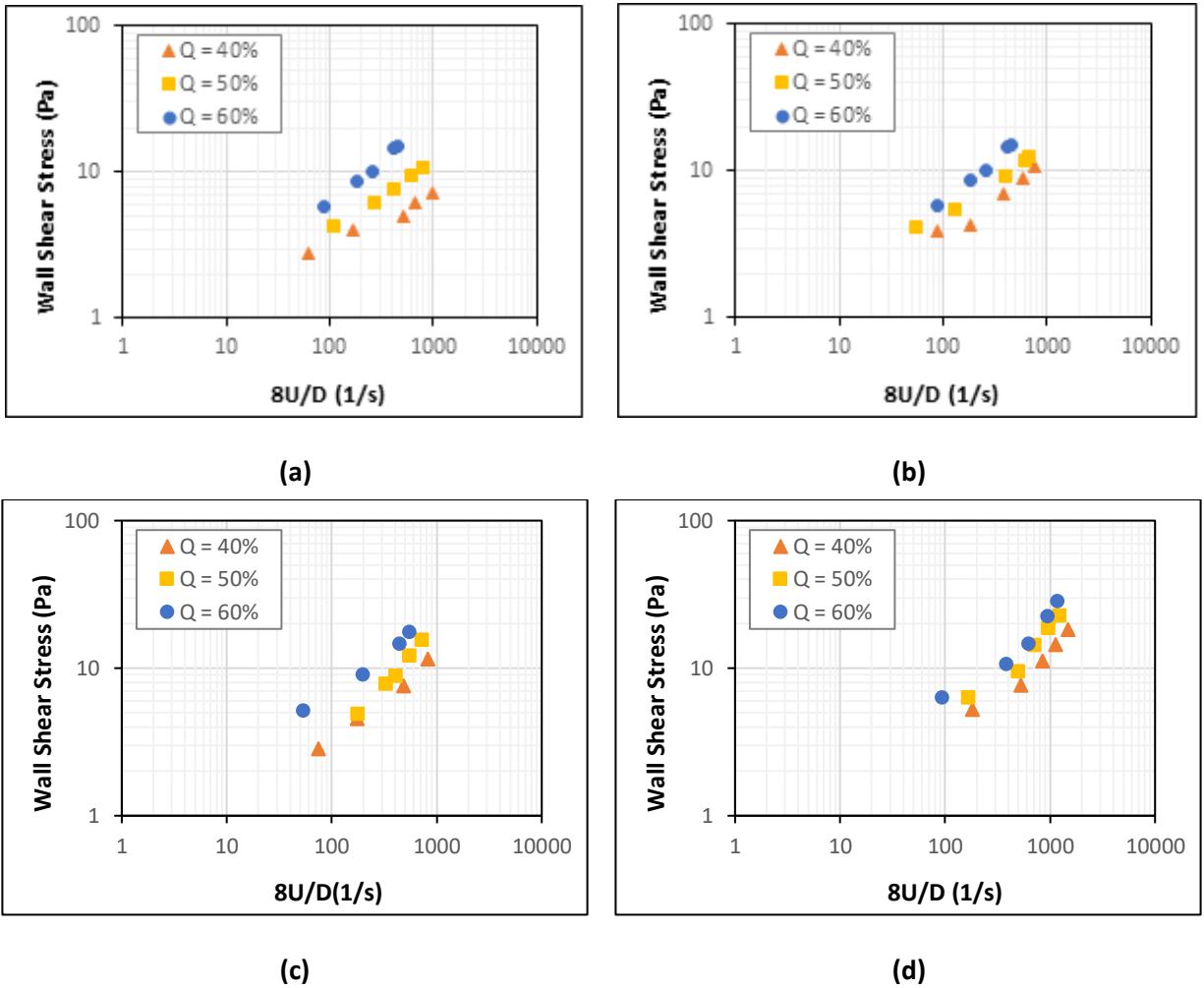
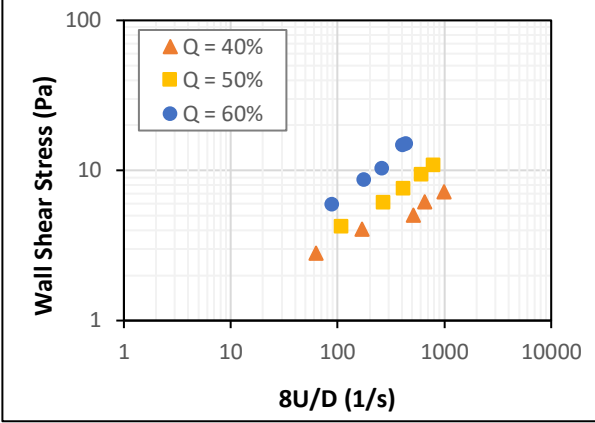
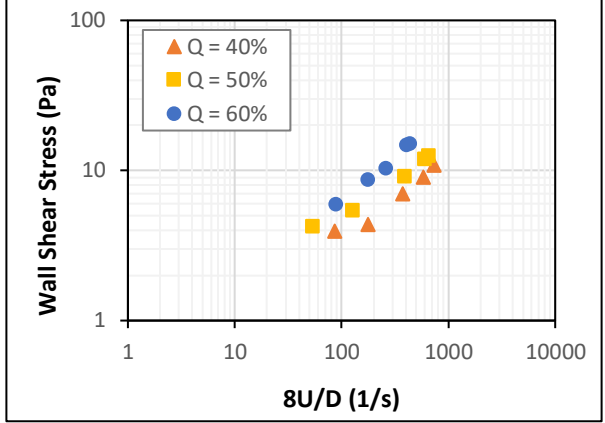


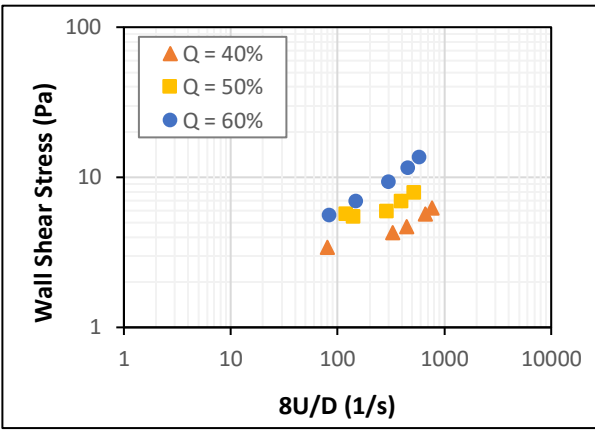
Figure B.1.1. Shear stress vs. nominal Newtonian shear rate for: a) 5%; b) 9%; c) 14%; and d) 18% NaCl foams



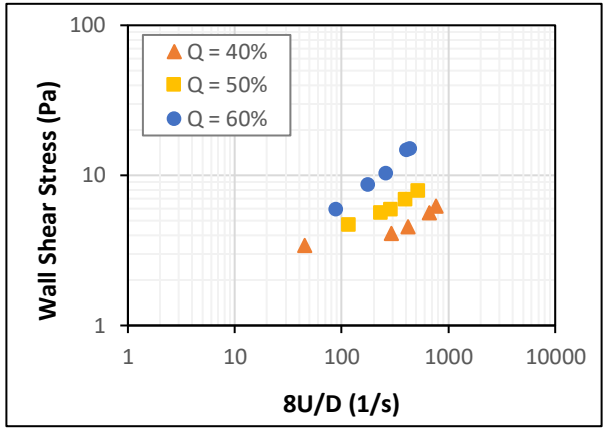
(a)



(b)



(c)



(d)

Figure B.1.2. Shear stress vs. nominal Newtonian shear rate for: a) 5%; b) 9%; c) 14%; and d) 18% CaCl₂ foams

B.2 Results for Oil Contaminated Foams

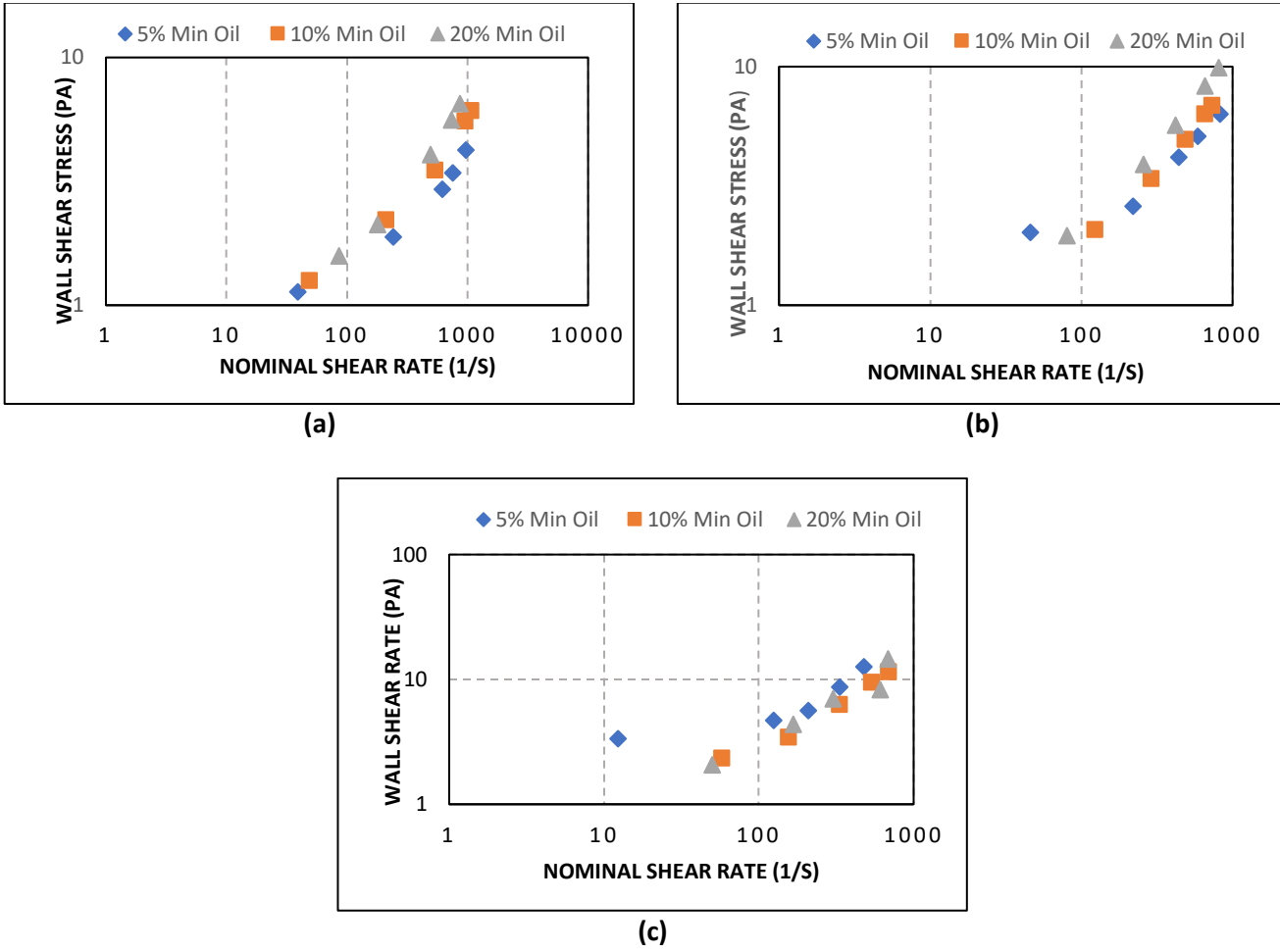
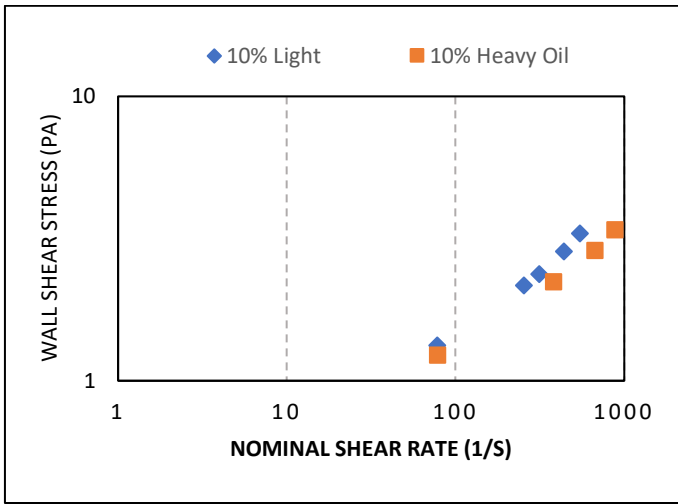
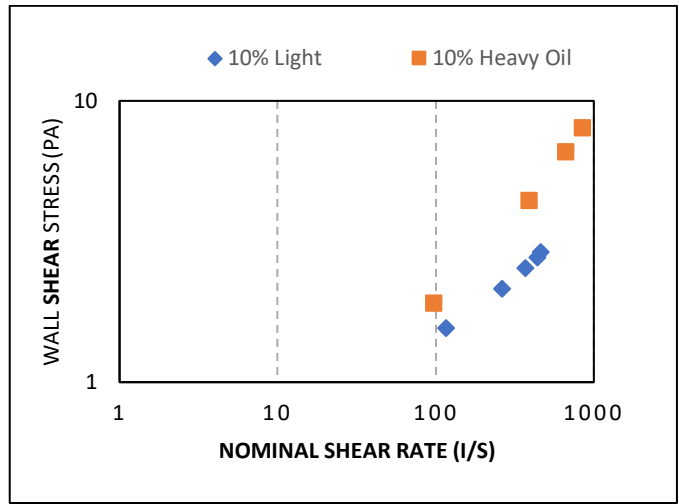


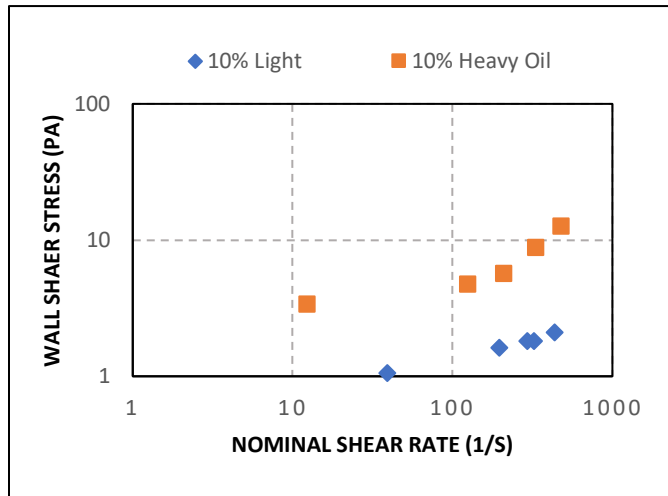
Figure B.2.1. Effect of the Mineral Oil on Foam Rheology a.) 40% Quality b.) 50% Quality
c.) 60% Quality



(a)



(b)



(c)

Figure B.2.2. Effect of the Crude Oil on Foam Rheology a.) 40% Quality b.) 50% Quality c.) 60% Quality

Appendix C: Mathematical Modelling Results

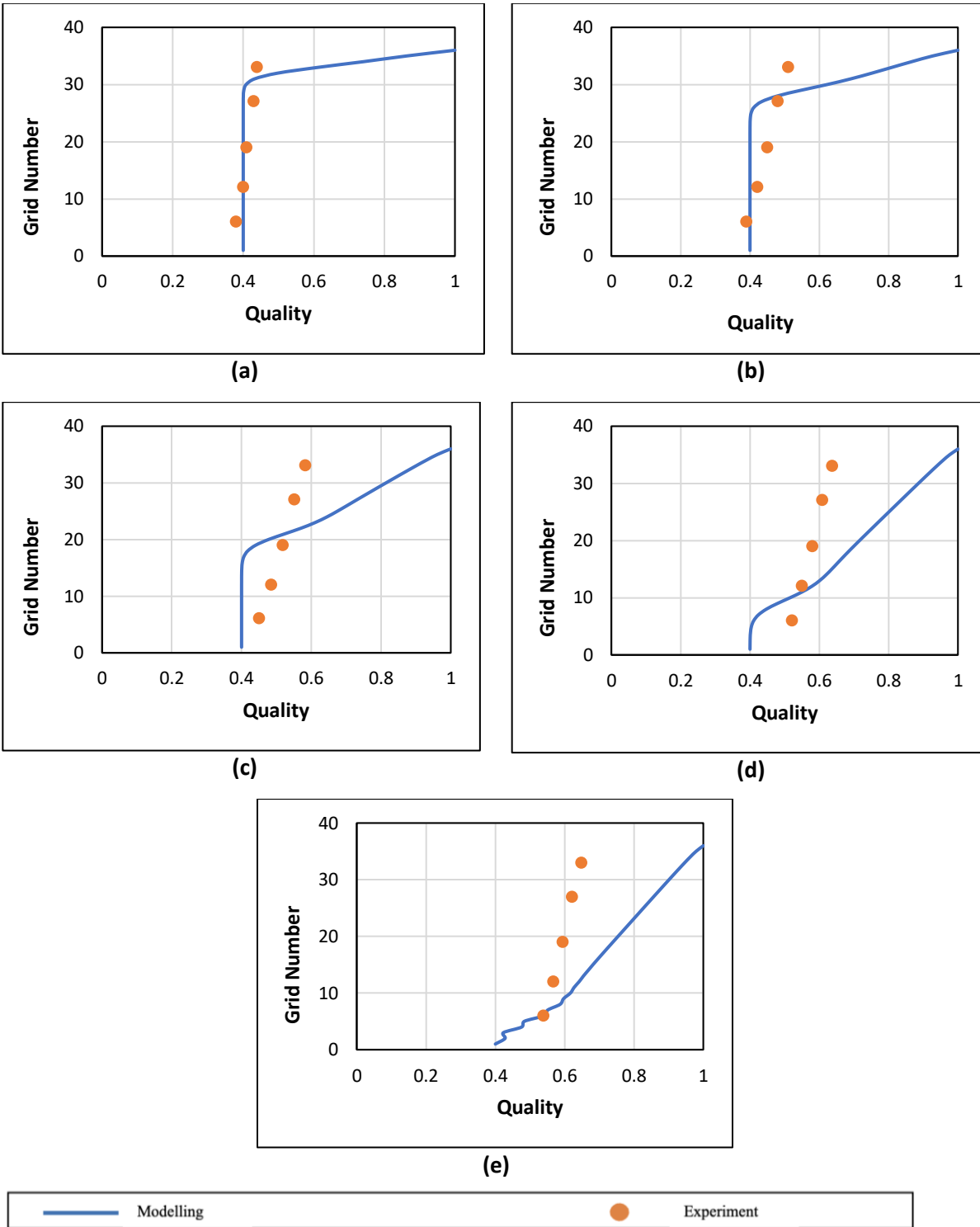


Figure C.1. Drainage Rate at 40% Quality of Model vs Experiment at 0% Salt (a) 15 Minutes (b) 30 Minutes (c) 60 Minutes (d) 100 Minutes (e) 120 Minutes

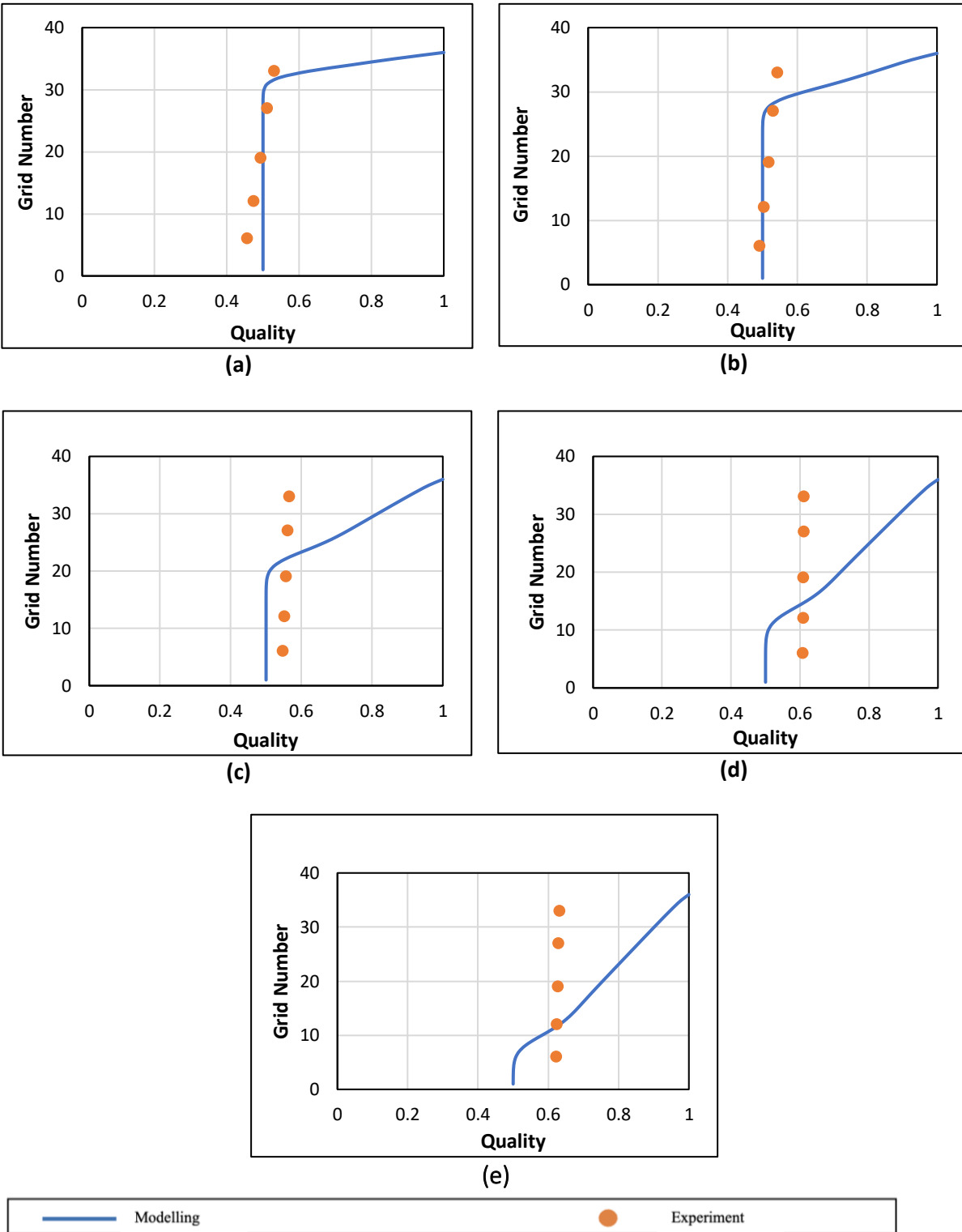
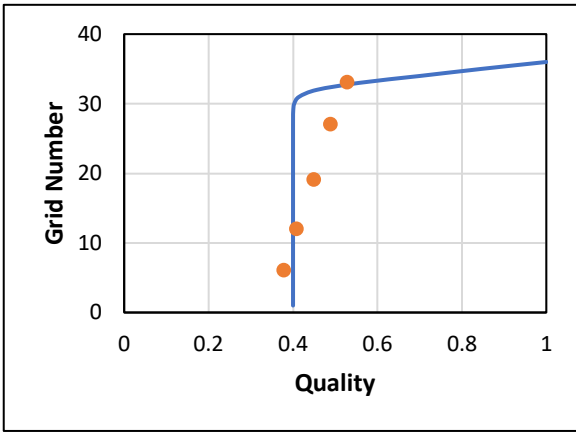
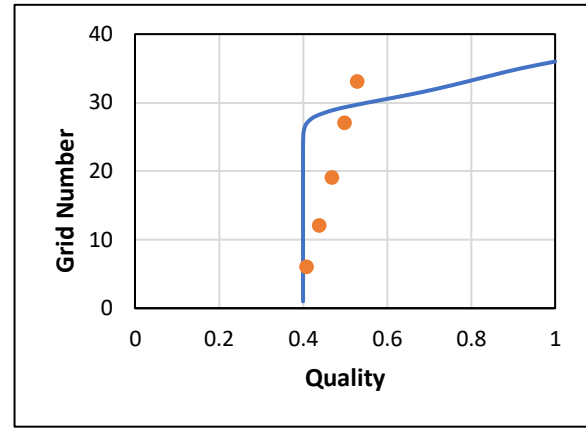


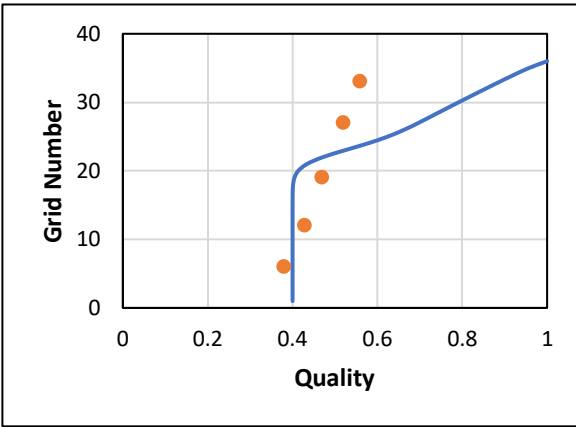
Figure C.2. Drainage Rate at 50% Quality of Model vs Experiment at 0% Salt (a) 15 Minutes (b) 30 Minutes (c) 60 Minutes (d) 100 Minutes (e) 120 Minutes



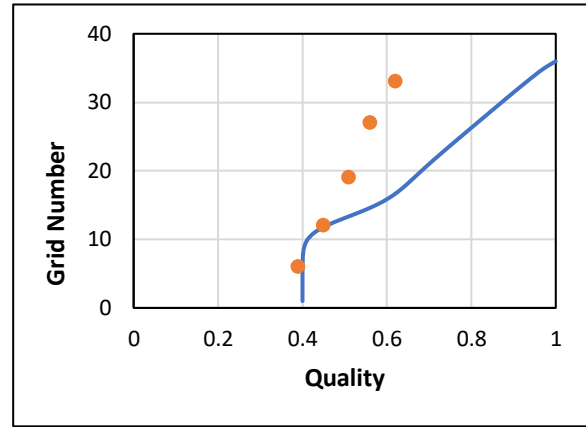
(a)



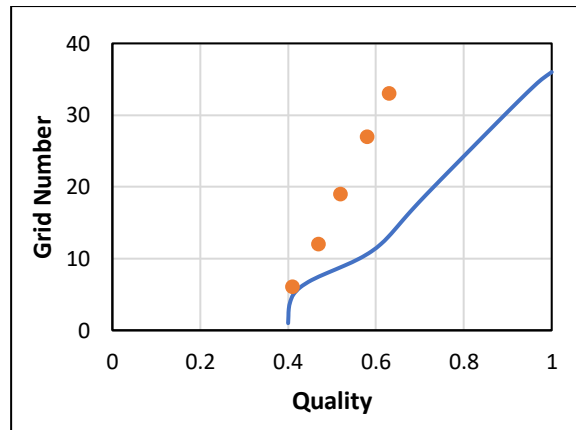
(b)



(c)



(d)



(e)



Figure C.3. Drainage Rate at 40% Quality of Model vs Experiment at 9% Salt (a) 15 Minutes (b) 30 Minutes (c) 60 Minutes (d) 100 Minutes (e) 120 Minutes

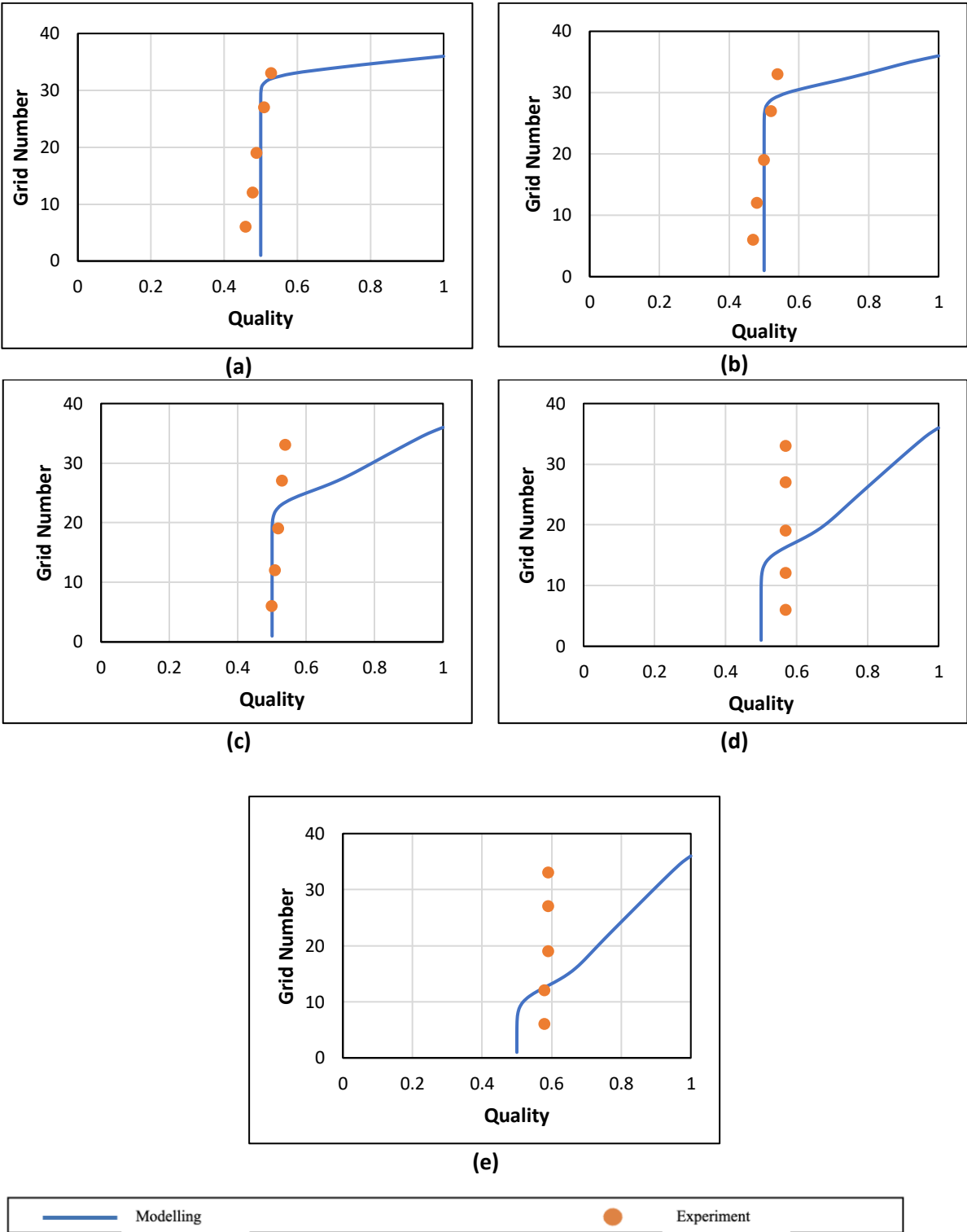


Figure C.4. Drainage Rate at 50% Quality of Model vs Experiment at 9% Salt (a) 15 Minutes (b) 30 Minutes (c) 60 Minutes (d) 100 Minutes (e) 120 Minutes

Appendix D

Mathematical Modelling Code

```
clear all;
mu = 0.005; %viscosity of base liquid with surfactant (kg/ms)
rho = 1000; %density of base liquid with surfactant (kg/m3)
%change the density to the salt foam density.
g = 9.81; %acceleration due to gravity (m/s2)
deltaE = 0.1711; %value taken from Nosa thesis - constant (dimensionless)
K1 = 0.0063; % value chosen from paper - Koehler et al. (2000) %0.05
L = 0.00005; %value taken from Nosa thesis - foam length (m)
gamma = 0.25; %value taken from Nosa thesis - surface tension (kg/s2)
%constants below:
A = mu;
B = 2*K1*rho*g*L^2;
C = gamma*deltaE^0.5*K1*L/4;
D = gamma*deltaE^0.5*K1*L/2;
%model parameters:
deltaT = 10; %timestep (s) %2
grids = 36; %seven grids + two imaginary grids
H = 1.1; %total height of foam column
%change the length of this to the length of only the stable middle section.
%
z = H/(grids-2); %each grid length
E = zeros(grids,1);
%Q = zeros(grids,1);
E(:,1) = 0.40; %this is liquid content

%computations:
T1 = table;
T3 = table;
T2 = table;
for index = 1 : grids
x1(index) = E (index, 1);
x2(index) = 1-x1(index);
y1(index) = grids - index;
end

figure(3)
plot(x1,y1);
hold on;
for n = 1:360
E(1, 1) = 0;
for i = 2:grids-1
%nosa equation
E(i,1) = (deltaT/A)*(C*(E(i,1)^-0.5)*((E(i+1,1)-E(i,1))/z)^2 +
D*(E(i,1)^0.5)*(E(i+1,1)-2*E(i,1)+E(i-1,1))/(z^2) - B*E(i,1)*(E(i+1,1)-
E(i,1))/z) + E(i,1);
end

for index = 1 : grids;
x1 (index) = E (index, 1);
x2 (index) = 1 - x1(index);
```

```
%x_1 = 1 - x1;
y1(index) = index;
end

x = table(x2);
z_1 = table(x1);
y = table(y1);

T1 = [T1; x];
T3 = [T3; z_1];
T2 = [T2; y];

figure (3)
plot(x1, y1); hold on;
%axis([0 1 0 40]);
set(gca, 'XDir', 'reverse');

end
```